Organic & Biomolecular Chemistry

ROYAL SOCIETY OF CHEMISTRY

REVIEW

View Article Online
View Journal | View Issue

Cite this: *Org. Biomol. Chem.*, 2024, **22**, 5470

Synthetic approaches of carbohydrate based self-assembling systems

Guijun Wang, * Anji Chen, Pramod Aryal and Jonathan Bietsch

Carbohydrate-based self-assembling systems are essential for the formation of advanced biocompatible materials *via* a bottom-up approach. The self-assembling of sugar-based small molecules has applications encompassing many research fields and has been studied extensively. In this focused review, we will discuss the synthetic approaches for carbohydrate-based self-assembling (SA) systems, the mechanisms of the assembly, as well as the main properties and applications. This review will mainly cover recent publications in the last four years from January 2020 to December 2023. We will essentially focus on small molecule self-assembly, excluding polymer-based systems, which include various derivatives of monosaccharides, disaccharides, and oligosaccharides. Glycolipids, glycopeptides, and some glycoconjugate-based systems are discussed. Typically, in each category of systems, the system that can function as low molecular weight gelators (LMWGs) will be discussed first, followed by self-assembling systems that produce micelles and aggregates. The last section of the review discusses stimulus-responsive self-assembling systems, especially those forming gels, including dynamic covalent assemblies, chemical-triggered systems, and photoresponsive systems. The review will be organized based on the sugar structures, and in each category, the synthesis of representative molecular systems will be discussed next, followed by the properties of the resulting molecular assemblies.

Received 18th April 2024,
Accepted 21st May 2024

DOI: 10.1039/d4ob00636d

rsc.li/obc

1. Introduction

Carbohydrate-based self-assembling systems are important for the formation of advanced biocompatible materials with

Department of Chemistry and Biochemistry, Old Dominion University, Norfolk, VA 23529, USA. E-mail: g1wang@odu.edu; Fax: +(757) 683-4628; Tel: +(757) 683-3781

Guijun Wang

Professor Guijun Wang obtained her BS and MS in chemistry from Tsinghua University Beijing, China. She received PhD in Organic Chemistry from Michigan State University. After postdoctoral research at Yale University, she was appointed as an assistant professor at the University of New Orleans in 2002. In 2012, she moved to Old Dominion University, where she is currently Professor of Chemistry and Biochemistry. Dr Wang's group is conducting research in organic chemistry with an emphasis on the synthesis of chiral small molecules, natural product analogs for biomedical applications, catalysis, and carbohydrate-based self-assembling systems and biomaterials. She has coauthored 80 publications and 20 patents.

Anji Chen

Dr. Anji Chen completed his doctoral studies in organic chemistry at Old Dominion University in 2018 under the guidance of Professor Guijun Wang. His thesis focused on the synthesis of novel glycolipids, glycoclusters, and glycomacrocycles as functional materials. Anji joined TCG GreenChem as a Post-doctoral Researcher in February 2019. After being promoted to a Senior Scientist in February 2021, he worked as a process chemist to develop reliable, safe, and sustainable synthetic approaches to APIs. He is currently an Associate Principal Scientist in the analytical department focusing on method development and impurity identification using MS and NMR techniques.

different functions and they have numerous applications. In this review, we will discuss the recent development of sugar-based small molecules and their self-assemblies, as well as the construction of large molecular assemblies by noncovalent interactions and dynamic covalent interactions. The main sections of the review are based on the structures of carbohydrates: monosaccharides, disaccharides, oligosaccharides, and branched systems. The formation of the self-assembling carbohydrates for functional materials including organogels and hydrogels, as well as the applications for optical probes, and biomedical applications for diagnostics and therapeutics, will be discussed. In the last section, various stimulus-responsive carbohydrate-based assemblies will be reviewed, with an emphasis on dynamic covalent, chemical triggered, and photo-responsive systems. The formation of dynamic covalent bonds is often used for the preparation of functional assemblies and reversible supramolecular gels.

Carbohydrate-based self-assembling systems encompass a broad range of materials and fields. Many important reviews discuss various aspects of these systems. These include, for example, carbohydrate-based macromolecular materials,[1] supramolecular chemistry and glycoconjugates,[2] and click chemistry and its applications in glycoscience.[3,4] The preparation of glycomimetics and multivalent glycoconjugates and their applications for lectin binding have been reviewed.[5–7] Carbohydrate-based chiral assemblies[10] and carbohydrate-derived amphiphiles and their applications for materials and medicines have also been reviewed recently.[8,9] Carbohydrate-based molecular gelators as special classes of carbohydrate-based molecular assemblies have been examined.[11–13] However, the reviews for gelators typically did not include their syntheses. In this review, we wish to summarize the general methods in the preparation of carbohydrate-based self-assembling systems and aim to provide not only the structures of compounds that can form gels or other SA architectures, but also the general methods for their chemical synthesis.

We will first discuss self-assemblies from monosaccharides, disaccharides, and oligosaccharides, and lastly stimulus-responsive sugar derivatives. Most of the synthesis starts from commercially available starting materials. The structures of sugar scaffolds that are often used for the synthesis of self-assembling systems are shown in Fig. 1. These include the common hexoses **1–5** and disaccharides **6–7**. The sugars discussed in this review are D-sugars unless specifically defined. Monosaccharide derivatives are a major class of compounds that form low molecular weight gelators (LMWGs) and other assemblies, and this section will include more detailed examples.

2. Monosaccharide derivatives

Common hexoses such as glucose (Glc), galactose (Gal), mannose (Man) and glucosamine (Fig. 1), and sugar alcohols such as sorbitol (glucitol) and mannitol, as well as some pentoses, have all been utilized as building blocks for the formation of carbohydrate-based self-assembling systems. In this section, the carbohydrate derivatives are organized into three main categories based on the glycoside linkages: *O*-glycosides, *N*-glycosides, and all other types of glycoside derivative including glycopeptides and glycolipids. These will be discussed in the same order in the following sections.

2.1 *O*-Glycosides

The formation of *O*-glycosides can be obtained by the reaction of monosaccharides with the corresponding alcohols *via* straightforward reactions. The synthesis of both anomers from

Pramod Aryal

Pramod Aryal received his BS and MS degrees in Chemistry from Tribhuvan University, Nepal. During his master's he dedicated his research efforts to isolating bioactive compounds from medicinal plant extracts. Then, he joined the National Forensic Science Laboratory, Nepal, and worked as a forensic chemist for four years. Currently he is pursuing his doctoral degree at Old Dominion University (PhD) under the mentorship of Professor Guijun Wang. In the Wang lab his research is focused on the synthesis of glycoconjugates and photochromic molecules, and natural product derivatives for medicinal applications.

Jonathan Bietsch

Dr. Jonathan Bietsch received his Ph.D. in organic chemistry at Old Dominion University, VA, under the mentorship of Prof. Guijun Wang in 2021. His research focused on the synthesis of novel carbohydrate-based self-assembling systems. After graduation, Jonathan briefly continued work in the Wang group to take part in a project synthesizing dithienylethene-based molecular switches. In August of 2022, Jonathan joined TCG GreenChem as a Senior Scientist. He currently works in the Analytical Department where he supports process development. The focus of his current work is on structure elucidation, molecular conformation determinations and impurity identification by NMR and LCMS.

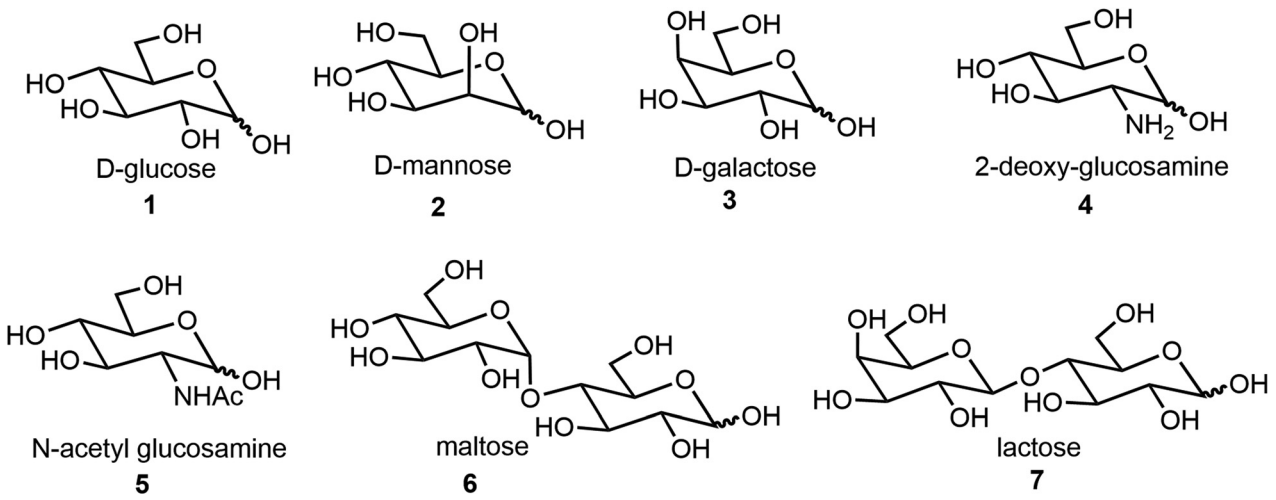

Fig. 1 Structures of the common monosaccharide and disaccharide starting materials, all D-sugars.

free sugars can be achieved readily by several methods. An advantage of the formation of glycoside is that the sugar structures can be synthesized in optically pure forms and anomers can be obtained as single isomers. In addition to fixing the configuration, different functional groups can also be introduced to the anomeric positions. Many derivatives with alpha-methoxy glycosides have been synthesized due to the ease of formation, and the methoxy group is the smallest *O*-glycoside.[11] As shown in Scheme 1, *N*-acetyl-D-glucosamine (NAG) **5** has been used extensively for the formation of various self-assembling systems due to the presence of the 2-amino group, which can be utilized for further functionalization.[14,15] NAG **5** can be converted to glycoside **8**, the 4,6-hydroxyl groups are then functionalized by the formation of the acetal **9**, the pure alpha isomer can be obtained by recrystallization or chromatography, and deacetylation under alkaline conditions using a microwave synthesizer leads to the corresponding sugar amine alcohol **10.** The 2-amino group can be further functionalized with different functional groups to obtain LMWGs (Scheme 2). Compound **10a** can be converted to the corresponding amides **11**, ureas **12**, and carbamates **13**. Several series of derivatives with the general structures **11a**, **11b**, **11c**, **12a**, **12b**, **13a**, and **13b** have been synthesized and have demonstrated gelation properties in organic solvents, mixtures of alcohol with water or dimethyl sulfoxide (DMSO) with water, and water, depending on the nature of the R group.

N-Acetyl-D-glucosamine-based 3-*O*-carbamates **15** were prepared by first acylation of 3-OH with 1,1′-carbonyldiimidazole (CDI) followed by displacing the imidazole group with a primary amine.[16] Alternatively, functionalizing 3-OH with isocyanate in the presence of DBU[17] in one step can also afford the 3-*O*-carbamates **15.** Many derivatives in this series were effective LMWGs, especially for aqueous mixtures. The gelator **15** (when R′ = *p*-methoxyl benzyl) formed spontaneous gels when adding aqueous solutions of metal ions to the gelator solution dissolved in a small amount of DMSO. Wang's group also reported several C-2 *N*-linked carbamates of the 4,6-*O*-phenylethylidene acetal protected D-glucosamine derivatives **16,**[18] which were prepared by commercially available chloroformate and the previous literature-reported amine headgroup.[19]

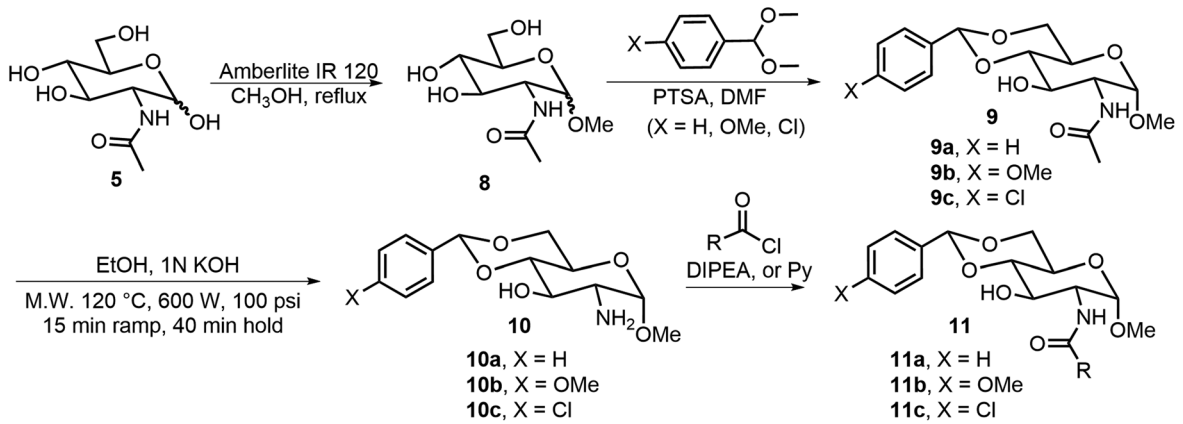

Scheme 1 Synthesis of methyl glycoside **8**, the derivatives **9** and **10** as headgroups, and the amides **11** as LMWGs.

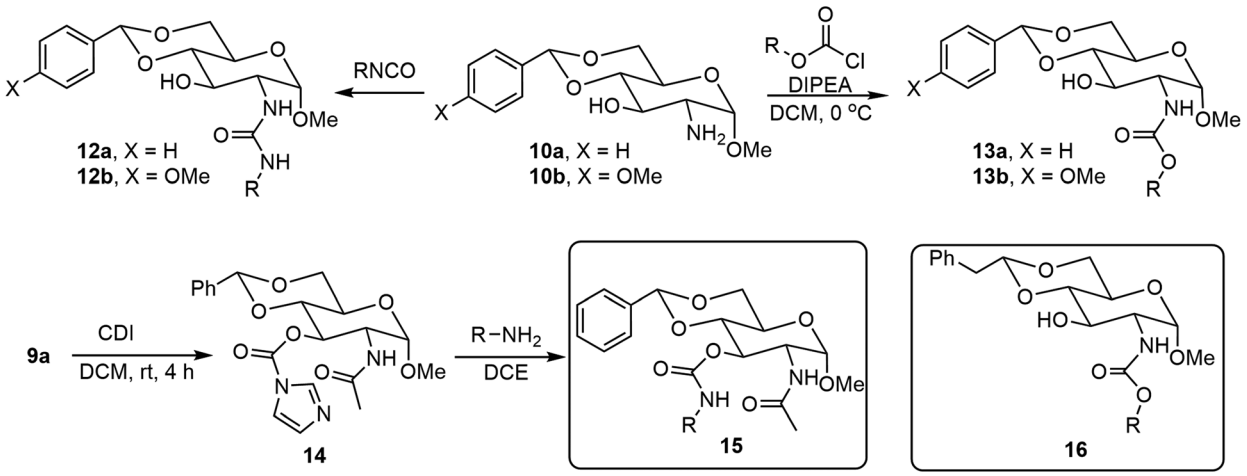

Scheme 2 Synthesis of urea and carbamate derivatives as organogelators and hydrogelators.

Among the synthesized carbamates, the isopropyl derivative (**16**, R = iPr) is a hydrogelator and can form hydrogel at 0.2 wt%. This hydrogelator gels with tetra alkyl ammonium salts to create effective gel electrolytes.

Ludwig *et al.* synthesized a series of boronate derivatives of *O*-glucosides and studied their organogelation properties.[20,21] The synthesis was carried out by heating the glucosides with the corresponding boronic acids and the removal of water, as shown in Schemes 3. A few boronate derivatives were able to form gels in toluene. The 4,6-boronate group can be hydrolyzed with the addition of a small amount of water, resulting in the degradation of the corresponding organogels. The extent of the water sensitivity of the gels formed by **21** was evaluated.[21] The monomethyl and *p*-methoxy group on the phenyl ring did not affect gelation, but dimethyl substituted and CF_3 groups increased the solubility and reduced the gelation tendencies. Also, the alkyl chain lengths seem to affect the water sensitivity more significantly than the aryl substituents.

The glycosylated tripeptides **22** and **23** were synthesized from the corresponding Fmoc protected Ser or Thr glucosides *via* solid-phase peptide synthesis (Fig. 2).[22] The presence of the glucose unit affected the tripeptides' aggregation properties, with enhanced disorders and dynamics due to the introduced CH–π interaction. Glycopeptides containing disulfide linkages were also synthesized and the self-assembling properties were investigated.[23] Compound **24** is one of these compounds from a library of glycopeptides which contain different monosaccharides; these glycopeptides were syn-

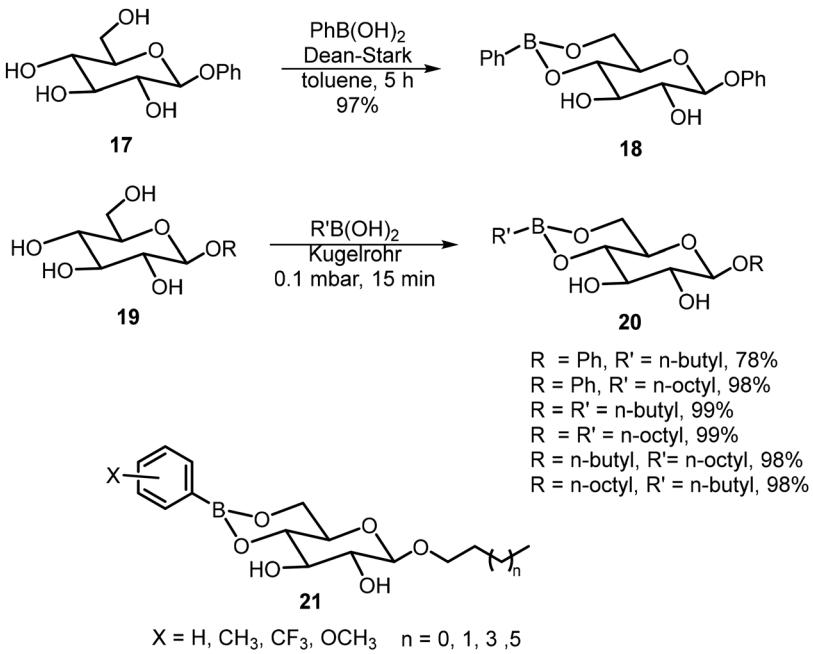

Scheme 3 Synthesis of boronate derivatives as organogelators.

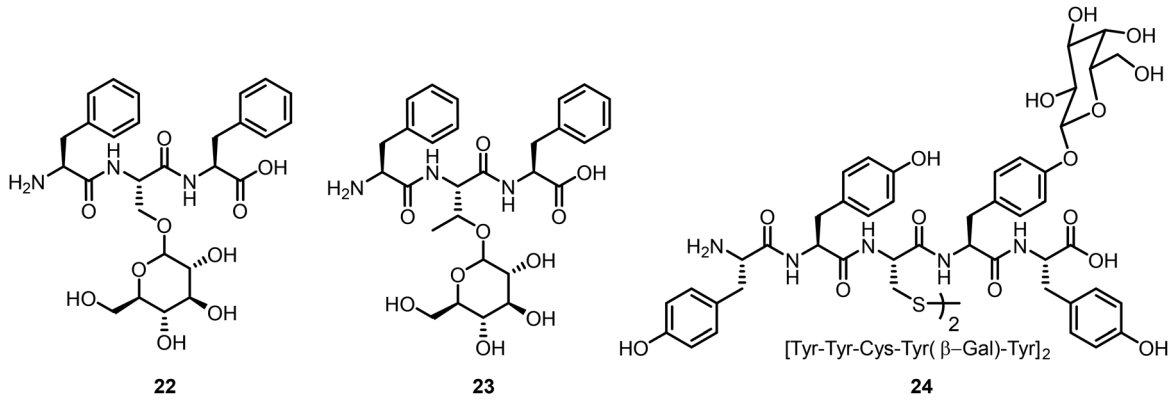

Fig. 2 Structures of *O*-glycoside and peptides derivatives.

thesized by peptide coupling reactions from glycosylated tyrosines. Various monosaccharides were attached to the tyrosine residue and certain glycopeptides were able to form hydrogels, presumably through enhanced CH–π interaction with the sugar moieties.

Pathak *et al.* synthesized a library of phenolic glycopyranosides from pentoses **25a–d** and studied the structure to gelation relationships (Scheme 4).[24] The sugar scaffolds used in this library included arabinose, xylose, lyxose, and ribose. Four organogelators (**28–31**) were obtained, two β-arabinose and two α-xylose derivatives. Compound **28** was used to entrap curcumin in a mustard oil gel and its sustained release was studied at various pH values. Slower release was observed under basic conditions.

Tsutsumi *et al.* synthesized glycosylated *N*-alkyl-2-anilino-3-chloromaleimide-based chromophore (AAC) derivatives and studied their self-assembling properties.[25] The synthesis of beta-D-Gal-AAC-C6-Fn **34** is shown in Scheme 5. This compound was prepared from the AAC containing bola-amphiphilic glycolipid **32**. The conjugation of **32** with mono, di, tri, and tetrapeptides of phenylalanine (F) yielded the glycolipopeptides **34**. The compound **34** (n = 3), betaGal-AAC-C6-F3, formed transparent gels at 0.19% in solvent 200 mM HEPES–NaOH buffer (pH 8.0). The same team also synthesized and analyzed five H-AAC-C6-Ph-MS compounds **35a–e**;[26] the monosaccharides used include α- and β- glucose, galactose, and α-mannose. The glucosyl and galactosyl amphiphilic compounds exhibited aggregation-induced emission (AIE) features, but the mannose derivatives did not exhibit fluorescence.

Several *O*-glycosides containing anthracene groups at the anomeric position were synthesized and their self-assembling properties as well as fluorescence properties were analyzed.[27,28] The structures of some of these compounds are shown in Scheme 6. Glycosylation of the hydroxyl methyl anthracene derivatives **36** with tetraacetyl glucosyl bromide **37**, followed by deacetylation, afforded the anthracene glycosides **38**. Other sugar bromides were also used, including derivatives of D-Glc and L-Glc, Gal, and Lactose (Lac). The glucose derivative **38a** formed chiral assemblies in aqueous solutions, the π–π stacking of the anthracene moiety is the driving force for the assembly

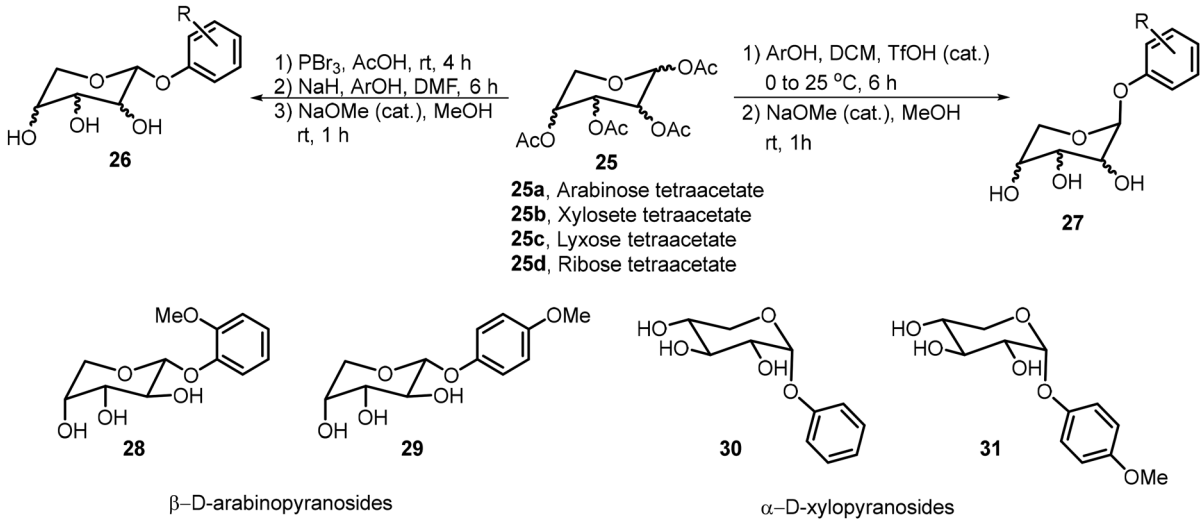

Scheme 4 Synthesis of phenolic glycosides of pentose sugars – arabinose, xylose, lyxose and ribose.

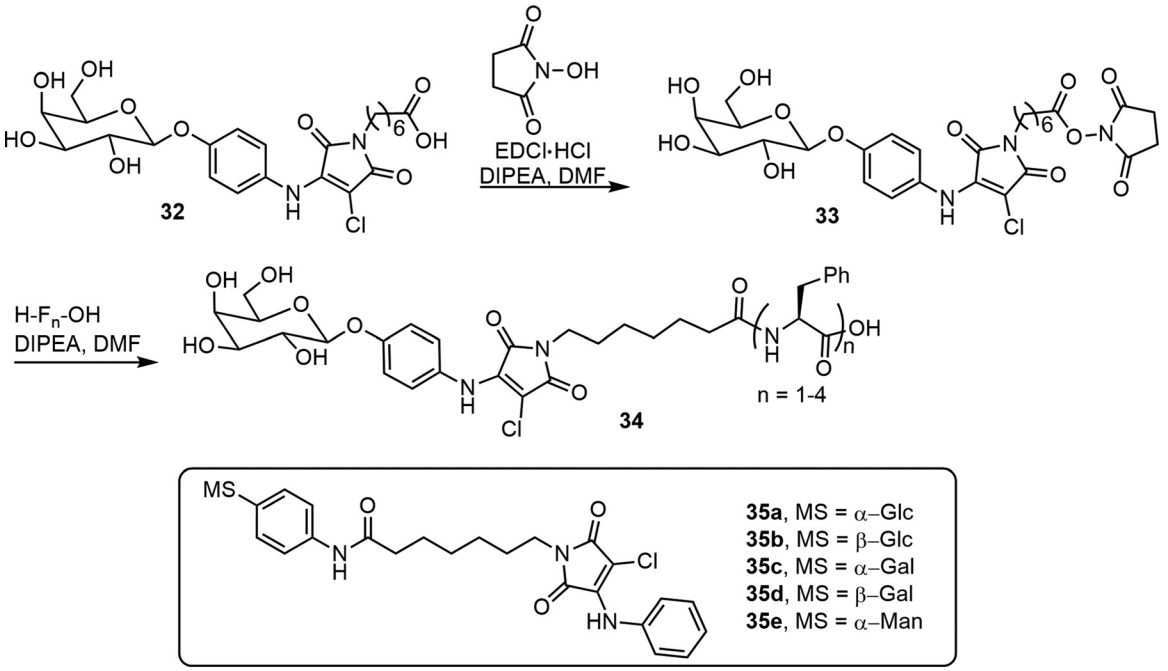

Scheme 5 Synthesis of glycosides of AAC derivatives **34** and **35a–e**.

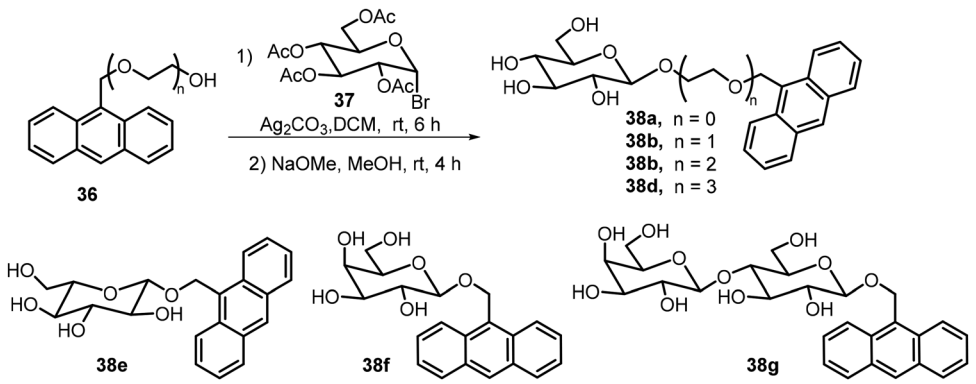

Scheme 6 Synthesis of anthracene derivative of glycosides **38** with different linkers and sugar moieties.

and the chirality of the assemblies is dependent on the nature of the sugar structures. Irradiation at 365 nm disrupted the assembly structures due to (4π + 4π) photochemical reactions of the anthracene moieties. Circular dichroism (CD) was used to characterize the chirality of the SA structures of the anthracene glycosides; the CD spectra indicate left-handed chirality for **38a** and right-handed chirality for **38e** (L-Glucoside). Galactose derivative **38f** exhibited right-handed chirality and lactose derivative **38g** showed no or little chirality. The team also synthesized anthracene glucosides with different chain lengths of ethylene glycol linkages (**38b–d**) and analyzed their SA properties.[28] They found that the introduction of ethylene glycol linkages changed the SA morphologies significantly, though the glucosides still produced chiral aggregates.

Mousavifar *et al.*[29] synthesized and analyzed a series of mannosyl neoglycolipids with different chain lengths and evaluated their effectiveness as liposome-based drug delivery vehicles (Scheme 7). These glycolipids **43** were prepared starting from the peracetylated mannose **39**. Glycosylation with 6-chloro-1-hexanol followed by azide displacement afforded intermediate **41**. Staudinger reduction of the azido group followed by amide ligation with carboxylic acids afforded compound **42** as shown in Scheme 7. After de-acetylation, glycolipids **43** with lipid tails of 8–16 carbons were prepared. The alkyl groups with the formula of C_nH_{2n+1} are all linear alkyl chains. These compounds were able to form liposomes. Liposomes formed by the C14 lipid exhibited ideal properties and were further studied for their drug delivery capabilities.

Two *N*-acetylgalactosamine (GalNAc) based glycolipids **50α** and **50β** were synthesized and evaluated as potentially useful supramolecular materials (Scheme 8).[30] Preparation of the epimers **50α** and **50β** started with the glycosylation of 2-azido

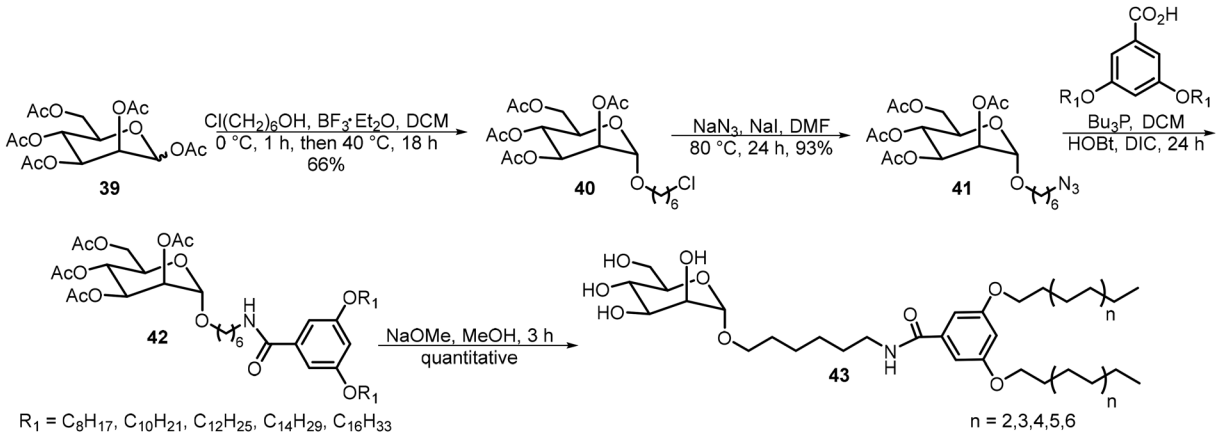

Scheme 7 Synthesis of neoglycolipids **43**.

thioglycosyl donor **44** with *N*-Fmoc and benzyl protected serine acceptor **45**. The resulting 2-azido glycoside **46** was then reduced and further acetylated to form **47**. The benzyl group was then removed by catalytic hydrogenation, followed by the formation of the pentafluorophenyl ester **48**. Amide coupling reactions with 2-aminoethanol were then carried out, subsequent removal of the Fmoc and Ac groups afforded intermediate **49**. The amine in **49** was then reacted with a long chain lipid containing pentafluorophenyl ester to afford the glycolipids **50**, which were isolated to obtain the **α** and **β** epimers. These GalNAc-based epimers on their own can self-assemble into ribbons in aqueous solutions while the mixture of the epimers (50 : 50) forms spherical micelles due to carbohydrate–carbohydrate interactions (Scheme 8).

Baccile's group studied the self-assembling properties of a class of natural glycolipids and their derivatives;[31,32] an example **51** is shown in Fig. 3. These compounds have been studied extensively and the glycolipids exhibited interesting

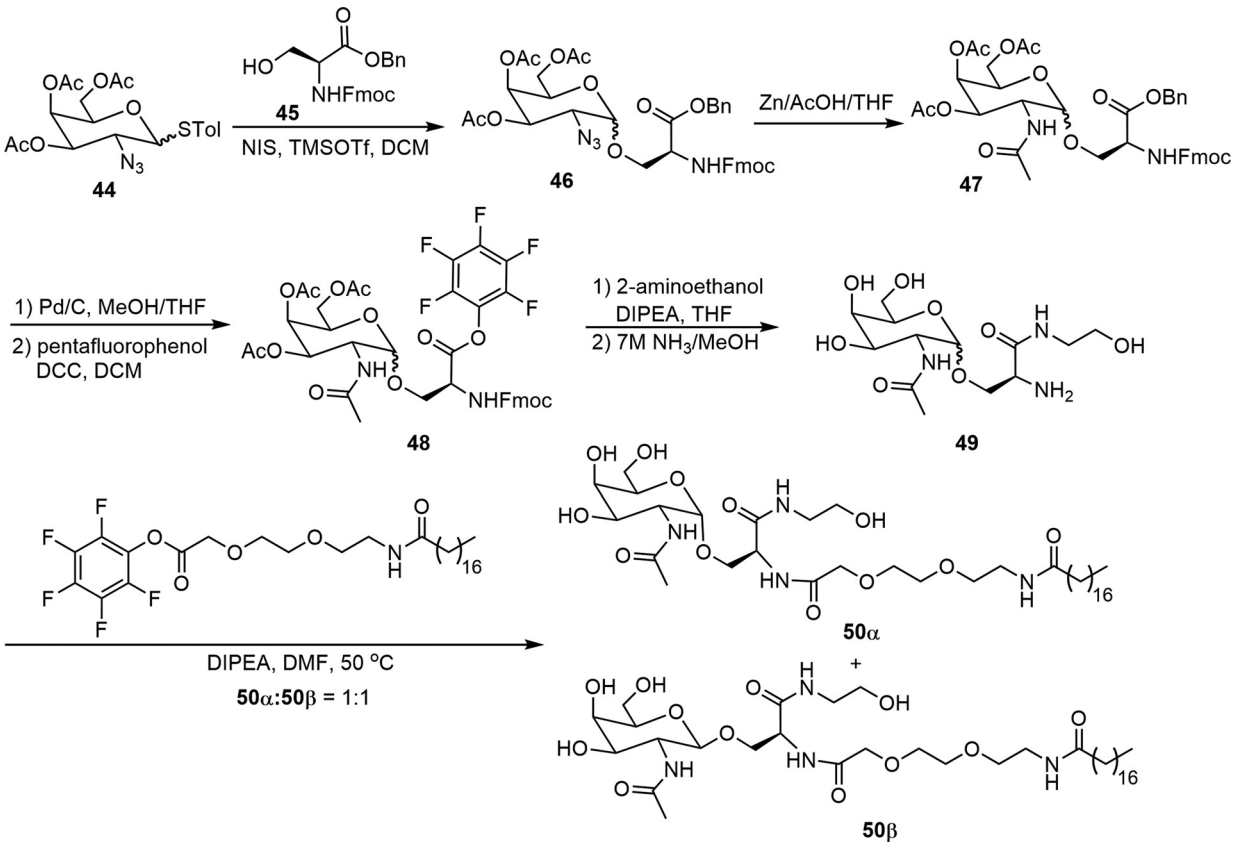

Scheme 8 Synthesis of GalNAc-based anomers **50α** and **50β**.

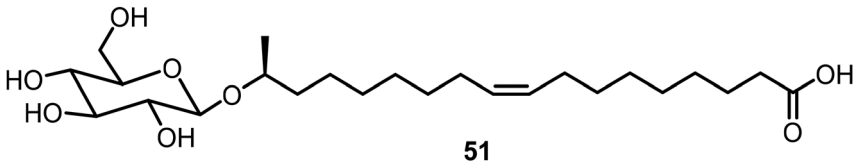

Fig. 3 Chemical structure of natural glycolipid **51**.

properties as LMWGs, and the carboxyl substituted lipids also formed metallogels in the presence of various metals.[33–35]

2.2 *N*-Glycosides

Besides the common *O*-glycoside derivatives, several *N*-glycosylated systems have been synthesized and their molecular assemblies evaluated. The synthesis of these compounds typically was done by reaction of an amine with a reducing sugar to form the *N*-glycosides. Several examples are discussed in the next section for monosaccharide derivatives. Rachamalla *et al.* explored *N*-glycosylation reactions under various conditions to create a library of amphiphilic *N*-glycosyl naphthalimides.[36] The synthesis of these carbohydrate derivatives utilized ammonium sulfate as a catalyst and exclusively produced the β-anomers (Scheme 9). The scope of the reaction was explored using glucose, galactose, and xylose, along with several long chain alkyl groups, to create a library of compounds. The mechanism of the *N*-glycosylation reaction was proposed and supported by a relative energy profile diagram. Several glucose derivatives from the library were found to form gels in chloroform and compound **53a** also formed gels in a DMSO–H_2O (40% v/v) mixture. Additionally, thin drop cast films of **53a** possess semiconducting behavior and it was capable of being anchored on cotton fabric, resulting in increased conducting properties.

Mohan Das *et al.* have reported several glucose-derived gelators **54**. These are 4,6-alkylidene acetal-protected glucose derivatives with various β-arylamines introduced at the anomeric positions.[37] 4,6-*O*-Ethylidene and butylidene were used as the protecting groups, whereas on anomeric positions C8, C12 and C16 chain-length ester groups were attached to the phenyl ring at the *para* position (Fig. 4). These compounds formed gels in several organic solvents, and they have high selectivity towards the organic phase from a mixture of aqueous and organic phases. The toluene gel formed by **54e** was studied for metal ion responsiveness and a gel–sol transition was observed upon the addition of Cu^{2+} metal ions. The structure of coordination of Cu^{2+} with compound **54e** was determined by NMR titration, which showed a dimeric gelator to one copper ion. The same team introduced a photoresponsive azobenzene moiety to the anomeric position and synthesized a series of derivatives, of which the best performing gelator, compound **55**, was further studied.[38] These compounds formed phase-selective gels in organic solvents and also exhibited the effective removal of dyes. Long aliphatic chains resulted in the formation of hydrophobic interaction and van der Waals interactions to form organogels in toluene and acetonitrile. These organogels were selective for the removal of cationic dyes from the mixture of cationic and anionic dyes. Photoisomerization of azobenzene leads to the transition of gel-to-sol when exposed to UV light. More recently azophenol and azonaphthol derivatives were also synthesized and the azonaphthol derivatives **56a–d** were able to form gels in DMF/water and DMSO/water mixtures.[39] The synthesis of compound **56** is described in Scheme 10. Diazotization from the amine **57** with naphthols afforded intermediates **58** and **59**. Hydrolysis and glycosylation with compound **62** led to compounds **56a–d**. Gelator **56b** formed gels in the presence of various metal ions except copper ions. The addition of Cu^{2+} ions resulted in a gel-to-sol transition. This was rationalized by the formation of complexes with Cu^{2+} as shown in Fig. 4.

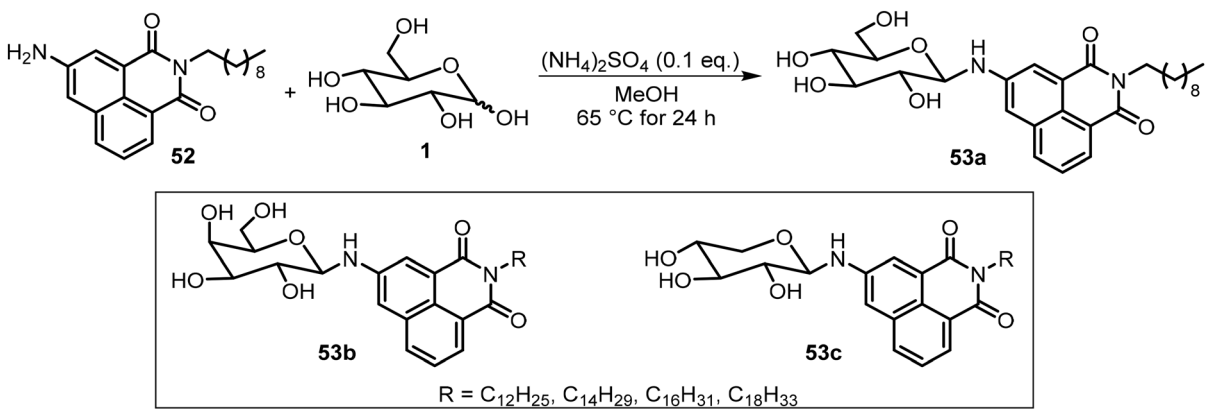

Scheme 9 Synthesis of glycosylarylamines **53**.

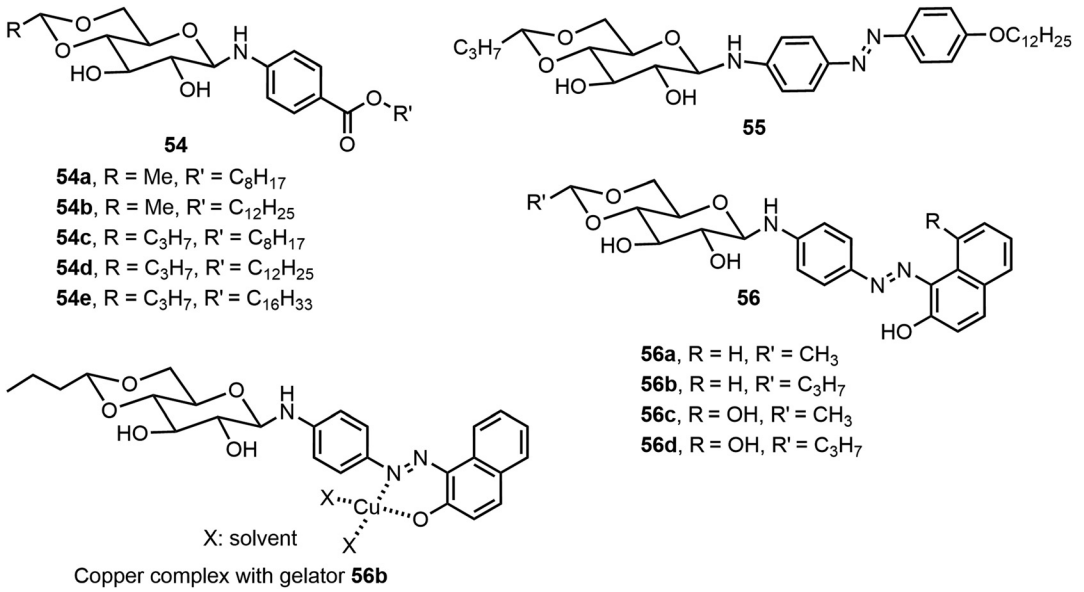

Fig. 4 Structures of arylamine glycoside gelators **54**–**56b** and copper complex with gelator **56b**.

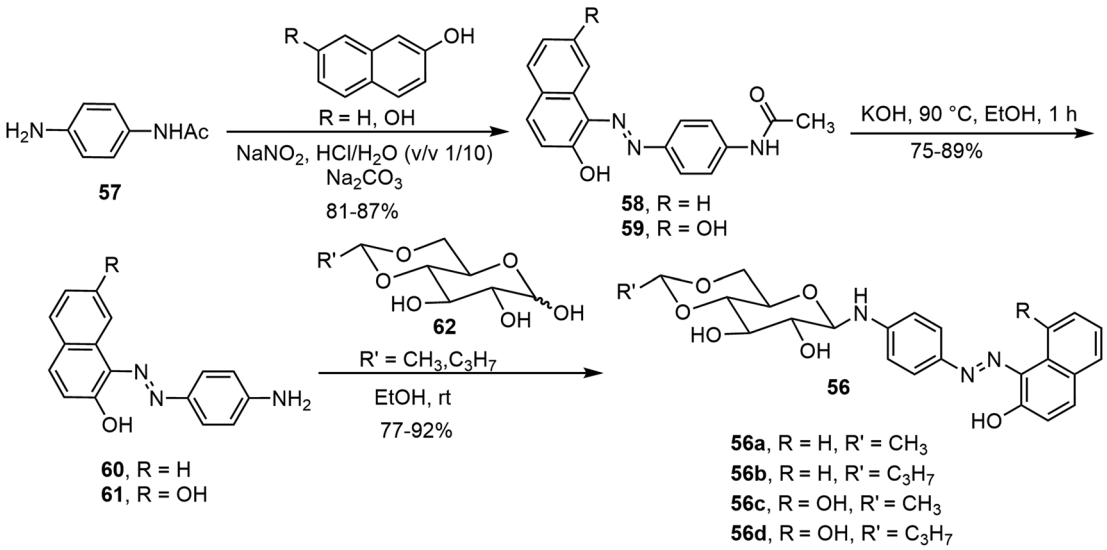

Scheme 10 Synthesis of photoresponsive azobenzene naphthol derivatives **56**.

2.3 Glycolipids and other glycosides

Several glycolipids derived from 3-deoxy-D-manno-2-octulosonic acid (Kdo) were prepared and their self-assembling properties were studied (Scheme 11).[40] The key intermediate **63** bearing both azido and ethyl ester functional groups was prepared starting from D-mannose in 8 steps.[40] The ester **63** was hydrolyzed and the resulting acid was coupled with octadecylamine to afford the amide **64**. Catalytic hydrogenation then afforded the glycolipid mimic **65**. In parallel, a Staudinger reduction of azide **63**, followed by an amide formation and ester hydrolysis, provided glycolipid **68**. Interestingly, these glycolipids formed different morphologies formed during the self-assembling process. The self-assembly of **65** resulted in thermodynamically stable bicelle formation; while the bicelle is only a kinetic intermediate of the self-assembly product with **68**, which eventually transformed into ribbons.The lipid **68** formed ribbons directly by using MeOH/H_2O (v/v 1 : 1) as the solvent.

Metelkina *et al.* synthesized two lectin-targeting phospholipids for *Pseudomonas aeruginosa*, both containing phospholipid 1,2-dipalmitoyl-*sn-glycero*-3-phosphoethanolamine (DPPE) moieties.[41] These lipids are LecA-targeted galactose derivative **76** and LecB-targeted fucose derivative **78** (Scheme 12). Either 1% or 15% (w/w) of these lipids was used to form liposomes together with 1,2-distearoyl-*sn-glycero*-3-phosphocholine

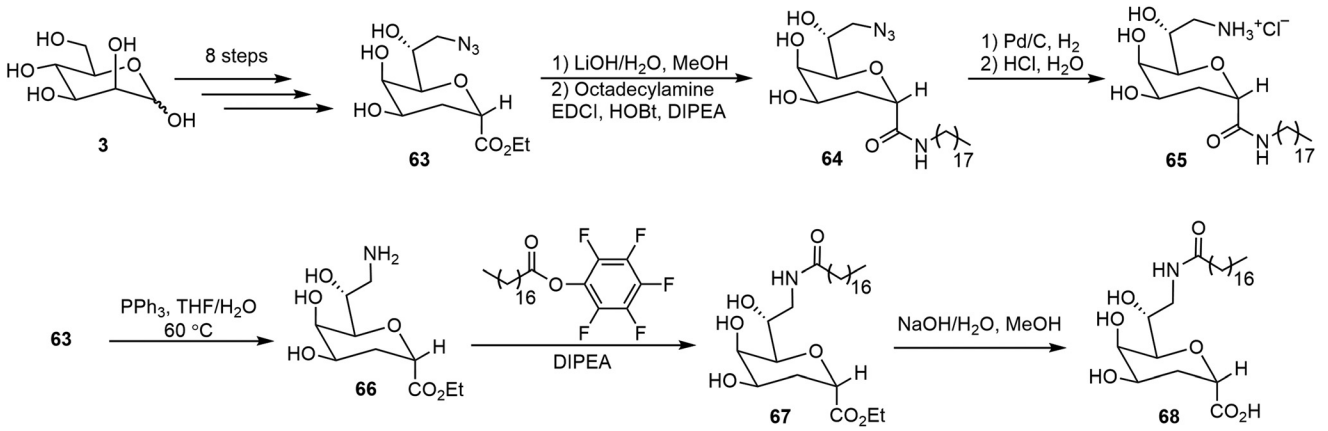

Scheme 11 Synthesis of Kdo-derived lipids **65** and **68**.

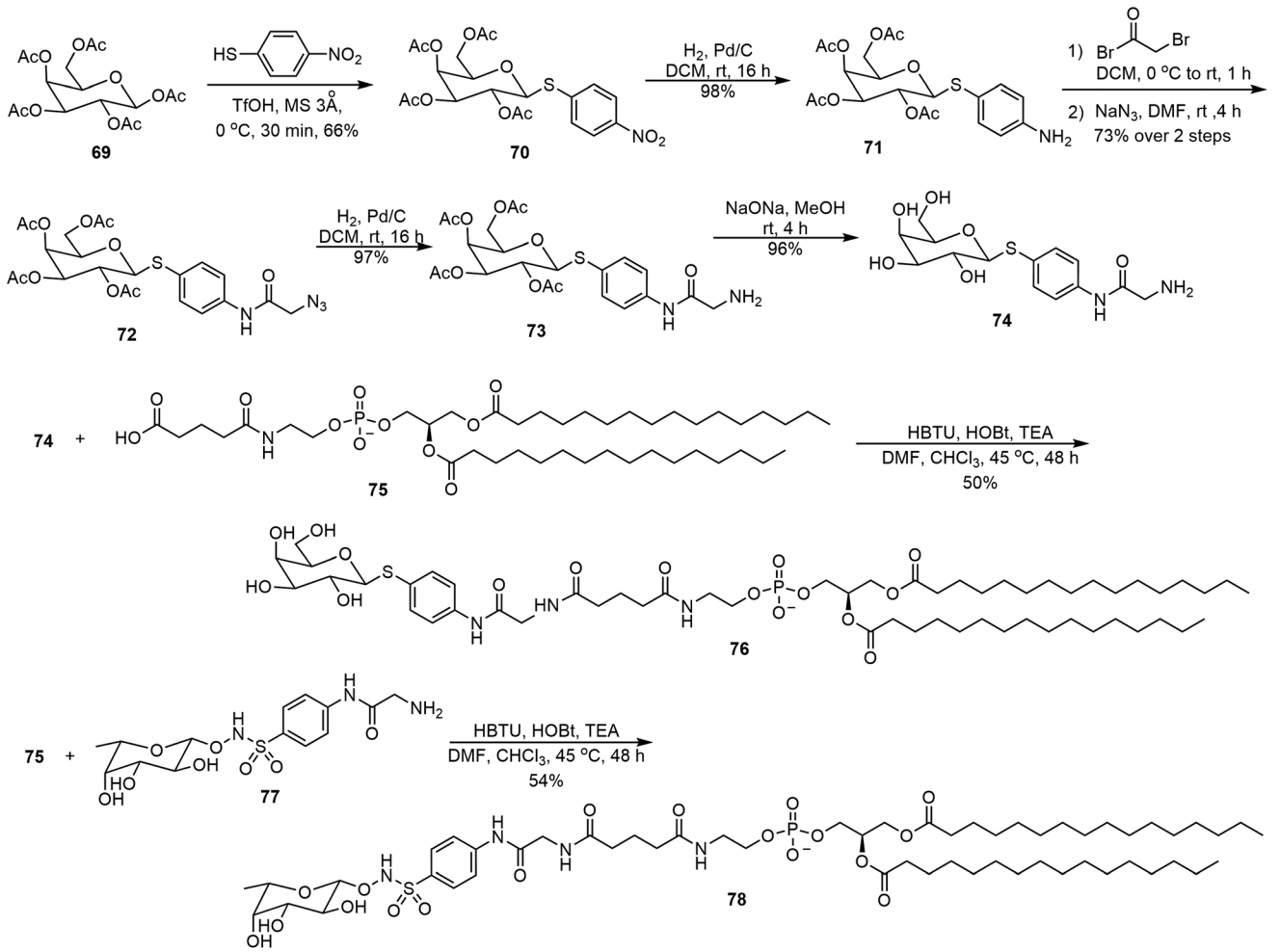

Scheme 12 Synthesis of phospholipid conjugates lectin-targeted lipids **76** and **78**.

(DSPC) and cholesterol. The synthesis method is shown in Scheme 12. Galactose pentaacetate **69** was glycosylated using 4-nitrobenzenethiol to afford **70**. Reduction of the nitro group led to the amine **71**, which was acylated with bromoacetyl bromide, followed by azide displacement of the bromide to form intermediate **72**. The azido group was then reduced to an amino group, followed by deacetylation to afford compound **74**. Compound **74** was then used for the amide coupling reac-

tion with the phospholipid derivative **75** to produce the glycophospholipid **76.** Alternatively, coupling of the acid **75** with the fucose derivative **77** afforded the lipid **78.**

A series of long chain ester derivatives of D-glucose and 1,5-anhydro-D-glucitol (AG) was synthesized and evaluated for its organogelation properties.[42] As shown in Scheme 13, γ-aminobutyric acid (GABA) was reacted with fatty acids of varying chain lengths to form the long chain acids **79a–d**, which were used for the per-esterification of the sugar units to give the derivatives **81** and **82.** Many of these compounds exhibited gelation properties in paraffin oil and some other organic solvents.

Heterocycle functionalized sugar derivatives are useful for the formation of self-assembled networks and for the formation of low molecular weight gelators (LMWGs). Glycoconjugates formed by sugar derivatives connected through the copper-catalyzed azide and alkyne cycloaddition reaction (CuAAC) are an effective method to generate new materials with interesting properties.

Several peracetyl β-*O*-alkyl triazolyl D-glucosides **85,** where two or three carbon linkers are placed between the anomeric position and triazole moiety, were prepared as versatile organogelators (Scheme 14).[43] Starting from pentaacetate of β-D-glucose **83,** $BF_3{\cdot}Et_2O$-mediated glycosylation with 2-chloroethanol or 3-chloro-1-propanol afforded the chloro intermediates **84.** The chloro group underwent an azide displacement reaction, followed by reactions with various terminal alkynes under copper-catalyzed click conditions to give several glucosyl triazole derivatives **85.** The gelator **85a** (n = 2, R = Ph) formed metallogels with several different metal ions (Hg^{2+}, Zn^{2+}, Ni^{2+}, and Pd^{4+}). Interestingly, the co-gel of the 9-fluorenol derivative **85b** with the gelator **85a** showed enhanced fluorescence upon gelation. Similar triazole derivatives starting from the galactose pentaacetate **69** were also synthesized, but the galactose deriva-

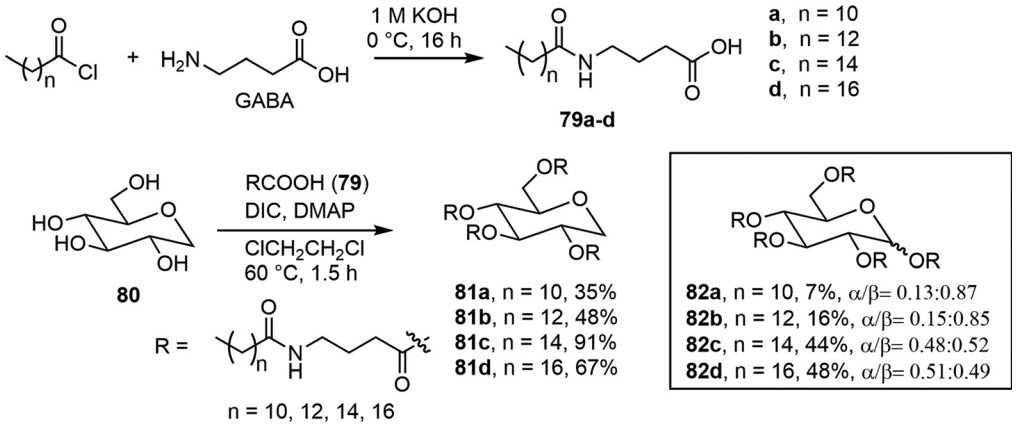

Scheme 13 Synthesis of 1,5-anhydro-D-glucitol and D-glucose ester derivatives **81–82**.

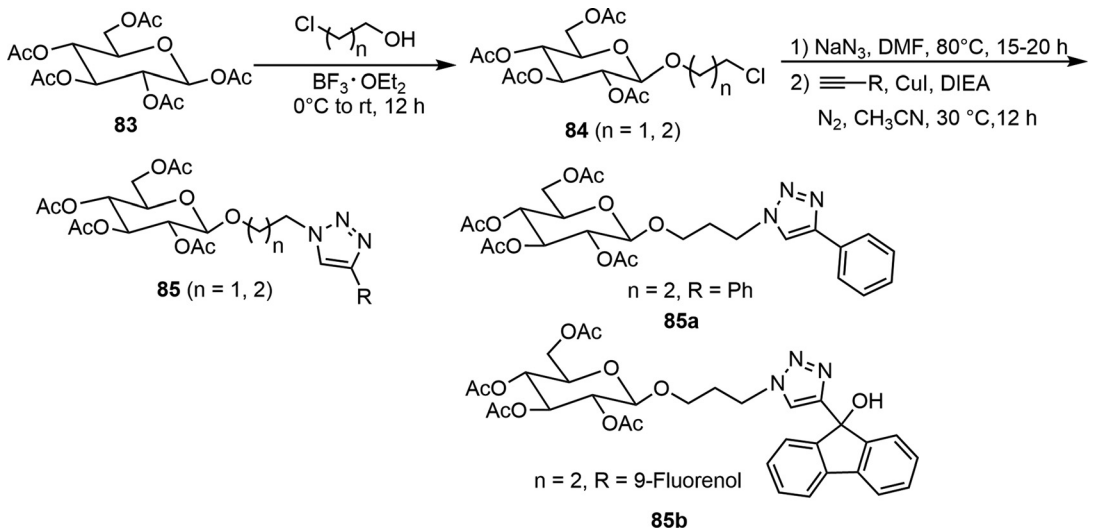

Scheme 14 Synthesis of D-glucose β-*O*-alkyl triazole derivatives **85**.

tives generally did not form gels and typically were soluble in many of the tested solvents.

Another glucose triazole-based gelator **86** was synthesized *via* a CuAAC reaction recently and the compound was found to be an efficient phase selective gelator for oil spill recovery (Fig. 5).[44] The combined effect of the van der Waals force of the long alkyl group and π–π stacking of the phenyl group and triazole group was the driving force for the formation of gels. Compound **86** was utilized for the selective removal of oil from a mixture of oil and water. Using click chemistry, a novel self-assembling cancer vaccine platform composed of Tn antigen Chol-GalNAc **87** and adjuvant CpG (unmethylated 5′-C-phosphate-G-3′) oligodeoxynucleotide (ODN) was developed, which is capable of inducing both humoral immune and cellular antitumor responses.[45] The Tn antigen **87** was formed through CuAAC reactions between the GlcNAc-based alkyne and cholesterol-derived azide (Fig. 5). To acquire the vaccine platform, liposomes of compound **87** were prepared *via* the membrane-ultrasound method followed by encapsulating TLR9 agonist CpG ODN adjuvant.

In addition to triazoles, recently a series of glucosamine derivatives containing isoxazole groups at the anomeric position were synthesized and analyzed, and many of these compounds were effective LMWGs.[46] The synthesis is shown in Scheme 15. Glucosamine- and glucose-derived propargyl glycosides were used to synthesize the 3,5 disubstituted isoxazole derivatives with different chloroximes. The structures of the 5-substituents and the nature of the sugars used were important for the gelation properties. Most of the synthesized derivatives were able to form hydrogels, representing the first class of isoxazole-based molecular hydrogelators. Compounds **89d–i** formed hydrogels at minimum gelation concentration (MGC) lower than 0.5 wt%. Compound **89d** formed hydrogels at 1.1 mg mL^{-1}, or 0.11 wt%, in water and also formed metallogels in the presence of earth metal ions such as Cu^{2+}, Zn^{2+}, and Ni^{2+}. Both gelators **89d** and **89h** were able to form stable hydrogels which can remove dyes from aqueous mixtures.

2.4 Open chain sugar non-glycosylated

In the next section, several examples of open-chain sugar derivatives capable of self-assembly will be discussed. These include several non-glycosylated derivatives in which the anomeric position exists as an aldehyde or hemiacetal, and open-chain sugar derivatives functionalized at the anomeric carbon through oxidative amidation or by con-

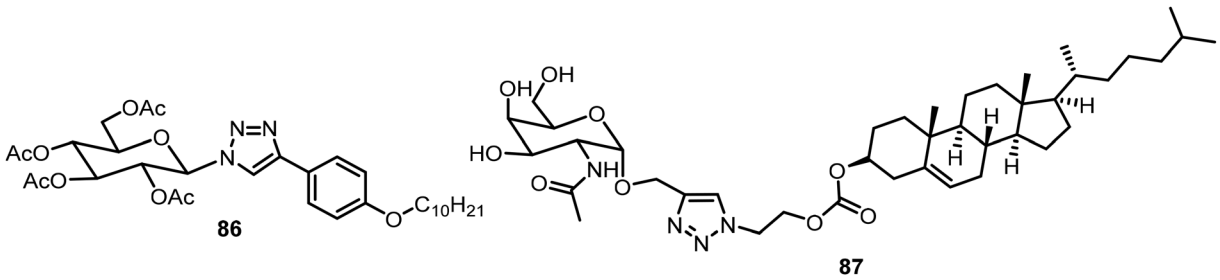

Fig. 5 Structures of glucosyl triazole derivative **86** and galactose triazole derivative **87**.

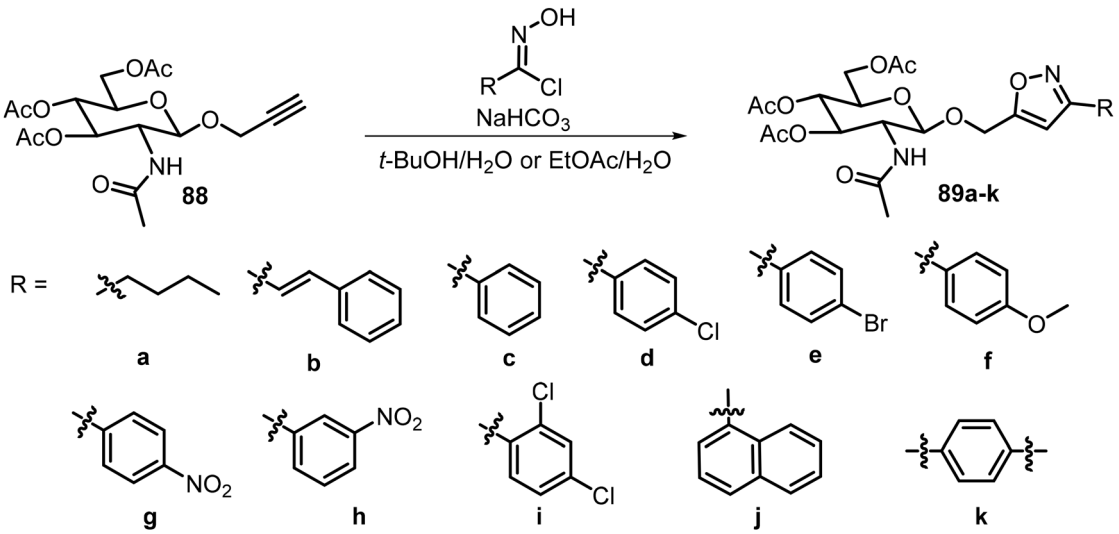

Scheme 15 Synthesis of β-*O*-alkyl isoxazole D-glucosides **89a–k**.

densation with amino groups followed by reductive amination to form amines.

Glucosamine and galactosamine were functionalized at the 2-amino position by reacting with *p*-nitrobenzyloxy carbonyl chloride to form the 4-nitrophenylmethoxycarbonyl (NPmoc) protected compounds **90a–b**.[47] The glucosamine derivative **90a** (Fig. 6) formed a hydrogel whereas the galactose carbamate **90b** only formed suspensions. Self-assembly of compound **90b** was hindered by the presence of an axial OH at the C4 position and resulted in the formation of non-networking spheres. Modeling supports that the combined effect of π–π interaction of the nitrophenyl group and hydrogen bonding of the C2-amide in compound **90a** was the driving force for self-assembly. The gel formed by compound **90a** turned into solution upon treatment with a reductant $Na_2S_2O_4$. The nitrobenzyl group can be reductively cleaved, resulting in gel disassembly. Three different glycoconjugates **91–93** were synthesized by reacting Cbz-protected amino acids (Phe, Val, Leu) with glucosamine.[48] These glycoconjugates formed gels in several different solvents including water. The phenylalanine derivative **91** formed a robust transparent to opaque hydrogel upon aging at 17 mM, the critical gelation concentration (CGC). Spectroscopic methods were used to observe the nanofibers formed by twisted β-sheet secondary structures. The gel has non-cytotoxicity with self-healing properties. In a more recent study, glycopeptide **94** was synthesized by coupling Fmoc-diphenylalanine (Fmoc-FF) with glucosamine-6-sulfate (GlcN6S) using NHS and DCC as the coupling agents.[49] The glycopeptide formed supramolecular hydrogels either by a thermal (heating–cooling) method or by a solvent switch (from DMSO to water). Adding cations formed salt bridges with the sulfates of GlcN6S to promote assemblies. Additionally, the gel prepared from the thermal method with supplemental protein had more fibers with a higher density of cross-linking compared with the gel made from the solvent switch method, which was confirmed by AFM, fluorescence spectroscopy and CD analyses. They found that in comparison with non-glycosylated peptide, the glycopeptide system exhibited a better performance for cell culture and was compatible with growth factors. The glycosylation is crucial for the gels' biocompatibility and biofunctionality.

Pyrene derivatives **95** and **96** were prepared by refluxing 1-pyrenebutyryl hydrazide with D-gluconolactone and D-glucose, respectively (Fig. 7).[50] The pyrene group contributed to fluorescence and hydrophobicity whereas the gluconic acid unit was responsible for the hydrophilic properties. Compound **95** formed gels in both ethanol and water, but compound **96** did not form gels. The gelation of compound **95** in ethanol was faster than in water. The gel was used for analytical study of the alcohol contents of beverages. Gluconolactone was also used for the synthesis of several amphiphilic molecules **97** which contain two gluconolactone derivatives and tris-alkoxy groups linked *via* an L-lysine (Fig. 7).[51] The 3,4,5-tris(alkoxy) benzoic acid was coupled with ethylene diamine and the resulting compound was further reacted with L-lysine. The amino groups of the lysine were reacted with D-gluconolactone to afford the target compounds. The self-assembly properties of these compounds were analyzed in different solvents and biphasic solutions of chloroform and water. Compound **97a** was able to form fibrous networks in the biphasic system, which was used for dye removal experiments and exhibited the effective removal of tartrazine. In a recent study, several single-chain amphiphilic pyridine-based gluconolactone derivatives **98** were also reported (Fig. 7). These compounds formed gels at 15–21 mg mL^{-1} concentrations in ethanol water (v/v, 1/9) mixture and similarly in DMSO–water mixtures. The gels were prepared in syringes and utilized for the absorption of dyes.[52]

2.5 Sugar alcohol derivatives

Four D-glucamine derivatives containing stearoyl and glycine groups were synthesized and analyzed.[53] As shown in Fig. 8, these glucamides **99a–d** were able to form hydrogels effectively. The thixotropic properties of the hydrogels were tuned *via* the effect of the presence or absence of a methyl group on the amide function of the molecules, which affected the mole-

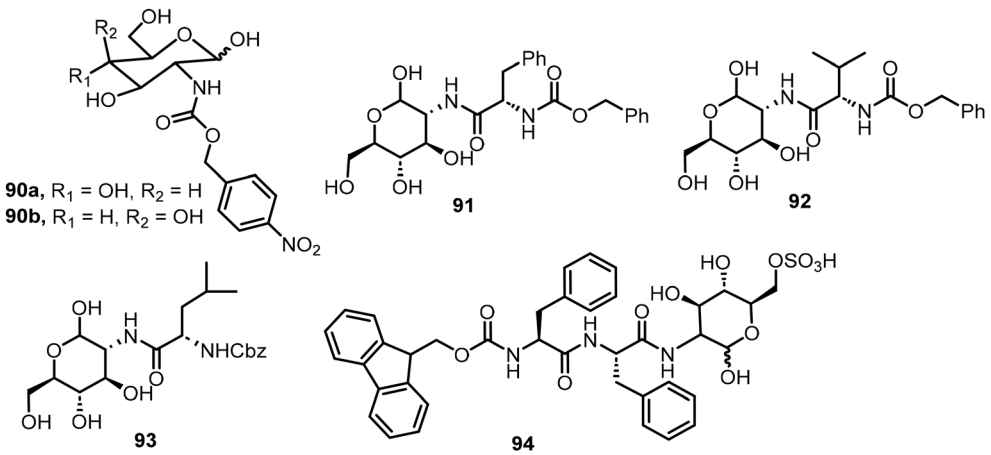

Fig. 6 Chemical structures of D-glucosamine-derived amide compounds **90–94**.

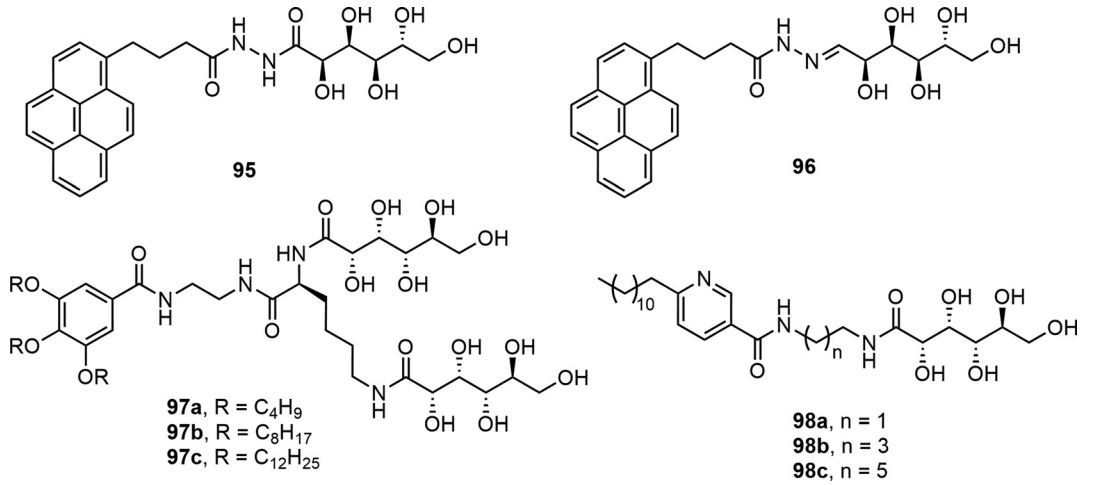

Fig. 7 Structures of pyrene derivatives **95–96** and gluconolactone-derived glycolipids **97–98**.

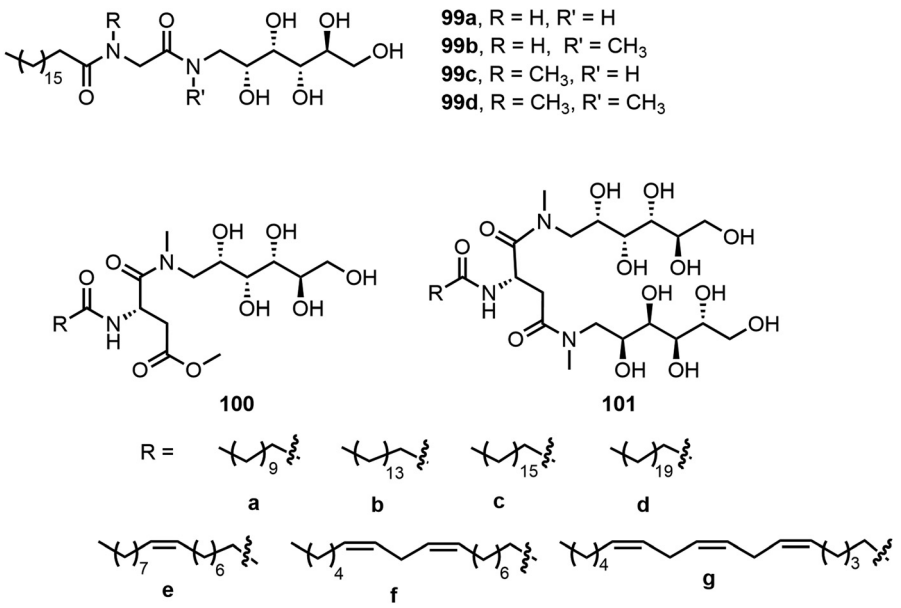

Fig. 8 Chemical structures of glucamine derivatives **99–101**.

cule's ability to form a hydrogen bond. *N*-Methyl-D-glucamine was also used for the preparation of self-assembling glycolipids by Nayak *et al.*[54–56] Two series of glycolipids which contain either mono or di *N*-methyl-D-glucamine moieties and different acyl chain lengths **100a–g** and **101a–g** were synthesized. Compounds with tails **a**, **b**, and **d** were analyzed in several solvents; **100a** and **101a–b** formed gels in hexanes, benzene, and other organic solvents. **101d** formed emulsions in these organic solvents and was soluble in water. Compounds **100b** and **100c** formed hydrogels and the hydrogels formed by **100b** were injectable and have thixotropic properties.[55] Glycolipids with different degrees of unsaturation were prepared to analyze the impact of unsaturation in the tail groups toward molecular self-assembly.[54] They have demonstrated that the increased unsaturation is correlated to enhanced critical micelle concentration (CMC) values. The lipids with one double bond (**100e** and **101e**) were deemed more suitable for loading hydrophobic drugs and solubilization. The glycolipids with di-unsaturated lipid tails (**100f** and **101f**) were more suitable for foamability and wettability. The team later on studied the gelation properties of gold nanocomposite gels formed by the glycolipid gelator **100e** with $HAuCl_4$.[56] Compound **100e** was analyzed with gold solutions of different concentrations and the maximum loading of gold without disturbing gelation was 57.60 mg g^{-1} (gold : gelator).

Smith *et al.* have studied the properties of pH-responsive gelators, the carboxylic acid of 1,3:2,4-dibenzylidenesorbitol **102** (DBS-COOH) and **103** (DBS-$CONHNH_2$) (Fig. 9).[57–59] The spatial and temporal diffusion of the resulting gels were characterized and applications of the gels for various organic reactions were

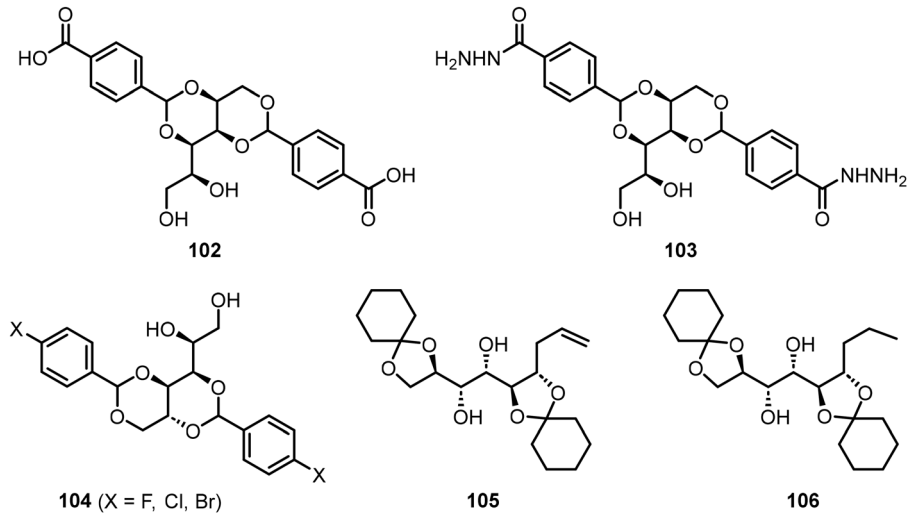

Fig. 9 Structures of dibenzylidene sorbitol derivatives **102–104** and mannitol derivatives **105–106**.

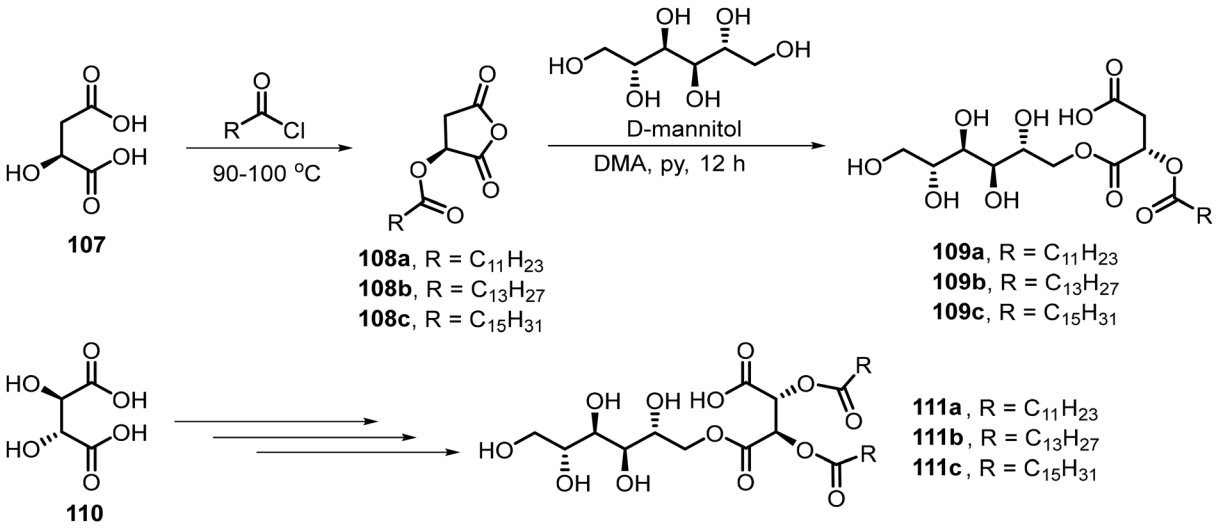

Scheme 16 Preparation of mannitol derivatives **109a–c** and **111a–c**.

studied. For instance, gelator **103** has been applied in the fabrication of gel beads which were used to catalyze the Suzuki–Miyura reaction.[58] Fan *et al.*[60] prepared supramolecular eutectogels utilizing halogenated dibenzylidene sorbitol derivatives **104** (X-DBS) and deep eutectic solvents (DESs). The gelators **104** were used to form gels with a mixture of choline chloride and alcohols or ureas. The resulting gels possessed self-healing properties and high conductivity. Two cyclohexanone acetal-protected mannose derivatives **105** and **106** were also shown to exhibit gelation properties in hexanes and related alkanes.[61] Two of the compounds were found to be capable of selective gelation of hydrocarbon solvents. The terminal alkene functionality allows for further chemical modification, and thus, further customization of the gelation properties.

Singh *et al.* synthesized a series of six amphiphilic D-mannitol derivatives **109a–c** and **111a–c** with various lengths of aliphatic chains linked through tartaric acid or malic acid (Scheme 16).[62] Most of the derivatives in the library were found to act as surfactants with low CMC and formed hydrogels. As shown in Scheme 16, among the six long chain esters except **109a**, five compounds formed stable hydrogels. Longer aliphatic chains led to increased thermal stability in the same series. The hydrogel formed by **111c** was used to stabilize silver nanoparticles (Ag NPs).

3. Disaccharide derivatives

A series of amphiphilic lactose derivatives containing urea-linked aliphatic chains were reported as LMWGs.[63] The gelation properties were tuned *via* the length of the aliphatic chain. As shown in Scheme 17, lactose urea derivatives **115**

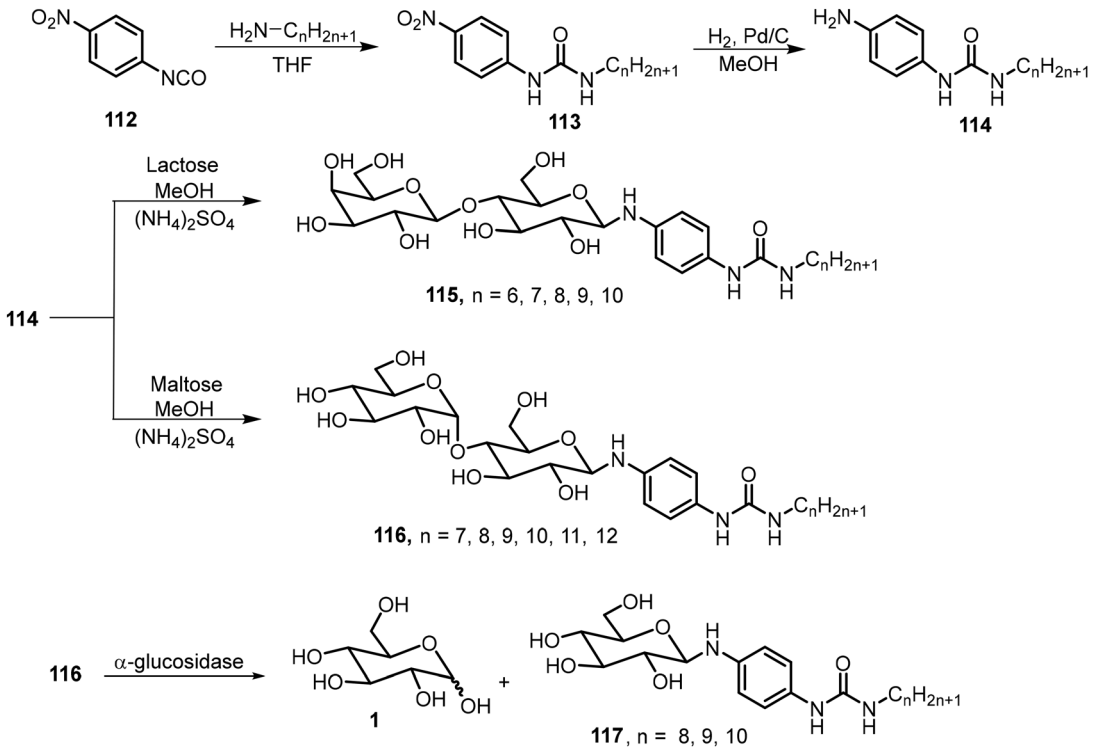

Scheme 17 Synthesis of lactose or maltose *N*-arylglycosides **115** and **116**.

were synthesized and tested. The derivatives with n = 6, 7, 8, and 9 were gelators, with MGCs of 2.0, 1.8, 1.2 and 0.9 mM respectively. The decyl derivative was insoluble in water. The gel-to-sol transition was controlled using β-galactosidase, which cleaves the lactose to form the corresponding glucose urea derivatives. The same team also synthesized mannose derivatives **116** (n = 7–12), and the alkyl chains with greater than eight carbons were found to be effective hydrogelators too.[64] The gels were found to undergo a gel–sol transition in the presence of α-glucosidase due to the hydrolysis of maltose and the formation of the glucose derivatives **117**.

A pyrene-based lactose derivative (PyLac) was prepared by refluxing 4-(pyren-1-yl) butanehydrazide **120** with lactose in methanol and chloroform.[65] The pyrene-appended lactose derivative **121** formed a fluorescent hydrogel, while the mannose derivative **122** was not a hydrogelator (Scheme 18). Using variable temperature CD experiments, the self-assembled structures were predicted to form a bilayer structure with the pyrene π–π stacking in the middle and the polar lactose at the exterior of the vesicle. The terminal galactose residue of **121** was able to bind to cholera toxin, and therefore the system was used for chlolera toxin's fluorescence sensing. In another study, the gelator **121** formed thermo-responsive hydrogels which were utilized for the sustained delivery of the anticancer drugs mitoxantrone and doxorubicin.[66] At physiological pH, the drug release amount from drug-loaded hydrogels was much higher at 37 °C than the release rate at 25 °C. The elevated temperature caused the disruption of the self-assembled networks and allowed the entrapped drug molecules to be released more rapidly.

Wang *et al.* synthesized thioglycolipids **125** and **126** from lactose and cellobiose with three alkyl thiols (Scheme 19).[67] The lactose derivatives **125** formed stable gels and the thiocellobiosides **126** formed metastable gels which precipitated over time. The thiolactoside hydrogels have thixotropic properties. The phase transitions of the gels were analyzed *via* fluorescence spectroscopy using a polarity sensitive fluorophore Prodan.

Yao *et al.* used Knoevenagel condensation to synthesize amphiphilic β-*C*-glycosyl barbiturates from unprotected glucose and maltose.[68] As indicated in Scheme 20, the Knoevenagel condensation of *N*-substituted barbiturates **128** with glucose or maltose directly afforded the corresponding β-*C*-glycosylbarbiturates **129a–d** or **130a–d**. They found that while the glucose derivatives **129a–d** were insoluble in water, the maltose derivatives **130a–d** were fully soluble in water upon heating. Upon lowering the pH or the addition of a divalent metal salt such as $CaCl_2$, **130c** and **130d** formed hydrogels at 2–5% MGC, and the gelators formed fibrous networks. *N*,*N*-Disubstituted β-*C*-glycosylbarbiturates **131a–d** were also prepared similarly, and compounds **131b** and **131c** formed vesicle hydrogels after two heating and cooling cycles due to the lower water solubility. These compounds were found to self-assemble into percolating multilamellar vesicles and connected vesicles, which further formed vesicle hydrogels. While for the monoalkylated urea derivatives, hydrogelation only occurred

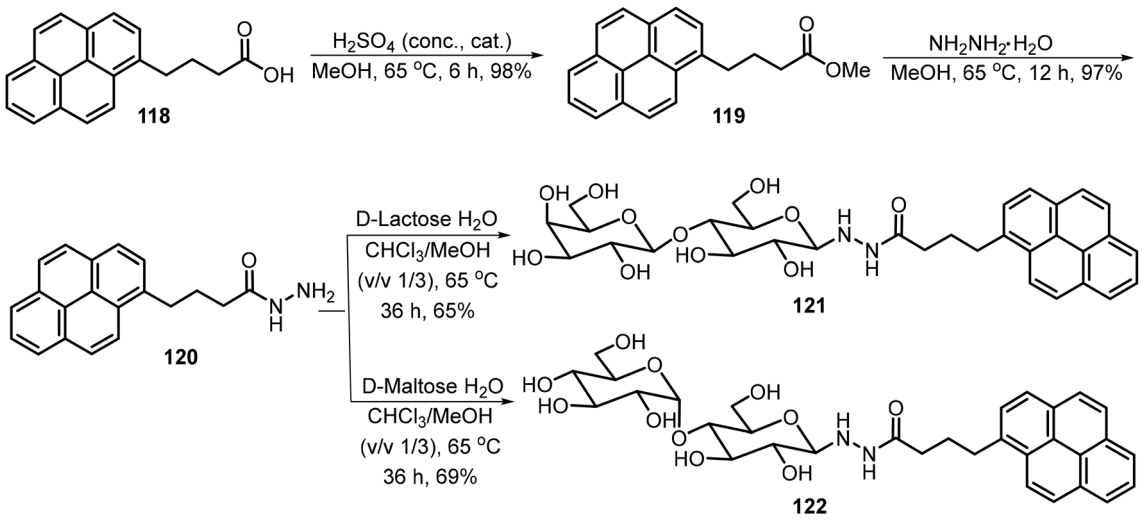

Scheme 18 Synthesis of lactose *N*-glycoside **121** and maltose glycoside **122**.

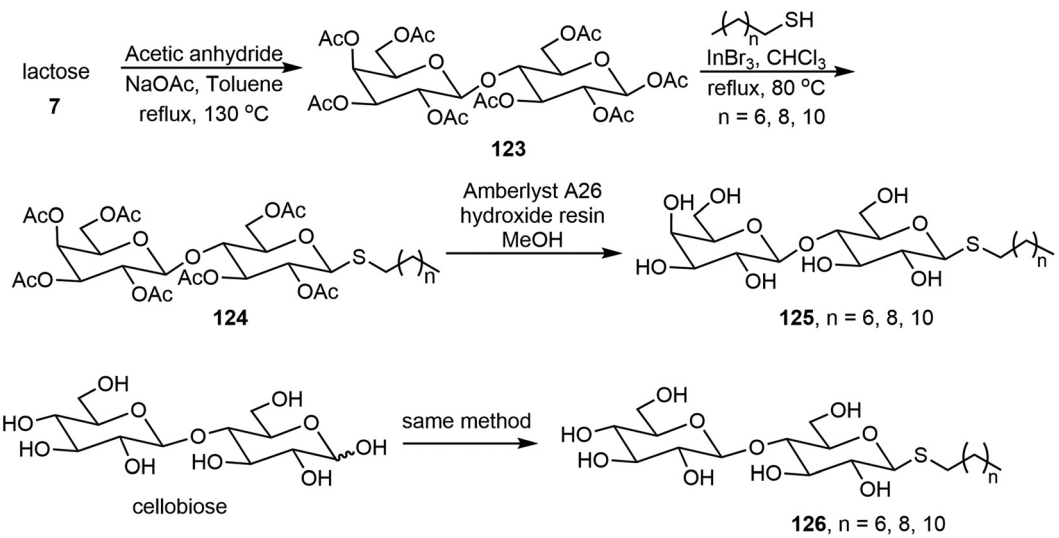

Scheme 19 Synthesis of thioglycolipids **125** and **126**.

under strongly acidic conditions or by adding metal ions at neutral conditions, under these conditions, the *N*-substituted maltosyl barbiturates **130** exist predominantly in the keto form. It was hypothesized that the keto forms would be able to self-assemble and form hydrogels. Therefore, they further modified the glycosylbarbiturate structures by oxidation using H_2O_2 to enable the compounds to adopt a fixed keto form to give **132** and **133**,[69] which were expected to enhance hydrogelation. The hydroxylated glucose and maltose derivatives were obtained in 54–72% yields, and these compounds were found to be more effective hydrogelators. The glucosyl derivatives **132b–d** and maltosyl derivatives **133c–d** formed stable hydrogels at neutral conditions.

Seeberger and Delbianco *et al.* have synthesized a series of disaccharides with different degrees of protection and studied their self-assembling properties (Fig. 10).[70,71] These disaccharides were prepared in both the **135DD** and **135LL** enantiomers, and interestingly, the disaccharides formed self-assembled helices that are relevant to their structures. It was found that the local crystal organization dictated the supramolecular morphology. The **135DD** isomer formed left-handed helices and **135LL** formed right-handed helices; however, the racemic mixture of **135DD** and **135LL** did not form helices; only planar sheets were observed. The synthesis of the disaccharides with the **135DD** configuration was carried out by a standard glycosylation reaction. The preparation of the enantiomer **135LL** is shown in Scheme 21 starting from the corresponding L sugar derivatives **141** and **142**.

The D-glucose-based disaccharide **135DD** formed highly crystalline twisted fibers. Systematic chemical modifications of **135DD** can provide important information responsible for the supramolecular assembly.[72] Substituting the hydroxyl group at

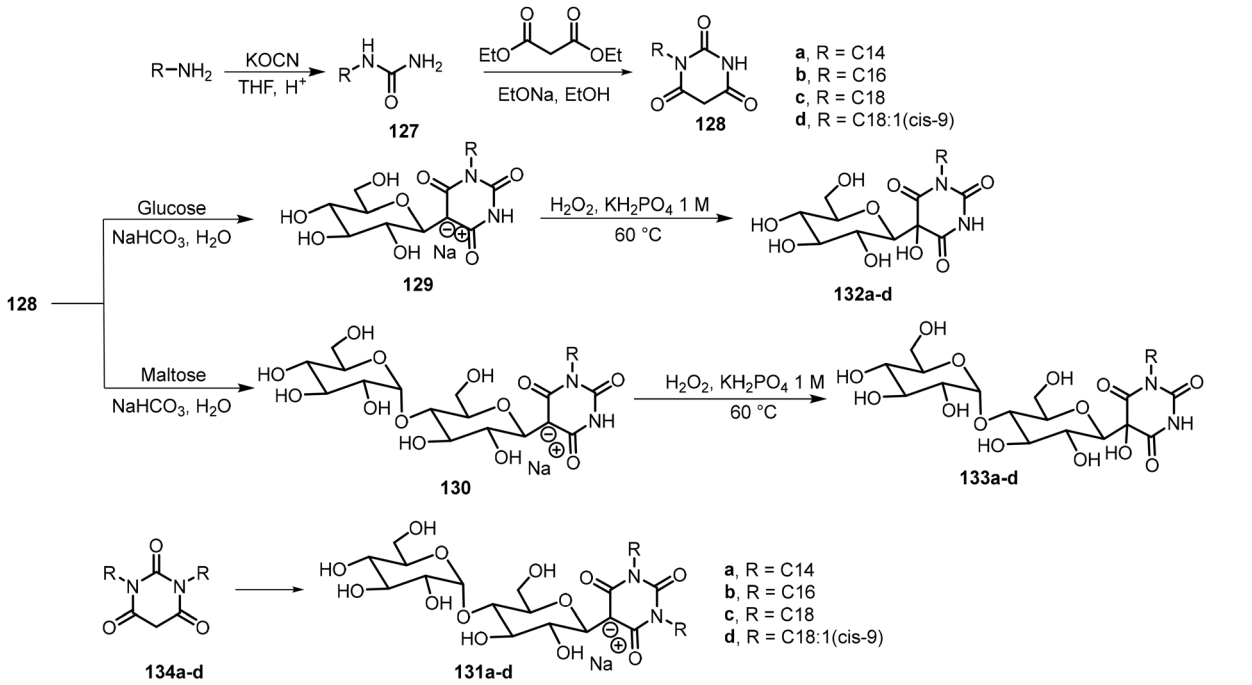

Scheme 20 Synthesis of β-*C*-glycosylbarbiturate derivatives **131–133**.

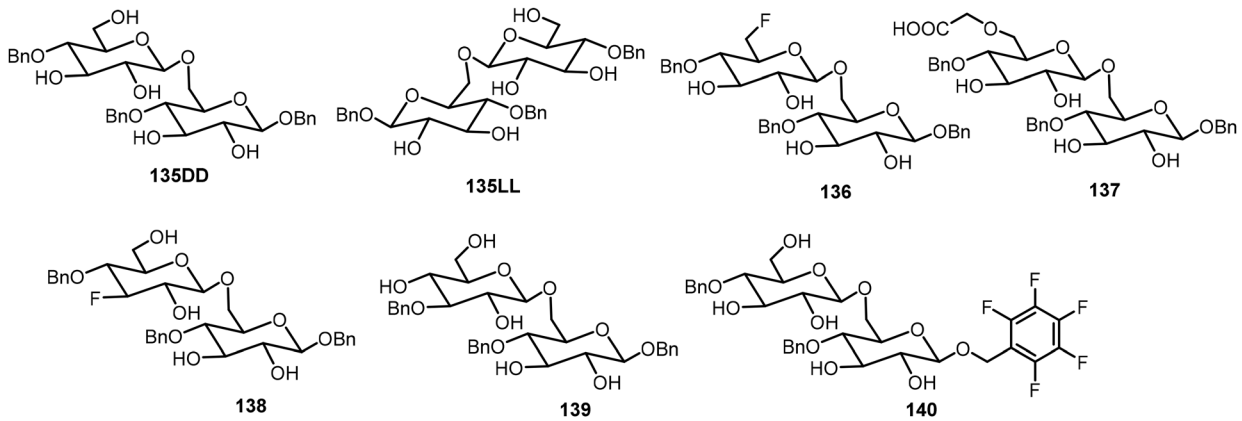

Fig. 10 Chemical structures of disaccharides **135DD**, **135LL** and **136–140**.

C-6 position with F (**136**) or –OCH_2COOH (**137**) preserved the self-assembly properties, while substitutions of the hydroxyl group at the C-3 position (**138** and **139**) or OBn group at the aromatic position with pentafluorobenzene group (**140**) disturbed the assembly. Structural modifications of **135DD** produced new geometries, such as hollow tubular structures, spherical colloidal particles, as well as highly twisted fibers/ribbons as characterized by electron tomography and electron diffraction. The disaccharide **137** was synthesized *via* glycosylation reaction of monosaccharides **143** and **144** as shown in Scheme 21.

In another study, the disaccharide trehalose **145** was functionalized *via* regioselective transesterification using Novozym 435 (Scheme 22).[73] Trehalose ester derivatives **147** at the primary hydroxyl groups with various length aliphatic chains (C3–C11) were synthesized. These derivatives formed organogels in ethyl acetate and oleogels in olive oil, canola oil, and grapeseed oil. The eight-carbon and ten-carbon fatty acid derivatives were found to be supergelators with MGC at <0.2 wt%. Powder X-ray diffraction (PXRD) studies identified the molecular assembly patterns of the gelators, and compound **147d** formed monophasic hexagonal columnar packing patterns. The trehalose lipids were used for the preparation of wax-free lip balms and may be useful for cosmetics.

Zhao *et al.* studied the gelation properties of a naturally occurring compound, glycyrrhizic acid **148** (Fig. 11).[74,75] They found that it formed hydrogels at 37 °C in a phosphate buffer solution and the gels can be injectable. The gel was found to

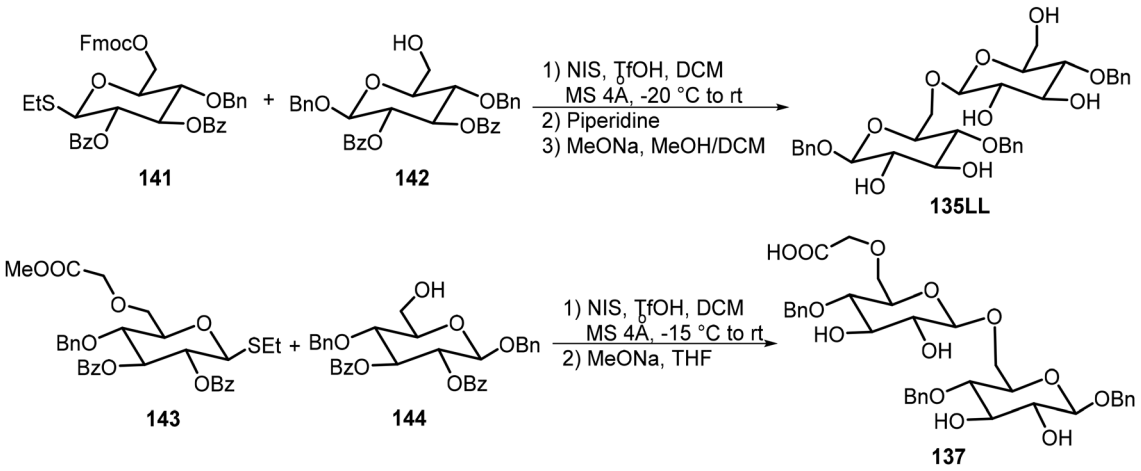

Scheme 21 Synthesis of disaccharide **135LL** and **137**.

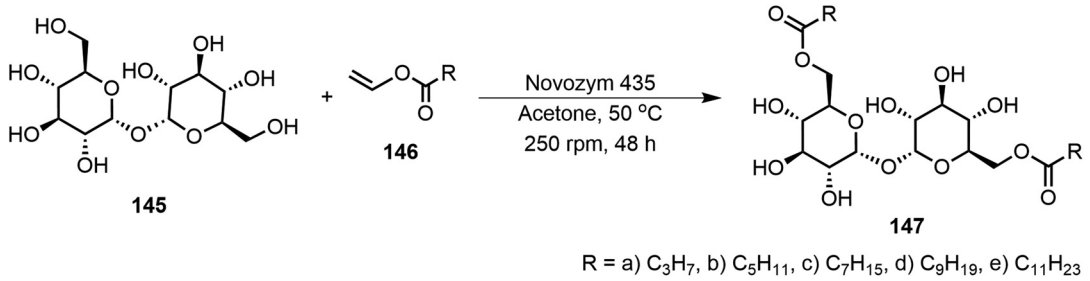

Scheme 22 Preparation of trehalose lipids **147**.

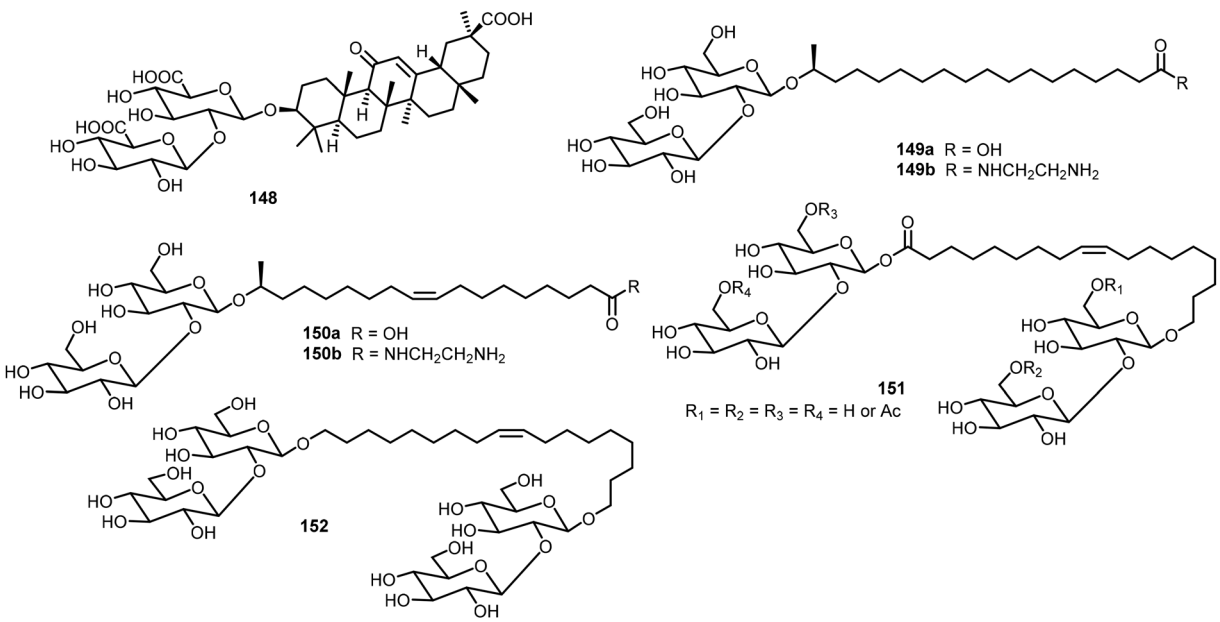

Fig. 11 Structures of natural product-based glycolipid **148** and sophorolipids **149–152**.

have good biocompatibility and possess inherent antibacterial activity. Baccile's group studied the self-assembling properties of sophorolipid derivatives **149–152** systematically, and these glycolipids were isolated from microbial sources.[76–78] The fatty acid formed different assemblies in the neutral and charged forms.[78] The acids can be further derivatized with amines to

form amides.[76] Several sophorolipids were found to be able to form hydrogels and metallogels. These biobased surfactants have also been reviewed recently.[79,80]

4. Glycoconjugates or branched systems

In this section, we review the recent literature on dimeric, trimeric, and multiple branched systems, and a majority of these systems employed click chemistry for the synthesis of glycoconjugates.

Scheme 23 shows the synthesis of two bisurea amphiphiles of sugar derivatives **156** and **157**.[81] These compounds were synthesized from either lactobionic acid **153** or maltobionic acid. The reaction of intermediate lactobiono-δ-lactone **154** with a diamine afforded the monoamine derivative **155**, which was further reacted with a diisocyanate to afford the corresponding bisurea **156**. The maltobionic derivative **157** was synthesized by the same method. The two sugar derivatives self-assembled and formed fibers and bundles which further formed hydrogels that can mimic ECMs.

El Hamoui *et al.* have synthesized glyconucleo-bola-amphiphiles (GNBs) linked through amide, urea, and carbamate functions and studied their self-assembling hydrogelation properties.[82,83] Some of these glyconucleoside-based LMWGs **158–159** are shown in Fig. 12. These hydrogelators were synthesized using a click reaction from the corresponding glycosyl

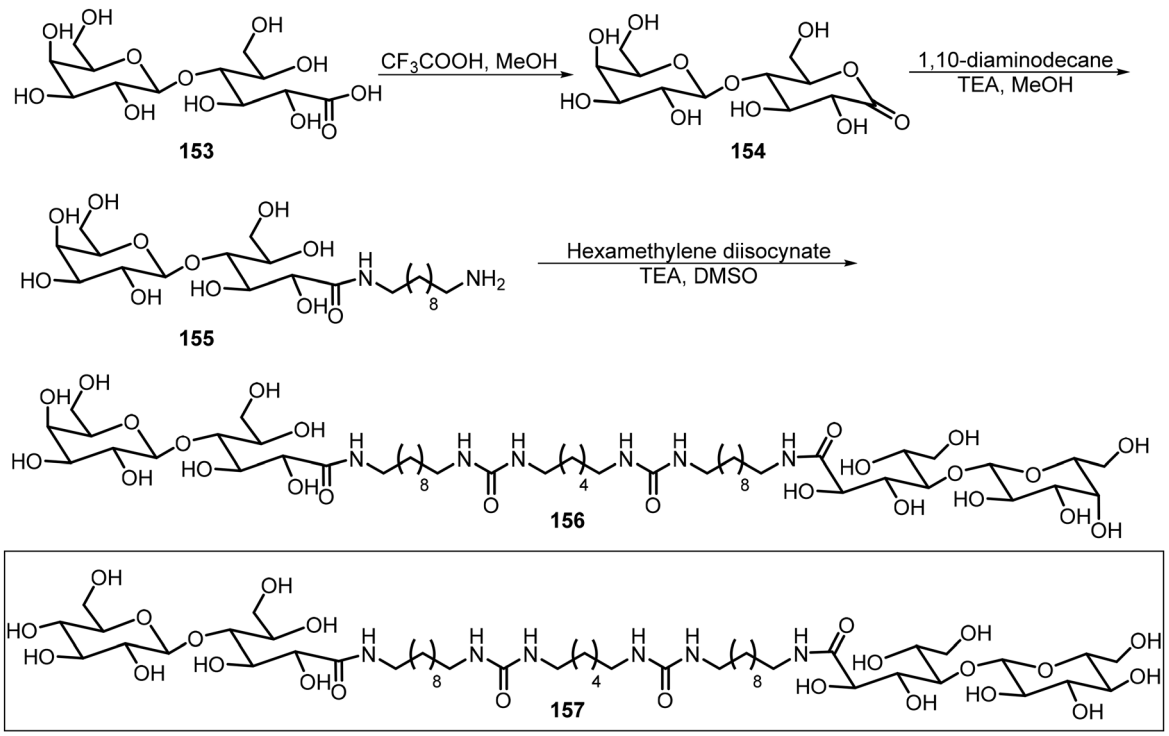

Scheme 23 Synthesis of bolaamphiphiles **156** and **157**.

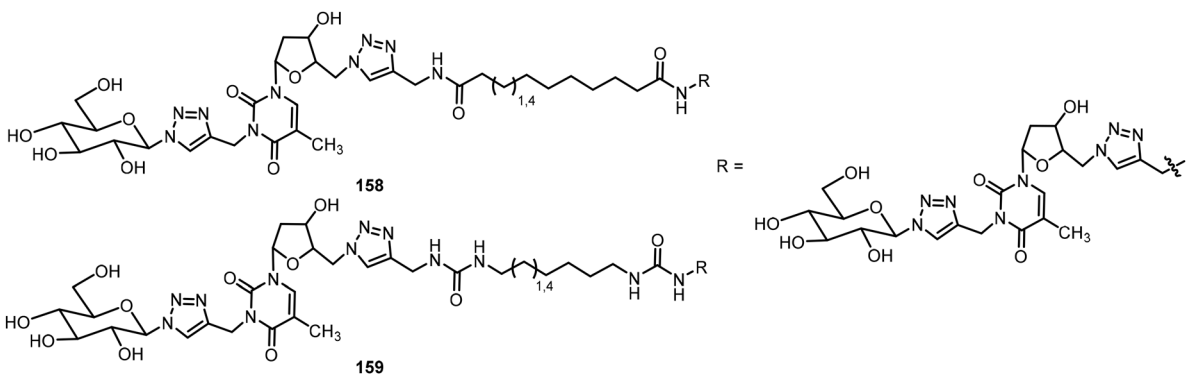

Fig. 12 Chemical structure of amide-linked GNB **158** and urea-linked GNB **159**.

azide and propargylated nucleoside. More recently, an *O*-nitrobenzyl group was attached to the nucleoside to prepare the glyconucleo-bola-amphiphile amide (GNBA) linked photocleavable gelator **164**.[84] The synthesis of **164** is shown in Scheme 24. A click reaction of *N*-propargyl thymidine with β-1-azido hepta-*O*-acetyl-β-D-lactopyranose afforded the intermediate **160**, which was converted to the azide derivative **161**. Methylthiomethylation at the 3′ position followed by introducing the nitrophenyl unit and removal of acetyl groups on the lactose unit afforded **163**. A second click reaction with the bisurea bisalkyne led to the formation of the nitrophenyl functionalized GNBA **164**. Compound **164** formed a hydrogel with enhanced stiffness. Upon cleavage of the nitrophenyl group, the resulting hydrogel became softer.

Meijer's group designed and synthesized four benzene-1,3,5-tricarboxamide (BTA) derivatives **167a–c** and **168** which contain sugars at the periphery and further studied their biomaterial applications.[85,86] The synthesis is shown in Scheme 25.

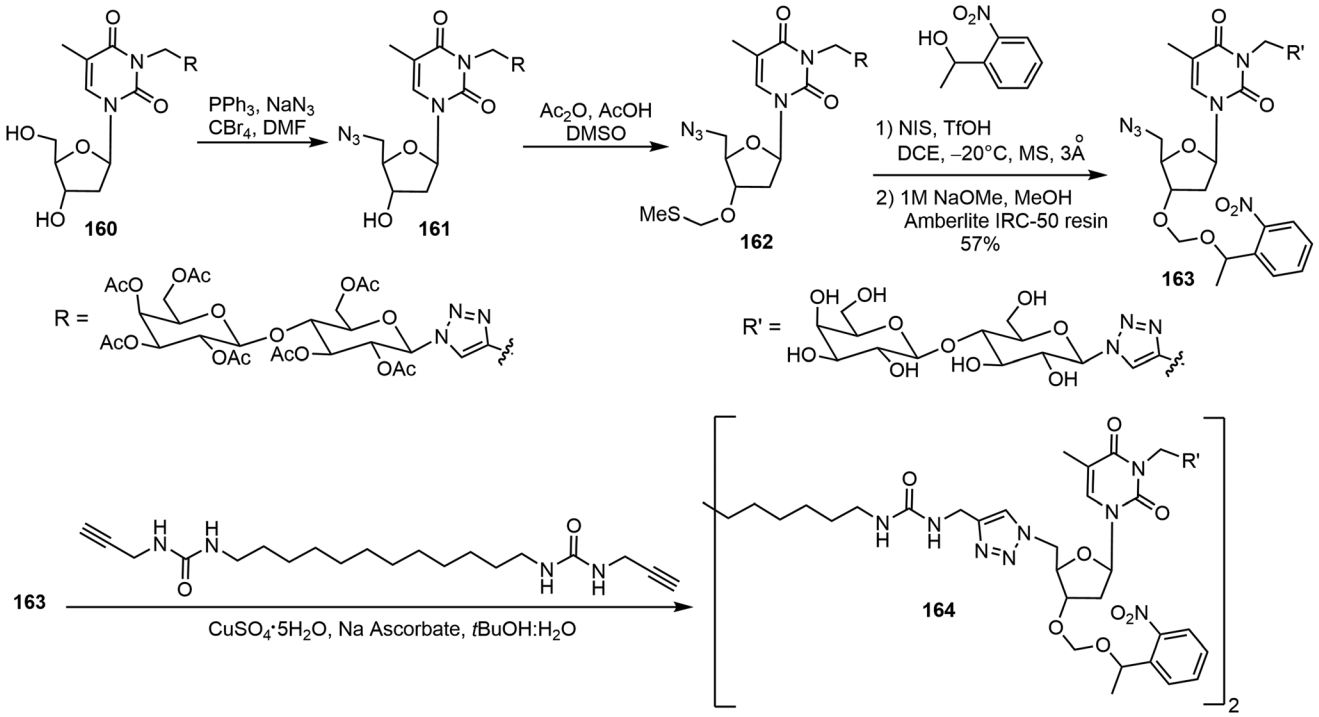

Scheme 24 Synthesis of nitrophenyl-protected GNBA derivative **164**.

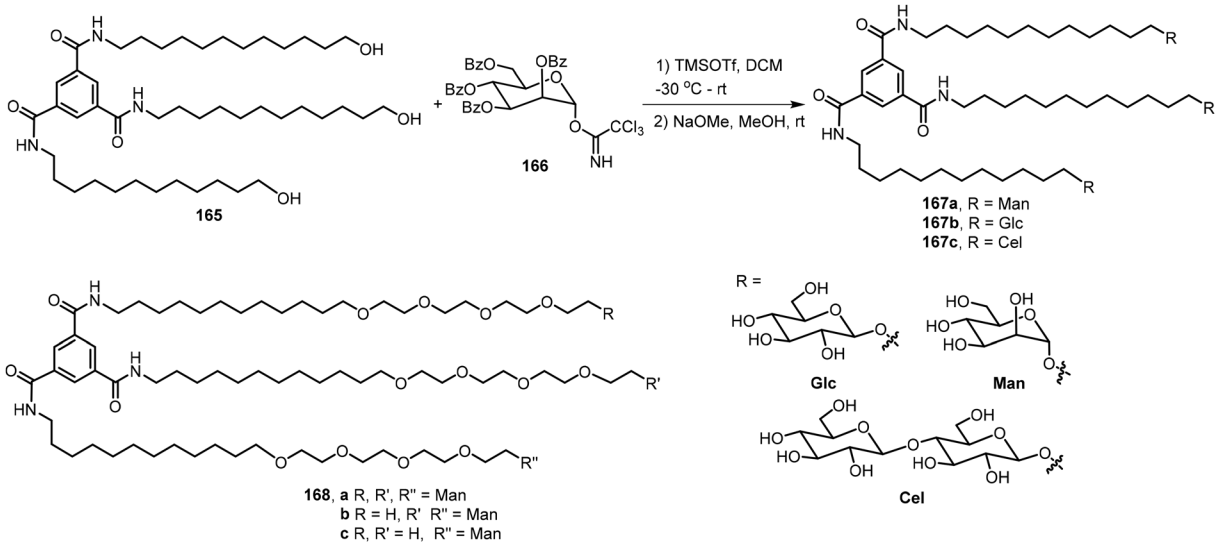

Scheme 25 Synthesis of trimeric branched glycoclusters **167a–c** and **168**.

Glycosylation of the BTA-derived trimeric alcohol **165** with corresponding protected sugar imidates followed by deprotection afforded the BTA derivatives **167**. An example using the mannose derivative **166** is included, and the product **167a** was obtained. Other derivatives with glucose and cellobiose at the periphery, BTA-Glc **167b** and BTA-Cel **167c**, and a derivative with tetraethyleneglycol (TEG) linked mannose BTA-TEG-Man **168** were synthesized by similar methods. These trimeric branched glycosides exhibited different morphologies. Cryo-TEM images indicated that the glucose and mannose derivatives **167a–b** formed fibrous networks, but the cellobiose derivative **167c** and compound **168a** formed micellar morphologies. They concluded that the trimer **167a** and **167b** self-assembled and formed 1D supramolecular polymers. Co-assembly of the compounds formed supramolecular polymers which resulted in very soft hydrogels. Rijns *et al.* synthesized and analyzed the self-assembling properties of three 1,3,5-tricarboxamide (BTA-TEG) derivatives containing one to three mannose moieties **168a–c**.[87] Derivatives containing one and two mannose groups **168b–c** were found to be able to form hydrogels.

Wang's group designed, synthesized, and characterized a series of glycoconjugates *via* a click reaction of various trimeric, tetrameric, and hexameric alkynes with glycosyl azides (Scheme 26).[88–90] Using pentaerythritol alkyne as the core structure, click reactions with azido sugars afforded a library of glycoclusters with different degrees of conjugation. The monomeric and dimeric glycosyl triazole derivatives tend to be soluble in most of the organic solvents tested, but compounds with three and four branches of sugar triazole units were found to be effective gelators for water and organic solvents.[89] The glycoclusters were expanded systematically into a series of seventeen glycoconjugates of three to six arms using eight different branched alkynes as the building blocks, **A1** and **A2** are inlcuded in Scheme 26. The self-assembling properties of these novel molecules and their catalytic activity as ligands in copper-catalyzed azide and alkyne cycloaddition (CuAAC) reactions were characterized.[88] The glycoconjugates containing six branches showed significant catalytic activities for CuAAC reactions. In an aqueous ethanol mixture, 1.0 mol% of six-armed glycocluster **171a** was able to accelerate the click reaction of **169b** with phenylacetylene significantly. Moreover, the co-gels formed by trimer **172** and hexamer **171a** together with $CuSO_4$ were able to form stable gels inside a column as the reaction matrix. The gel columns were used to catalyze click reactions and were reused for several cycles. The formation of triazoles using azide and alkynes, as well as the formation of isoxazoles using choroximes and alkynes, were demonstrated. These glycoconjugates can be used as supramolecular catalysts to efficiently catalyze click reactions in a flow-chemistry fashion. In a related study, eight trimeric glycoclusters from different sugar azides were prepared and analyzed.[90] The resulting glycoclusters formed different SA structures depending on the

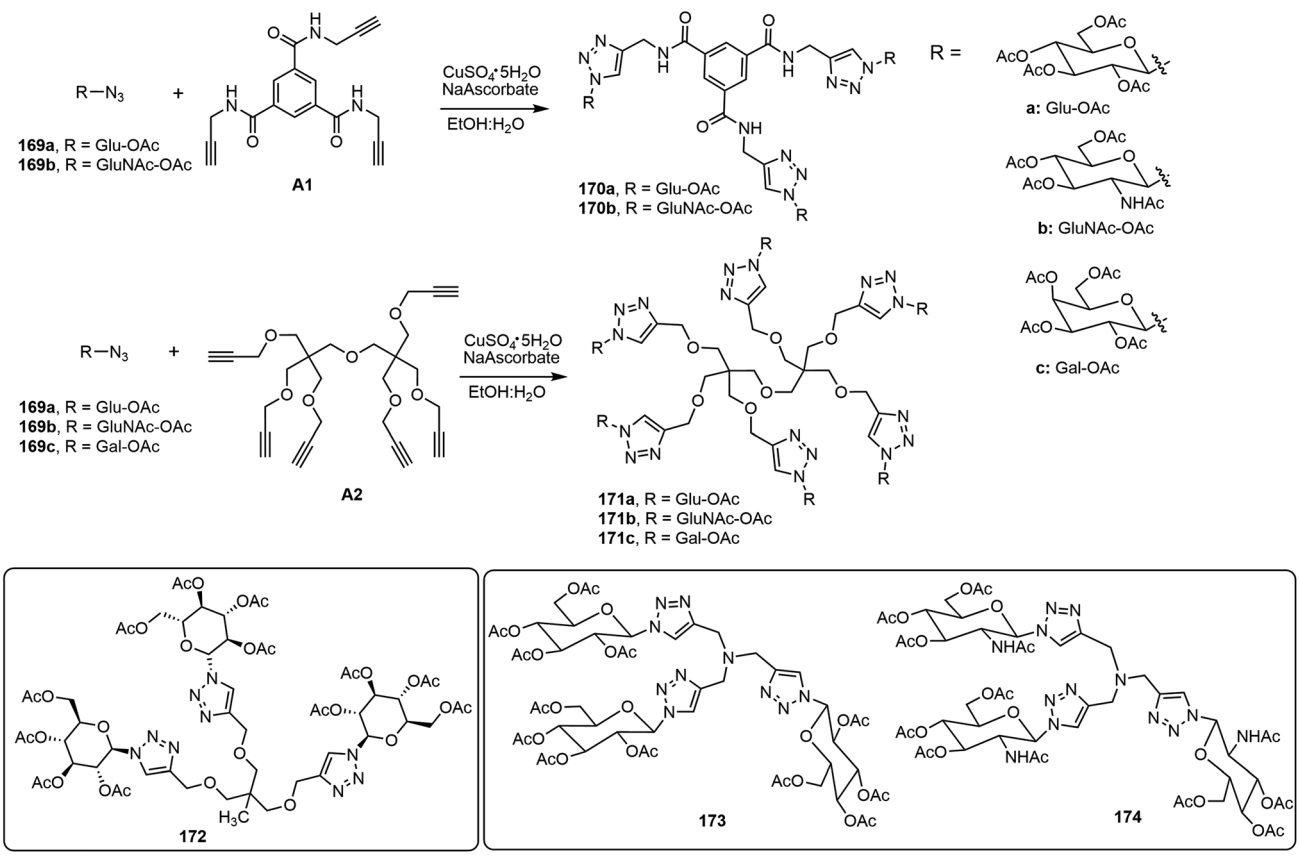

Scheme 26 Chemical structures of glycoclusters **170–174** synthesized using click chemistry.

sugar structures. Galactose and maltose derivatives did not form hydrogels. The glucose and glucosamine derivatives **173** and **174** both are effective LMWGs. Compound **173** was also able to form stable co-gels with $CuSO_4$ in gel columns and was used for running flow-like click reactions.

Percec *et al.* have synthesized several series of glycodendrimersomes *via* thiourea formation and click reactions and analyzed their self-assembling properties.[91–93] Janus glycodendrimers (JGDs) were synthesized *via* isothiocyanate-functionalized pentaerythritol derivatives and with amine-functionalized sugar derivatives (Scheme 27).[91] Different oligosaccharides were synthesized first and a pentyl amino linker was attached to the anomeric position with either alpha or beta stereochemistry. The oligosaccharides were synthesized *via* an automated glycan assembly (AGA) method. An example using a disaccharide is shown in Scheme 27. Lactose pentaacetate **123** was converted to intermediate **175**, followed by glycosylation and deprotection to afford the sugar amine **177**. The Janus glycodendrimers (JGDs) **178** and **179** were prepared *via* isothiocyanate and amine reactions which formed thiourea linkages. These JGDs formed self-assembled vesicles that exhibited lamellar structures with the glycans on the outer surface. Glycodendrimersomes formed by the self-assembly of JGDs exhibited lamellar nanovesicles. The thiourea in the glycoclusters contributed to the molecular assembly. Compound **180** formed a lamellar assembly morphology as indicated by AFM spectroscopy. These glycoclusters were synthesized *via* a method that resembles the CuAAC reaction in a "click" manner. Another series of GDS formed by JGDs and their formation of membrane-mimicking vesicles was also reported (Scheme 27).[92] These Janus glycoclusters were synthesized using azido alkyl sugars *via* click chemistry. The self-assembled vesicles of the JGDs with different sugar units at the periphery **180a–c** exhibited similar types of lamellar morphology, despite the sugar structures. However, the sugar structures did influence the thickness of the bilayers formed.

Murphy *et al.* synthesized three amphiphilic sulfate-substituted galactose-containing glycodendrimersomes and analyzed their interactions with galectins.[93] The synthesis of the clickable headgroup is shown in Schemes 28 and 29. The JGD-sulfatide **186a** and **186b** and sulfatide lactose headgroup JGD derivative **191** all contain 3-sulfate groups at the terminal sugar moiety, the presence of which is important for molecular assemblies and the interactions with lectins.

Mullerova *et al.* reported the preparation of carbosilane-based glycodendrimers and their application for anticancer drug delivery.[94] Different sugar azides were used for the synthesis of the glycoconjugates by click chemistry. In another study, a series of branched phenyl-cored block-*co*-oligomers (BCOs) **192** and **193** composed of maltooligosaccharides with 1-4 glucose units (**A**) as the hydrophilic component and solanesol (**B**) as the hydrophobic component were synthesized *via*

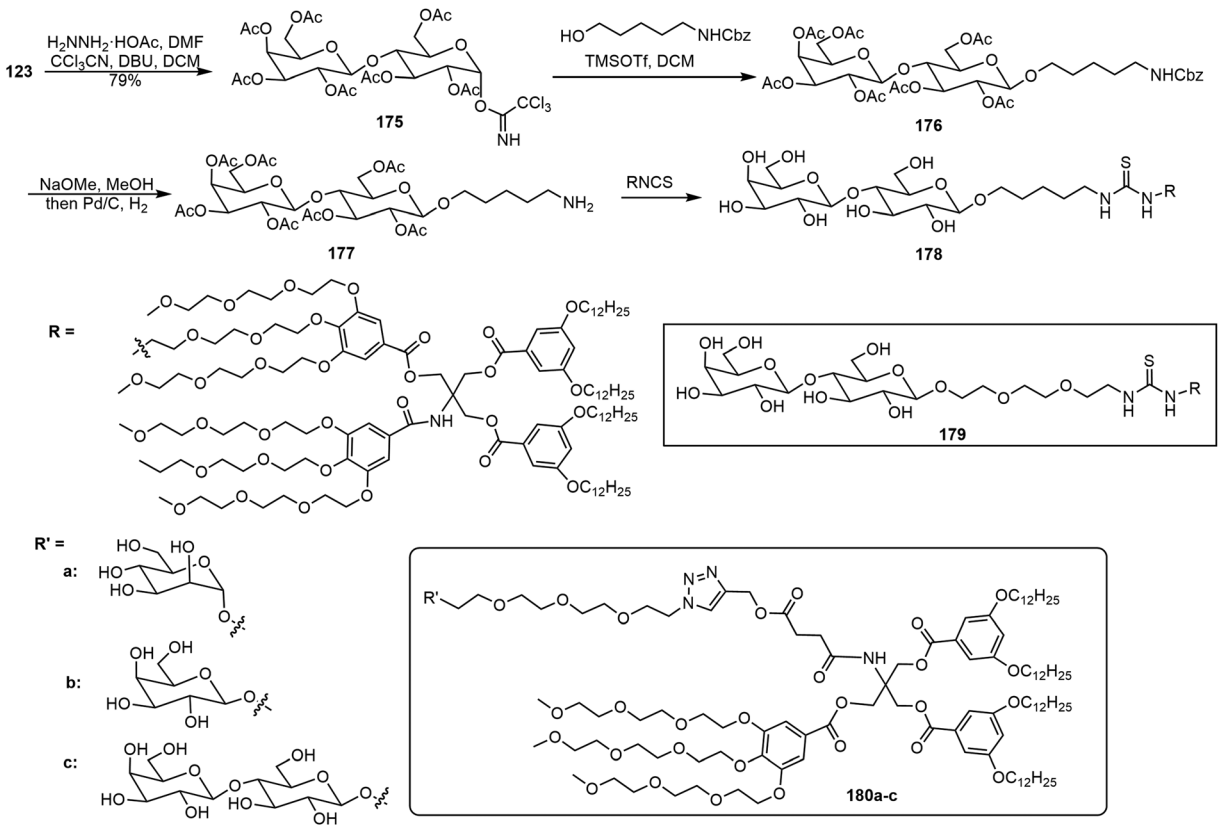

Scheme 27 Synthesis of Janus glycodendrimer **178** and chemical structures of Janus glycodendrimers **179–180**.

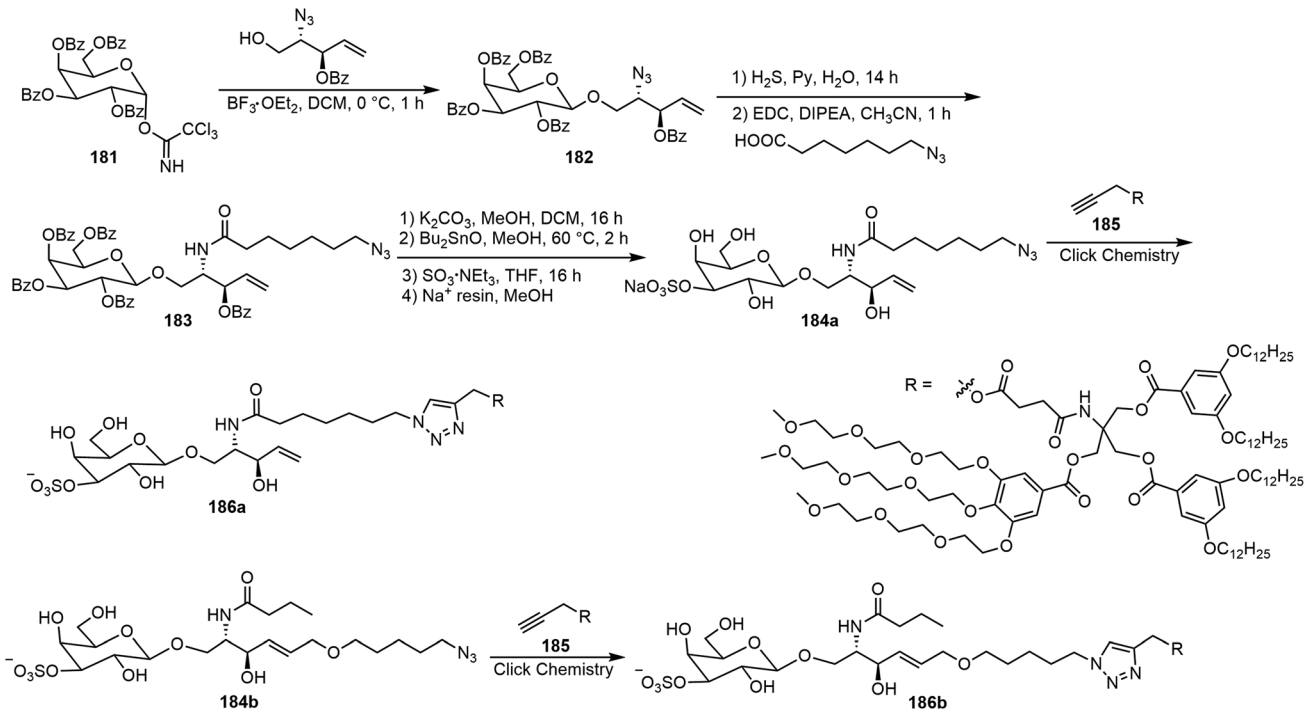

Scheme 28 Synthesis of sulfate-substituted galactose-containing glycodendrimersomes **186**.

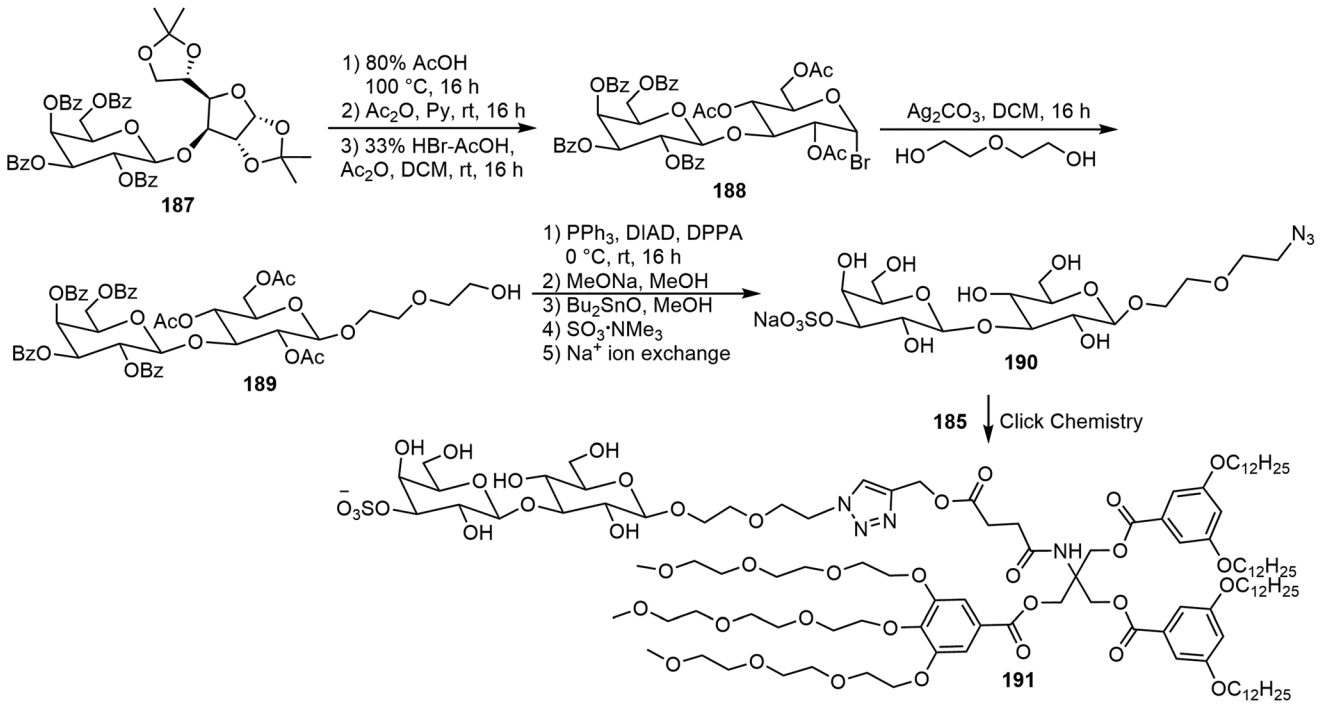

Scheme 29 Synthesis of sulfate-substituted lactose-containing glycodendrimersome **191**.

click chemistry (Fig. 13).[95] Besides these $\mathbf{A_2B}$, $\mathbf{AB_2}$ systems, several other $\mathbf{A_2B_2}$ systems were synthesized and studied. These BCOs self-assembled and formed different morphologies including lamellar, cylindrical, and spherical morphologies as well as double gyroid, *etc*.

Dong *et al.* have synthesized a series of tetraphenylethylene (TPE)-based glycoclusters and studied the self-assembling properties and fluorescence properties.[96,97] As shown in Fig. 14, water-soluble glyco-dots formed by TPE-based glycoclusters and dicyanomethylene-4*H*-pyran (DM) fluorescent probes (**194**)

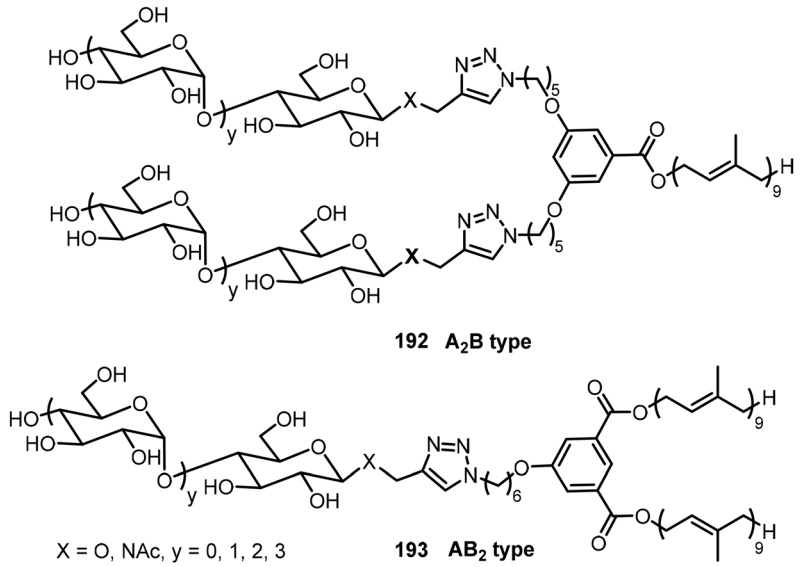

Fig. 13 Structures of phenyl-cored glycoclusters **192** (A_2B type) and **193** (AB_2 type).

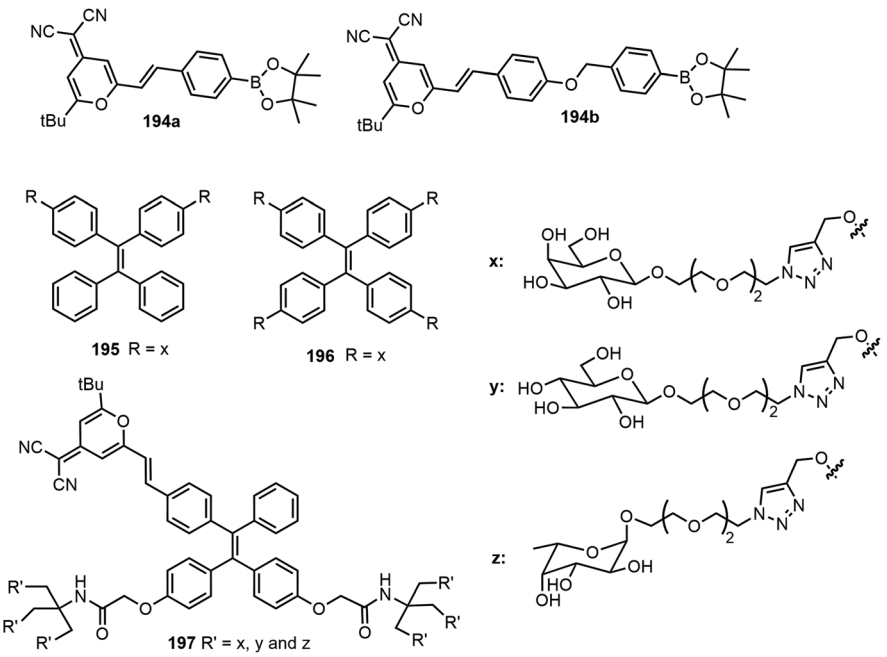

Fig. 14 Structures of fluorescent probes **194** and TPE-cored glycoclusters **195–197**.

were shown to enhance peroxynitrite sensing.[96] To take advantage of the multiple hydroxyl groups in the sugar moiety, the water-soluble TPE-cored glycoclusters were prepared from a propargylated TPE core and azido glycoside *via* click chemistry. When forming glycol dots with DM probes, among the synthesized glycoclusters, the galactose-appended tetrameric compound **196** exhibited a better sensitivity for peroxynitrite sensing in pure PBS buffer compared with the bivalent system using glycocluster **195.** The team also reported the AIE-based glycoclusters **197** as efficient fluorogenic glycosidase probes.[97] Hexavalent glycoclusters composed of a TPE core conjugated with a DM were found to be an optimal structural motif for glycosidase sensing through AIE. Structurally diverse glycoclusters with different sugars (D-galactose, D-glucose, and L-fructose) in the periphery were synthesized using click chemistry, by coupling an alkynylated TPE-DM core and various glycoside azides. Enzymatic hydrolysis of the glycoclusters by the corresponding glycosidases in water as well as within the cell produced significantly enhanced and stable fluorescence due to the formation of amphiphilic AIE-based aggregates.

BODIPY dyes have a common structure of BF_2 groups joined to a dipyrromethene group. 4,4-Difluoro-4-bora-3a,4a-*S*-indacene represents a large family of fluorophores. Various glycoBODIPY systems have been developed in recent years, and the synthesis and applications of these systems have been an intense interest as reported in a recent review.[98] We only show a few selected examples that are relevant to sugar-based molecular assemblies.

Diverse water-soluble mono-, di-, and trisaccharide BODIPY conjugates (glycoBODIPYs) with preserved chirality and high fluorescence efficiency were prepared by Werz's group.[99] As shown in Scheme 30, through a straightforward four-step synthesis including (1) ethyl pyrrole condensing with the reducing end of the sugar to give intermediate **198**, (2) triethyl silyl (TES) protection of the hydroxyl groups to form **199**, (3) BODIPY formation with $BF_3{\cdot}Et_2O$ and lastly (4) TES deprotection afforded glycoBODIPYs **201** smoothly. Some representative glycoBODIPYs synthesized from various sugars, L-fucose (**202**), D-cellobiose (**203**), D-lactose (**204**) and D-maltotriose (**205**), are shown in Scheme 30. Cell staining experiments showed that compound **202** (L-Fuc) is detected in the cytoplasm as well as in the nucleus. D-Cellobiose-based glycoBODIPY **203** illustrated staining in mitochondria, specifically contrary to its epimer **204**.

A lactosylated aza-BODIPY compound **206** was synthesized *via* click reactions (Fig. 15).[100] *In vivo* studies showed that the glycoconjugate **206** was capable of selectively entering HepG2 cells by forming J-aggregated nanofibers. The lactose moieties tuned the aza-BODIPY organization preciously to allow the dye to adopt the J-aggregate structures. Synergistically, these J-aggregates can generate superoxide radicals ($O_2^{\bullet}$) by photo-induced electron transfer, facilitating type I photodynamic therapy (PDT) to enhance the tumor suppression efficacy. Kamkaew *et al.* reported a novel glyco-BODIPY compound **207** as a promising targeted PDT agent, which is composed of two glucose motifs conjugating to iodine-functionalized NIR aza-BODIPY dye *via* a click reaction (Fig. 15).[101] Because of the presence of overexpressed glucose transporters (GLUTs) in cancer cells, GLUTs can be used as anti-cancer targets. A higher level of glucose triazole derivative **207** was detected in breast cancer cells than in normal cells. After exposing the cancer cells targeted with glycoconjugate **207** to light, singlet oxygen was generated, which enables high cancer cell toxicity through the type II PDT mechanism.

The tetravalent glucose functionalized aza-BODIPY conjugate **208** was designed to target cancer and to increase the photoacoustic (PA) imaging by addressing the following issues: (1) solubilizing effect, (2) prevention of π-stacking of the appended dye, and (3) cancer cell targeting compared with a single glucose moiety (Fig. 16).[102] Based on a similar scaffold, affixing tri[(2-pyridyl)-methyl]amine (TPA) generated

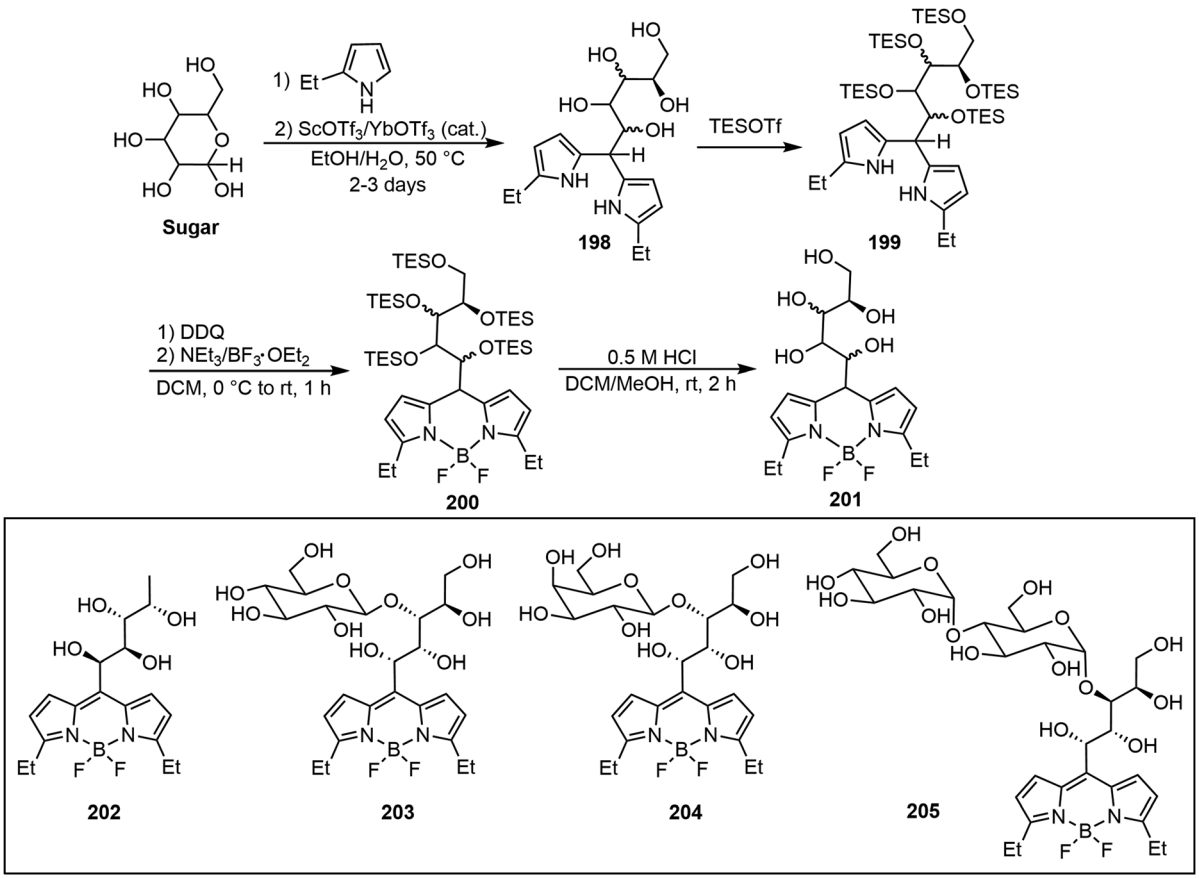

Scheme 30 Synthesis of glycoBODIPY **202–205** by Knoevenagel condensation reactions.

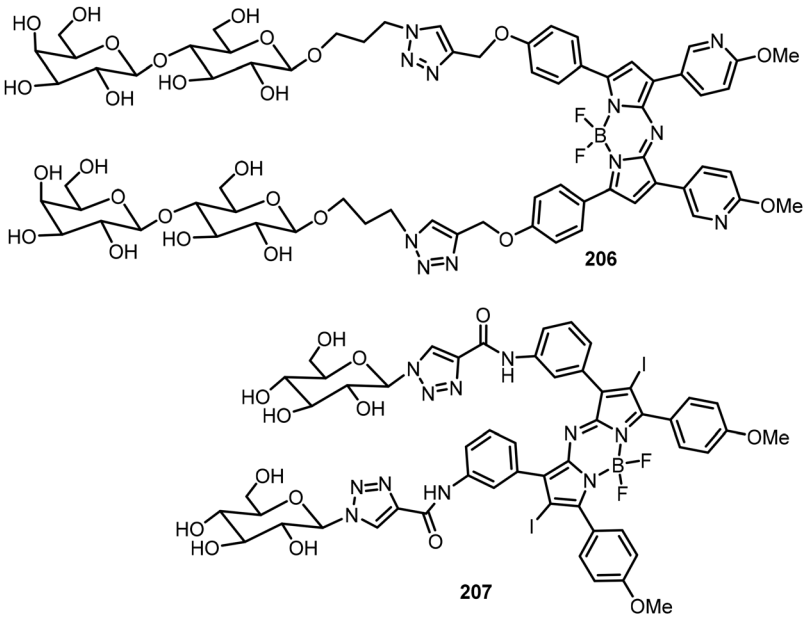

Fig. 15 Chemical structure of glyco aza-BODIPY **206** and **207**.

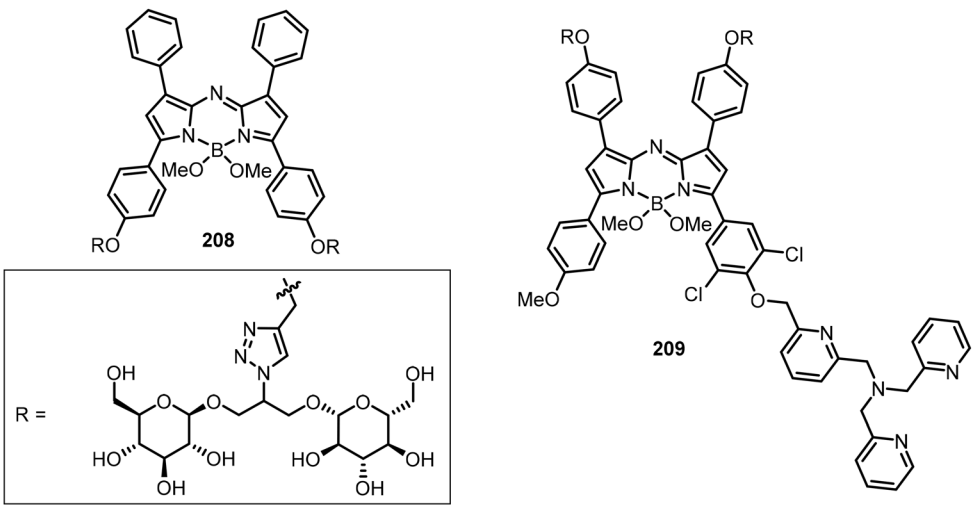

Fig. 16 Chemical structures of aza-BODIPY glycoconjugates **208** and **209**.

a copper(I) detection probe **209** (Fig. 16). Upon coordination of compound **209** with Cu(I), the triggered oxidative cleavage releases the dye, causing a significant PA signal absorption peak shift from 676 nm to 754 nm.

5. Oligosaccharides

The self-assembling properties of oligosaccharides either on their own or as part of glycopeptides have also been studied. In this section, several recent reports are included. Chen *et al.* reported two different series of glycopeptides and their self-assembling properties.[103] These include glycopeptide **210** composed of sialyllactose, a trisaccharide bearing a negative charged COO^- group, and triphenylalanine (Fig. 17).[103] The compound was prepared by an ytterbium(III) trifluoromethanesulfonate catalyzed *N*-glycosylation of sialyllactose with the peptide triphenylalanine hydrazide. The self-assembly of glycopeptide **210** formed double-strand fibrils, which were fully characterized by TEM and AFM. The self-assembling behaviors of several glycopeptide analogs were also studied *via* computational modeling. The sialyllactose portion contributed to hydrogen bonding and the peptide portion self-assembled through π–π stacking and hydrogen bonding.

Chen's team also synthesized several linear dimeric sugar peptide conjugates **213** as well as two amphiphilic dendritic

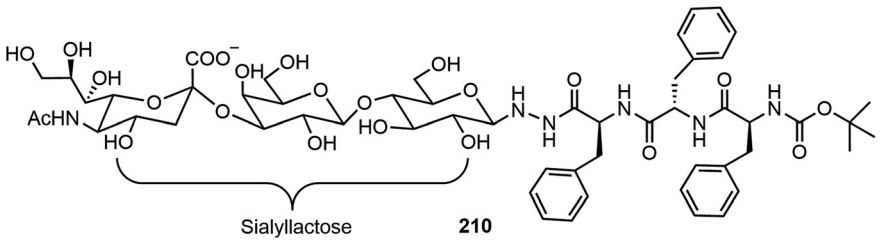

Fig. 17 Chemical structure of glycopeptide **210**.

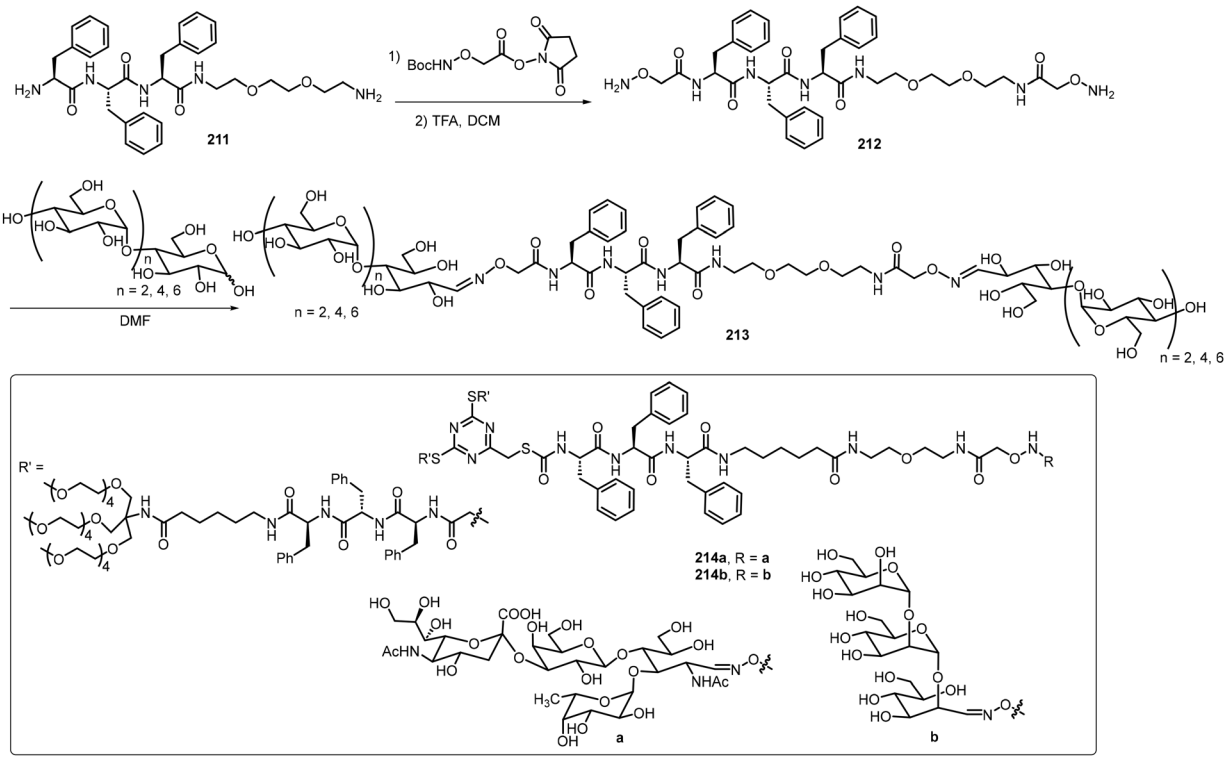

Scheme 31 Synthesis of the dimeric glycoconjugates **213** and **214**.

glycopeptide molecules **214a–b** with oligosaccharides in the periphery *via* an oxime-mediated strategy (Scheme 31).[104] They were synthesized by using hydroxyl amine reacting with the corresponding sugar aldehydes. The linear dimeric compounds self-assembled and formed spherical nanoparticles. The dendritic oligosaccharide-tripeptide monomers self-assembled to form uniform supramolecular nanorods in an aqueous solution. *In vitro* studies demonstrated that these supramolecular nano-rod like polymers have no cytotoxicity to macrophages, but can significantly affect the production of proinflammatory cytokines.

Delbianco *et al.* have synthesized oligosaccharides as mimics of cellulose and other polysaccharides by automated synthesis and studied the self-assembling properties of those oligosaccharides.[105–107] A series of phosphoethanolamine (pEtN)-modified oligosaccharides with defined sequences and structures were synthesized *via* the automated glycan assembly (AGA) method.[105] The synthesis of one oligosaccharide by AGA is shown in Scheme 32, where the suitably protected monosaccharide derivatives **215–217** are the building blocks for the automated synthesis. In order to elucidate the glycan–protein interactions, the synthetic oligosaccharides were co-assembled with a polypeptide **R5**, and the assemblies were analyzed using AFM. These pEtN-modified oligomers can form biofilm-inspired assemblies with synthetic polypeptide **R5**. It was found that mono-, di- and trisaccharide did not influence the secondary structure transition rate of peptide **R5** while the longer hexasaccharides such as **221** hindered the structural transition into β-sheets of the peptide.

Cellulose oligomers with defined sequence and chirality were also synthesized by the AGA method and their self-assembly was investigated.[106] Hexasaccharides composed of D- and L-glucose derivatives were prepared; these are denoted as **D6** and **L6**, and these oligomers formed self-assembled platelets

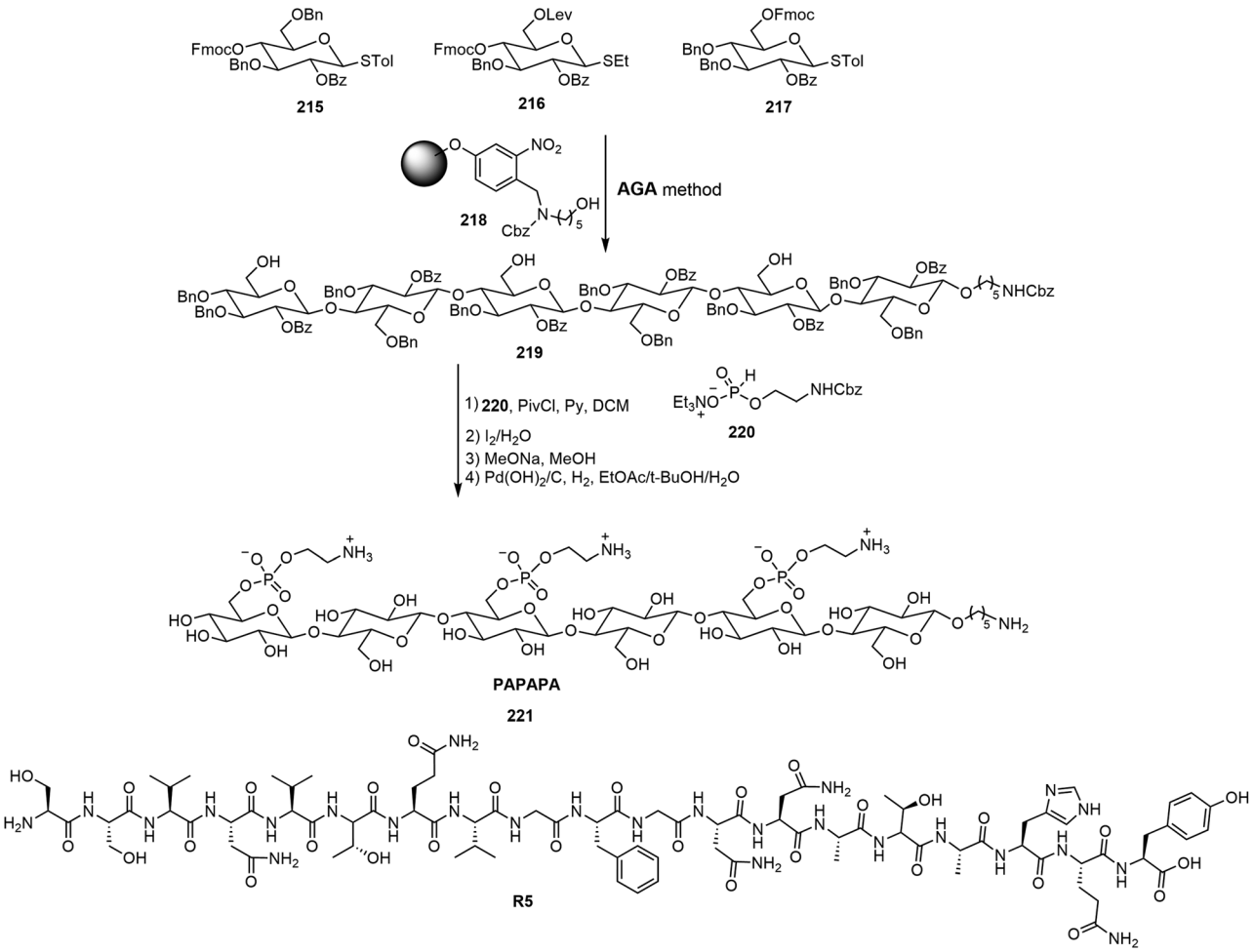

Scheme 32 Synthesis of oligosaccharide **221** by the automated glycan assembly (AGA) method.

and further assembled into bundles with a chirality directly related to the structures of the monosaccharides (Fig. 18). **D6** exhibited right-handed bundles and **L6** formed left-handed bundles. Oligomers composed of both D- and L-glucose were also synthesized; the hybrid DL-oligomers were prepared to help elucidate the assembling mechanism. The team also prepared six cellulose-based oliogosaccharides by the AGA method and studied their self-assemblies.[107] The synthetic oligomers formed different self-assembled aggregates depending on the sequence of the sugars. Modification of the glucose unit resulted in the formation of hydrogels. Modification at the terminal position with a 3,6-methylated D-glucose unit (**222**) or a mannose unit (**223**) resulted in self-healing supramolecular hydrogels, while the bis-mannose (**224**) compound failed to gelate in water, indicating that 3,6-methylated glucose unit is accountable for hydrogel formation.

Combining solid phase peptide synthesis (SPPS) with AGA, a series of peptides and glycans **225–228** were synthesized and their self-assemblies were analyzed (Fig. 19).[108] The peptides **225** FFKLVFF formed ribbon-like nanofibers and the lipid peptide **227** (palmitoyl-VVVAAAKKK) formed self-assembled fiberous aggregates observed on AFM. The complex peptide–glycans **226** and **228** were prepared efficiently and depending on the structures of the peptide, the chimera exhibited different self-assembled network structures. The glycopeptide chimera **226** did not form self-assembled fibers, even upon mixing the peptide **225** with glycopeptide **226**. Further dilution of the mixture resulted in the formation of micelles. The presence of glycans in the chimera interferes with the self-assembling of the peptides into fibers, and this may have implication for application in preventing amyloid fiber formation. Compound **228** did not form well-defined fibers but formed short fibers on its own, and the glycan did not block the self-assembly as in the case of **226**. Mixing **227** and **228** in different ratios resulted in well-defined fibers, as indicated by AFM experiment.

6. Stimulus-responsive carbohydrate derivatives

An advantage of the bottom-up molecular self-assemblies formed by non-covalent interactions of small molecules is that various functions can be designed into the molecular systems

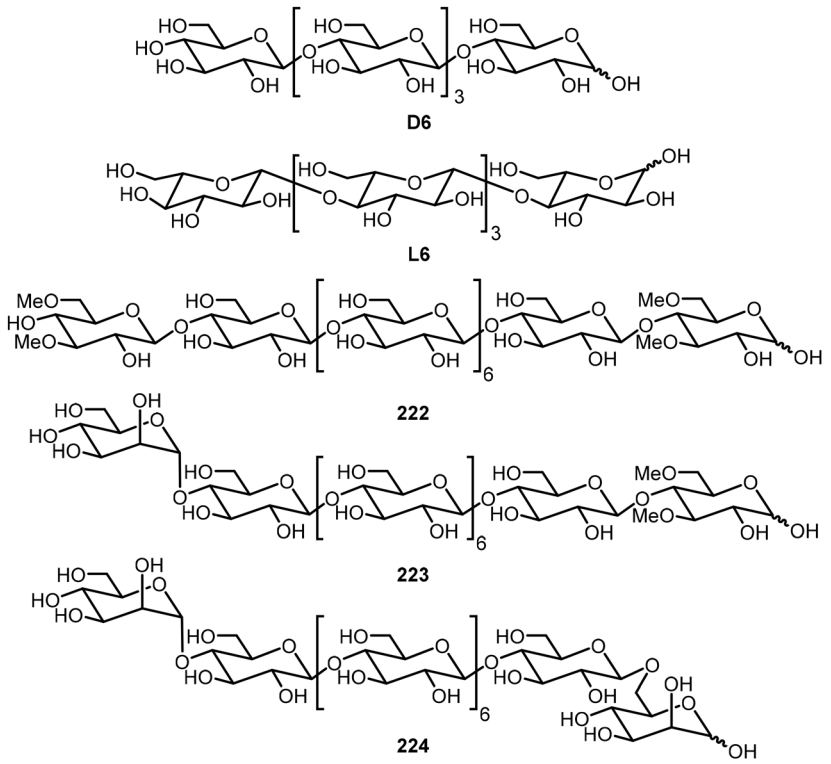

Fig. 18 Chemical structures of synthesized oligosaccharides **D6**, **L6** and **222–224**.

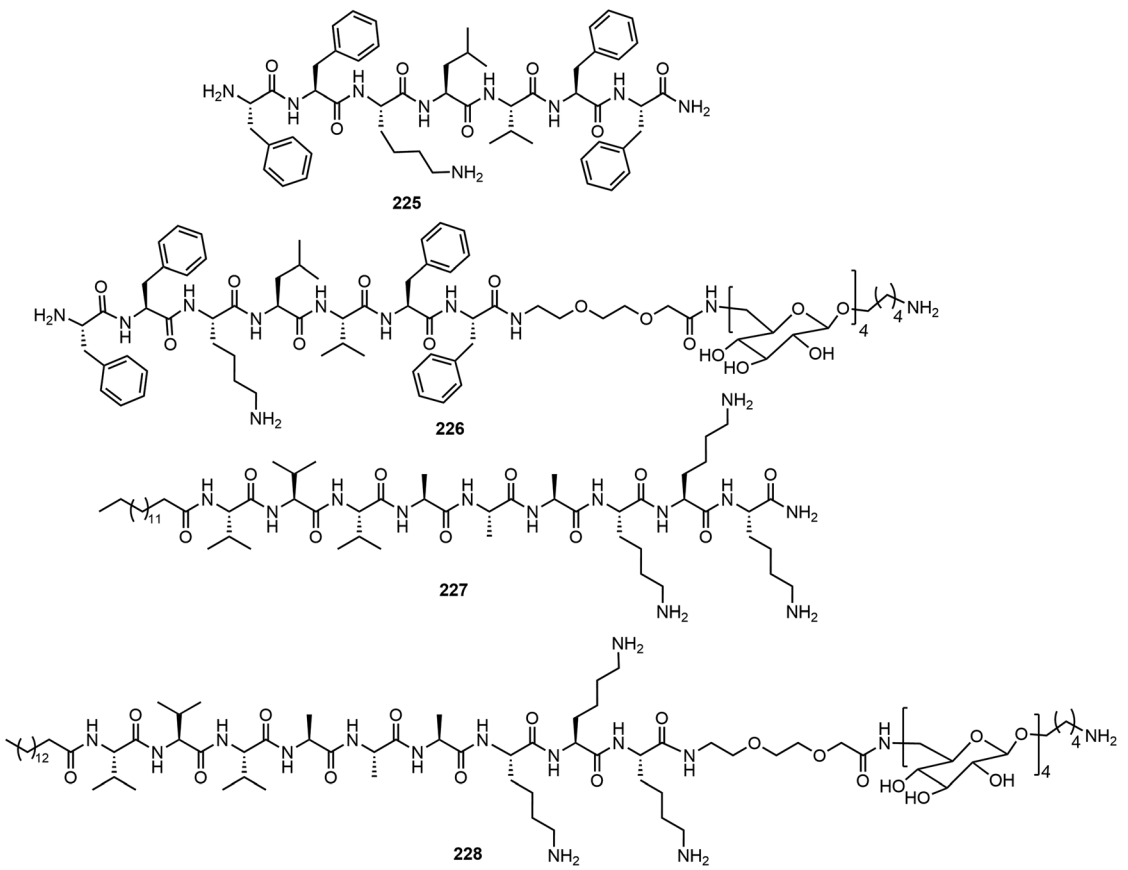

Fig. 19 Chemical structure of lipid peptide glycans **225–228**.

to achieve control of the resulting assemblies. In the field of LMWGs, this has been demonstrated in many examples. The stimuli or triggers in the various stimulus-responsive systems are photo, enzyme, pH, metal ion, chemical, *etc*. These are also utilized for carbohydrate-based assemblies. In this section, we briefly review a few recent examples, with the following systems: chemical-triggered, boronic acid dynamic covalant systems, and photoresponsive systems.

Several glucose derivatives containing an aldehyde functional group are shown in Scheme 33, and the 4,6-*p*-formylbezyldiene glucose derivative **229** is an organogelator.[109] Upon the addition of dithionite, gelator **229** was converted to the sulfonated derivative $GluSO_3^-$ **232**, which is not a gelator.[110] Therefore, the addition of dithionite can trigger the gel to solution transition. The solution can then be converted back to a gel upon the addition of formaldehyde (fuel), which can be prepared from hexamethylenetetramine (HMTA) and gluconolactone *in situ*. This mechanistic cause and effect was termed chemical-fueled gelation/supramolecular polymerization. In addition, two other glucose and formyl-benzaldehyde derivatives **230** and **231** were synthesized and studied. These glucose derivatives were mixed to obtain molecular assembling information on the co-assembly of either two or three components.[111] The three-component (**229** + **230** + **231**) system formed self-sorting gels and exhibited self-healing properties. More recently, a chemical triggered sol–gel–sol–gel–sol autonomous system was reported.[112] Compound **229** was condensed with homocysteine to form the sugar-thiaz derivative **233**, and by adding suitable reagents, the gel to sol transition was tuned (Scheme 33). At time zero, HCHO, piperazine, and homocysteine thiolactone (HCT) were added to the clear solution of **233**. The sequence of reactions then took place and the solution turned turbid and resulted in gel formation (G1) in one minute. The gel (G1) was formed by a mixture of gelator **229** and the imine derivative **234**. The gel (G1) turned into a clear solution after 10 minutes due to the disappearance of imine **234** and formation of aldehyde **229**. After a few minutes, this turned to the formation of another gel (G2) which was formed by **229**. The gel (G2) turned into solution after 3 days due to the reformation of compound **233**. Overall, the system represents chemical-fueled autonomous sol–gel transitions.

The dynamic covalent interaction between phenyl boronic acid and diols has been utilized in the design of self-healing hydrogels. For example, Webber's team has reported the preparation of 4-armed polyethylene glycol (4aPEG) hydrogels with different stiffnesses (Fig. 20).[113] The hydrogel's stiffness can be controlled by dynamic covalent PBA–diol interactions which are temperature, pH, and concentration dependent. The diol from the 4-arm PEG glucose derivative (4aPEG-GLD) **236** acts as a crosslinking component with 4-arm PEG 4-borono-2-fluorobenzoic acid derivative (4aPEG-BFBA) **237**.

Due to space limitations, we did not include a separate section for nucleoside- and nucleotide-based self-assembling systems and gelators, but these important classes of compounds were discussed in several recent reviews.[11,114–116] Recently guanosine and borate hydrogels were also used as

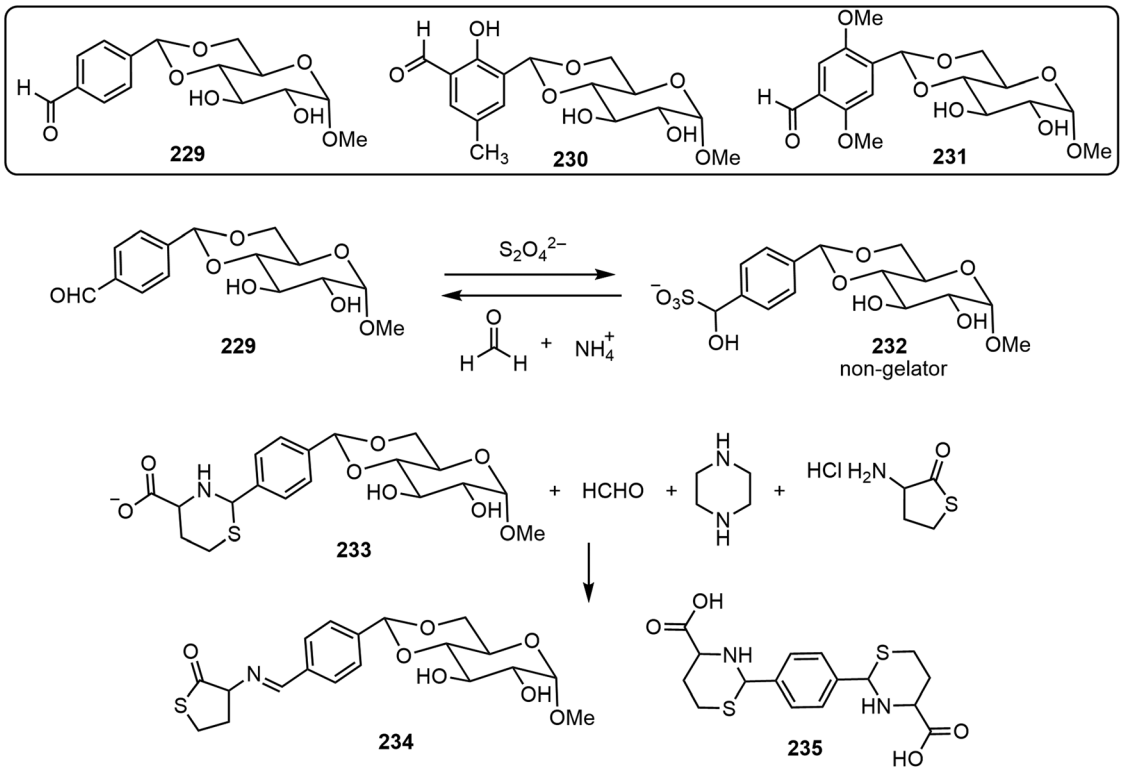

Scheme 33 Structure of glucose derivative gelators **229–234**.

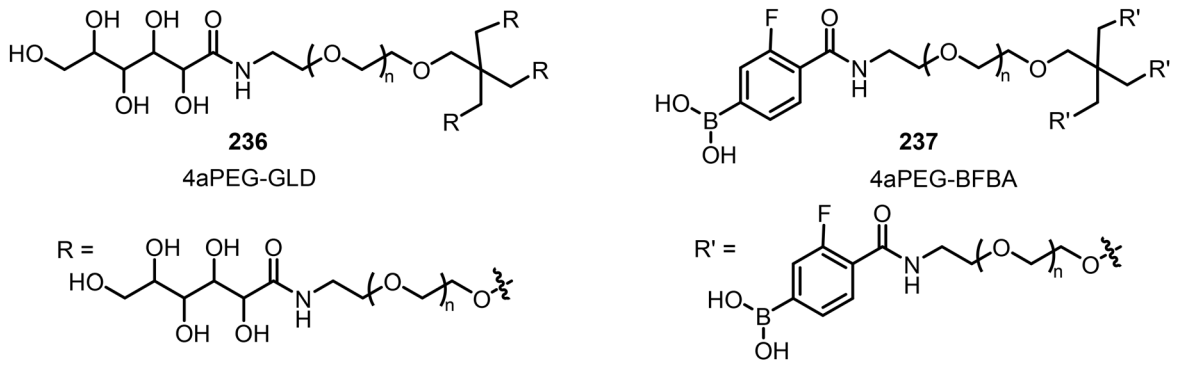

Fig. 20 4-Armed PEG glucose derivative **236** and phenylboronic acid derivative **237**.

organocatalysts for aldol reactions,[117] and the hydrogel formed by a GMP mixture with 1,4,5,8-naphthalene tetracarboxylic acid was used for controlled release of the anticancer drug doxorubicin.[118]

The next section will focus on a few recent examples of nucleoside-based gelators *via* chemical-triggered systems. Ghosh *et al.* reported a G-quadruplex hydrogel formed by guanosine (G), nucleopeptide, and 4-formylphenylboronic acid (4-FPBA).[119] The combination of these compounds was found to form stable hydrogels in the presence of potassium ions in water. The hydrogel system was named G4NP. Gelation is achieved through a combination of self-assembly and bioconjugation, as shown in Scheme 34. The nucleopeptide reaction with 4-FPBA (**239**) led to the formation of the imino adduct **240**, which then formed a conjugate with guanosine to afford the intermediate **241**. The formation of G4-quadruplex from this compound resulted in the formation of a hydrogel system which is injectable and capable of self-healing. The hydrogel system possessed inherent antibacterial activity and antifungal activity.

Tuning the G-quadruplex hydrogel through controlling the reaction of the diol and boric acid derivatives can be a useful strategy for creating transient hydrogels and new types of material. Using different boronic acid derivatives in combination with guanosine for the formation of G-quadruplex hydrogels, several other functional supramolecular gels with different properties have been reported.[120,121] As shown in Scheme 35, the self-assembling and chirality properties of the G-quadruplex hydrogels formed by guanosine and 5-fluorobenzoxaborole **242** (**B**) complex have been studied. The gel to sol transition can be controlled by adding various reagents (termed fuels). Under basic conditions by adding KOH, the resulting **GB** complex self-assembled and formed hydrogels. Under acidic conditions, the gels return to solution. The formation of dynamic covalent bonds between the *cis*-diols of guanosine with boric acid derivatives led to the formation of supramolecular gels under thermodynamic stable conditions by SA and forming a G-quadruplex. In a related study, acidic and basic conditions were used as chemical triggers or fuels to adjust the state of the molecular assemblies. KOH and 1,3-propanesultone (**243**) were utilized as the chemical fuels. Compound **243** was hydrolyzed in water to form the acidic 3-hydroxypropanesulfonic acid **245** (HPSA), which in turn reduces the pH values and breaks down the G-quadruplex back to the guanosine (**G**) and 5-fluorobenzoxaborole mixture. These cycles could be tuned multiple times using these two reagents. More recently, the team reported self-assembling properties of guanosine with 3,3′-piperazine-bis(benzoxaborol)

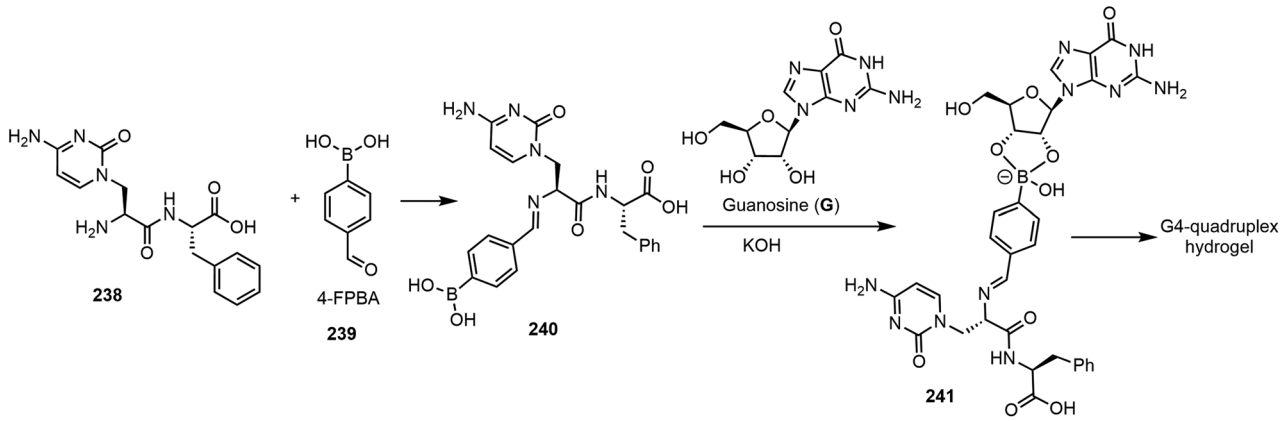

Scheme 34 Synthesis of G4-quadruplex.

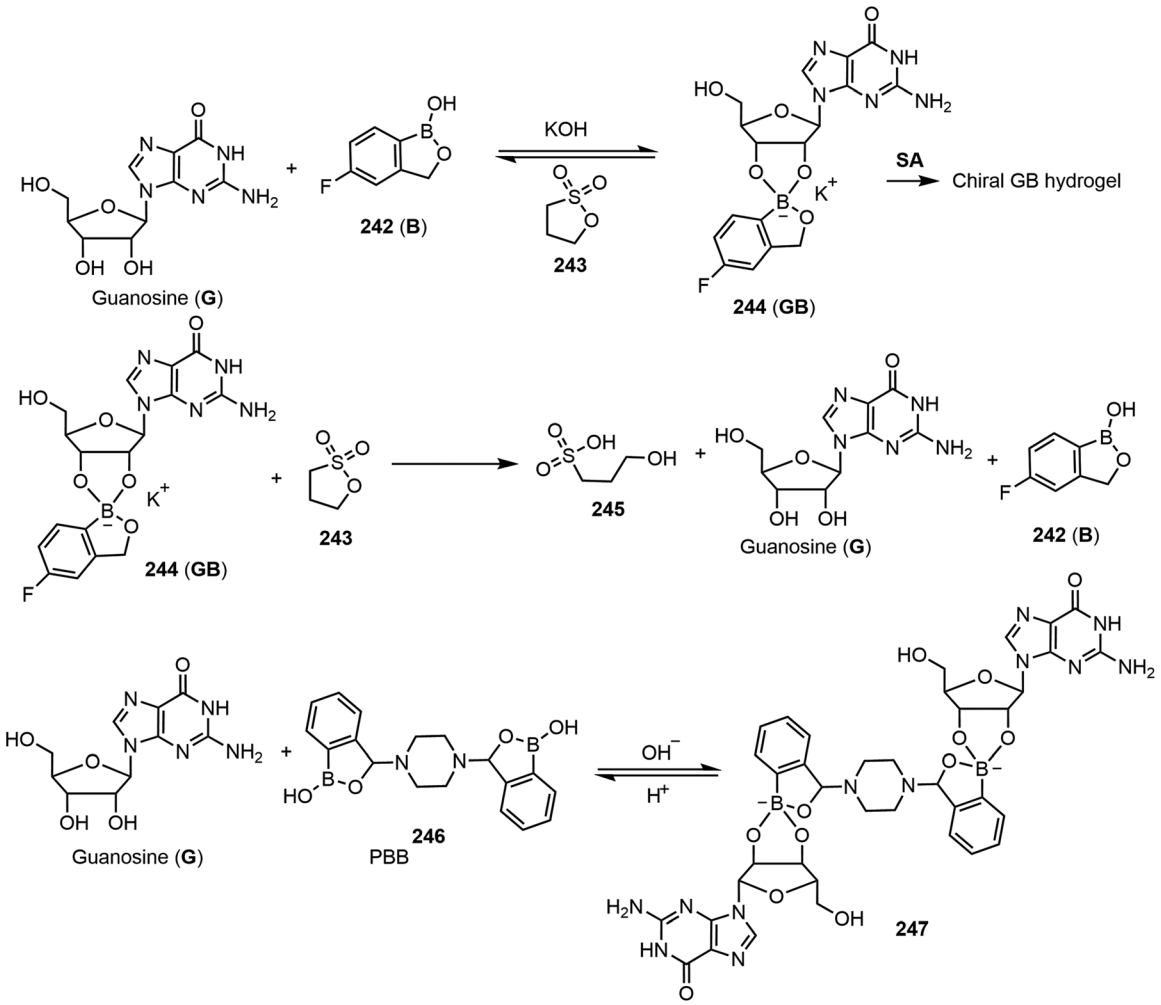

Scheme 35 Formation of guanosine (G) and boric acid complexes **244** and **247**.

(PBB) **246** and found that the supramolecular chirality can be programmed at different pH values, allowing the system to act as a multistate chiral optical switch.[121] A mixture of G and PBB (2 : 1 ratio) in the presence of potassium ions formed gels at a broad range of pH 1–14, and the formation of the G-PBB-G diester complex **247** resulted in the formation of stable hydrogels. At different pH values, the gelation and self-assembly were analyzed. The chiroptical properties of the assemblies under acidic conditions were deemed left-handed helical through a G···PBB quadruplex, and right-handed at basic conditions through N–H···O hydrogen bonding between G-PBB-G. They concluded that chemical fuels can be used to regulate the self-assembling pathways and lead to different supramolecular chiralities. 1,3-Propanesultone (PrS) was used to adjust the pH. The reaction of the G-PBB-G diester with PrS produces 3-hydroxylpropanesulfonic acid, which decreases the pH and increases the acidity, which results in the cleavage of the diester back to the G and PBB starting materials.

Photoresponsive carbohydrate self-assembling systems have also been investigated. These include azobenzene, diacetylene, and diarylethene based systems. In the next section, a few recent examples will be discussed. Several maltose-based nonionic surfactants **251a–c** containing a photocleavable azosulfide linker were synthesized and the self-assembling properties of these surfactants were explored (Scheme 36).[122] β-D-Maltose octaacetate **248** was converted to the corresponding thiolglycoside **249** through glycosylation using thiourea followed by reduction. The coupling reaction of the hydrolyzed product **250** with diazonium ions led to the formation of the maltose azo sulfide compounds **251**. Transmission electron microscopy (TEM) illustrated that the supramolecular assemblies formed by the synthesized surfactants **251** have micelle morphology. Upon UV light exposure, the light-switchable surfactant **251a** can rapidly degrade to photostable surfactant **252** indicated by surface tension measurements and LCMS. Biological applications using these surfactants for protein extraction were demonstrated. Surfactant **251b** (n = 7) provided the best protein solubility, while surfactants **251a** and **251c** exhibited slightly less effective results.

Wang *et al.*[123] synthesized glucoside or mannoside coumarin conjugates **256** from 2-allylethoxyl glucoside or mannoside **254** with 7-mercaptohexyloxy-4-methylcoumarin **255**

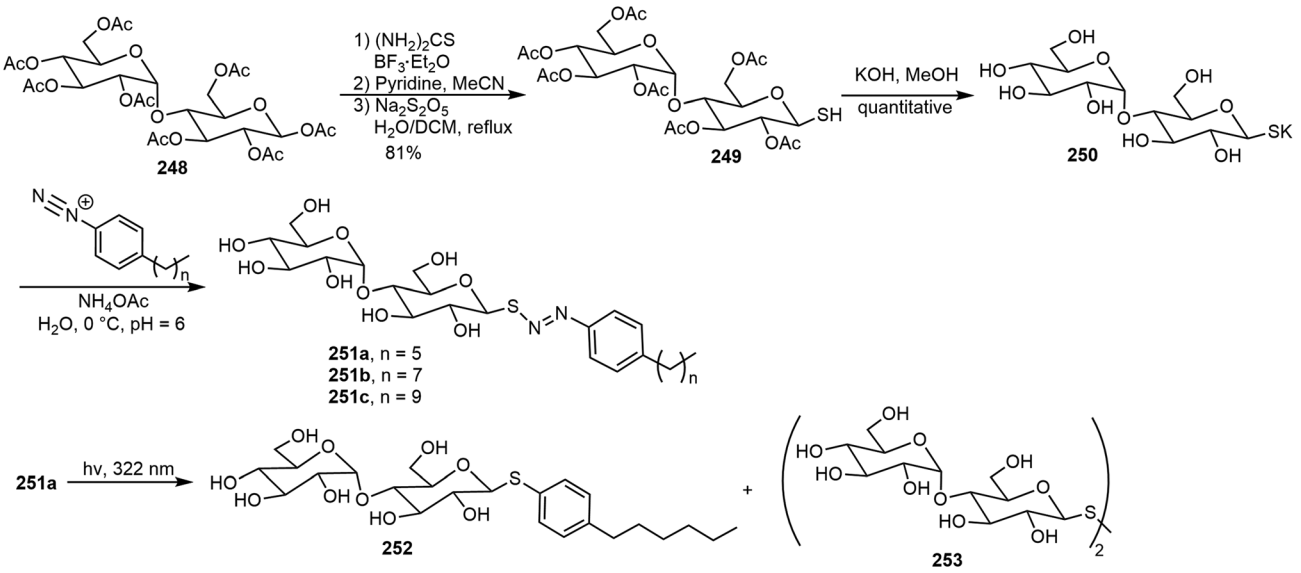

Scheme 36 Synthesis of photoresponsive thioglycoside derivatives **251a–c**.

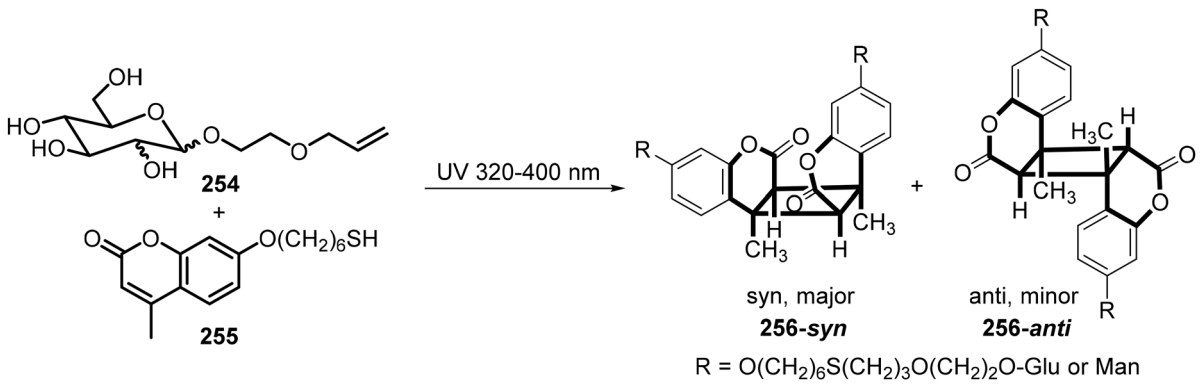

Scheme 37 Synthesis of sugar-based bolaamphiphiles **256** by thiol–ene addition and photodimerization of coumarin.

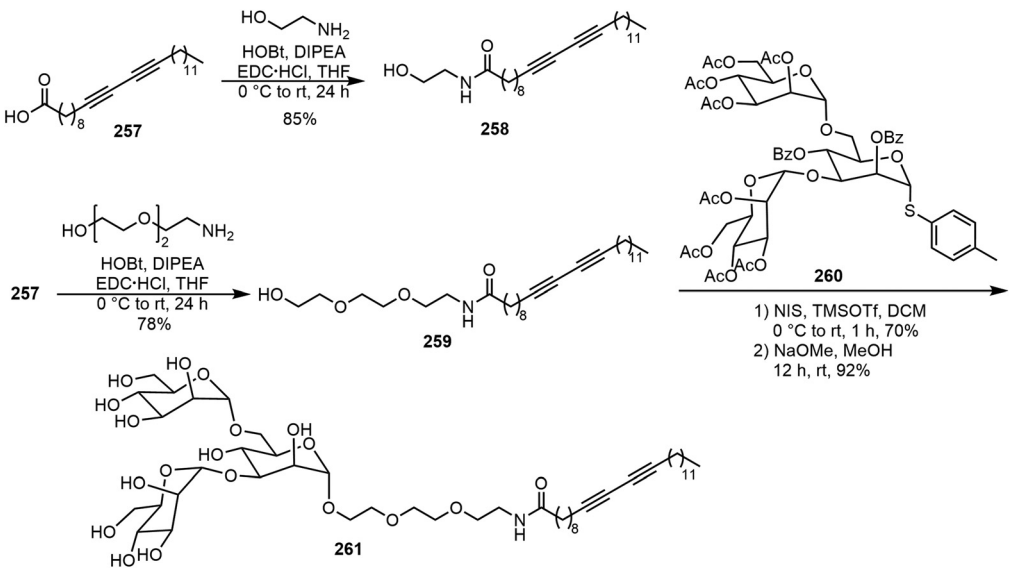

Scheme 38 Syntheses of manno-triose and ethanolamine-diacetylene lipids **261** and **258**.

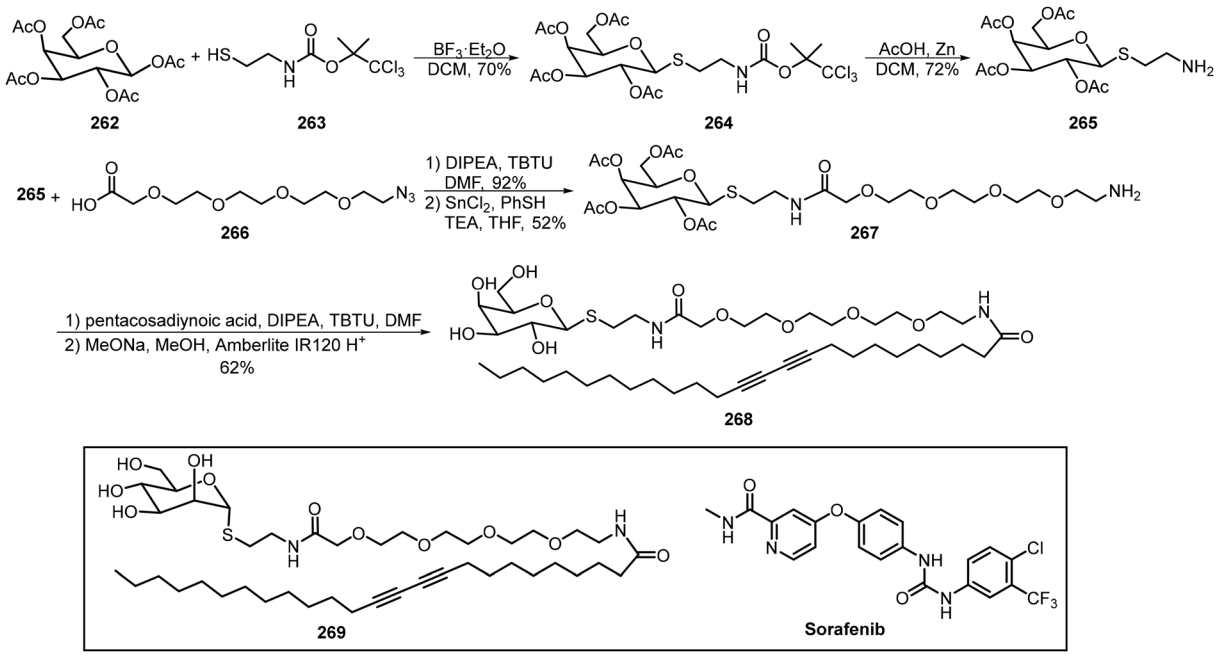

Scheme 39 Synthesis of PCDA functionalized thioglycosides **268** and **269**.

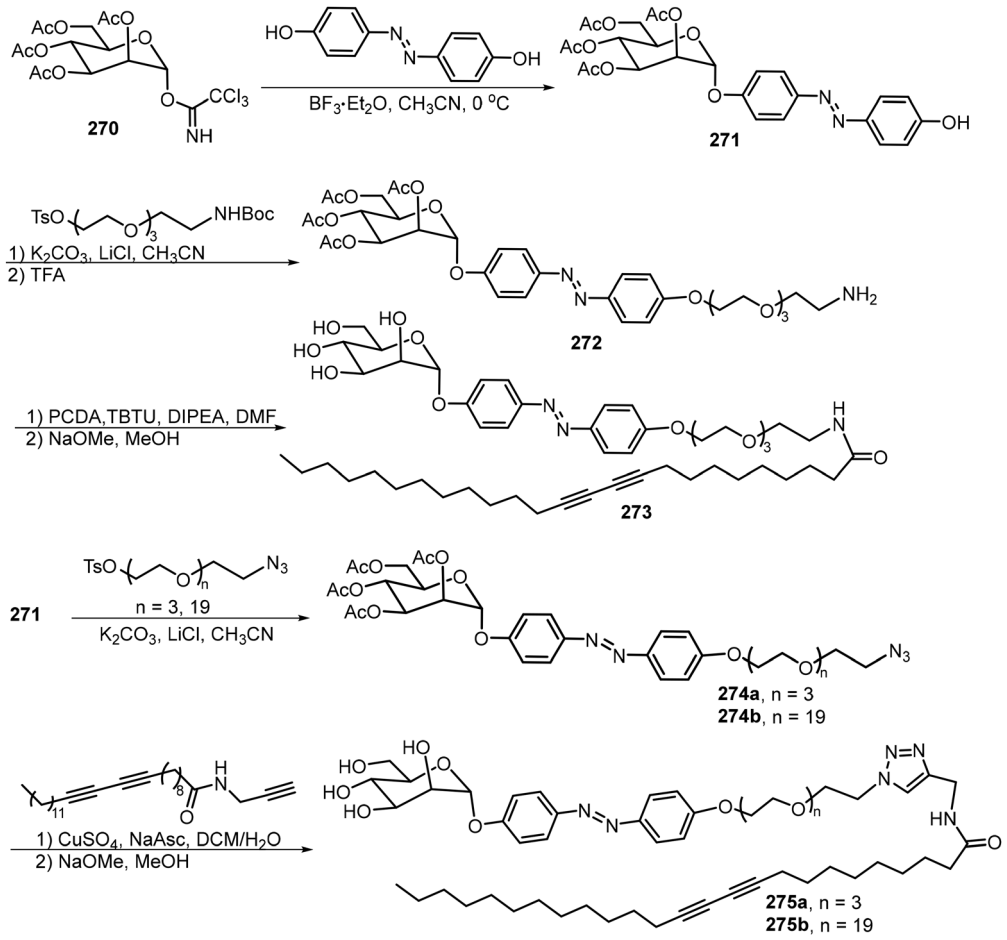

Scheme 40 Synthesis of azo-benzene-containing diacetylene glycolipids **273** and **275**.

through thiol–ene reactions under UV irradiation. The coumarin moiety in the resulting conjugate of **254** with **255** simultaneously dimerized through [2 + 2] photocyclization to form the sugar-based bolaamphiphiles **256**. This is illustrated in Scheme 37. Interestingly, these water-soluble compounds exhibited temperature-responsive properties as indicated by ^{1}H NMR spectroscopy in D_2O. At 30 °C, the aromatic signals were invisible, and the aliphatic signals were diminished. When increasing the temperature to 60 °C, both regions became sharp, which indicates that at lower temperatures strong intermolecular interactions exist, which diminish with increasing temperatures. They also observed a reversible transparent–turbid transition upon cooling and heating, which indicates micelle to vesicle transition.

Diacetylene functional groups have also been introduced to carbohydrate derivatives for the formation of glycolipids which can result in a variety of different molecular assemblies and applications. Yadav *et al.* synthesized glycovesicles prepared from diacetylene-containing glycolipid, as shown in Scheme 38.[124] Pentacosadiynoic acid (PCDA) **257** was converted to diacetylene lipids **258** and **259** by amide formation. The manno-triose headgroup **260** was coupled with the diacetylene lipid **259** through an alpha-glycoside linkage to afford the glycolipid **261**. The **258**–Con A interaction was analyzed as a function of the ligand density at inter- and intra-vesicular ligand–lectin interactions. For the tris-mannose lipid **261**, it was found that the intra-vesicular lectin interaction was favored over the inter-vesicular interactions.

Pentacosadiynoic acid has been incorporated into the anomeric positions of thioglycoside through amide coupling reactions. The resulting amphiphilic glycolipids formed micelles which were then crosslinked with UV light (254 nm) to form the photopolymerized vesicles. The diacetylene-containing galactose-based amphiphile **268** and mannose-based amphiphile **269** were synthesized and their self-assembling ability to form micelles was studied (Scheme 39).[125] The polydiacetylenic-based micelles were formed by dispersing the monomers **268** and **269** in distilled water at concentrations higher than their critical micelle concentration (CMC), followed by removing the excess monomers *via* dialysis and photopolymerization. The prepared micelles served as drug carriers to trap sorafenib, a drug to treat hepatocellular carcinoma (HCC). These nanomicelles-sorafenib carriers can target mannose and asialoglycoprotein receptors (MR and ASGPR) to induce cell apoptosis and reduce cell proliferation. It was found that the mannose-based micelles incorporating sorafenib were superior to galactose-based micelles incorporating sorafenib in treating hepatocellular carcinoma (HCC).

The preparation of glycoamphiphiles **273** and **275** started from the glycosylation of tetra-*O*-acetyl-α-D-mannopyranosyl trichloroacetimidate **270** with 4,4-dihydroxylazobenzene to afford the azobenzene-containing glycoside **271**, which serves as the

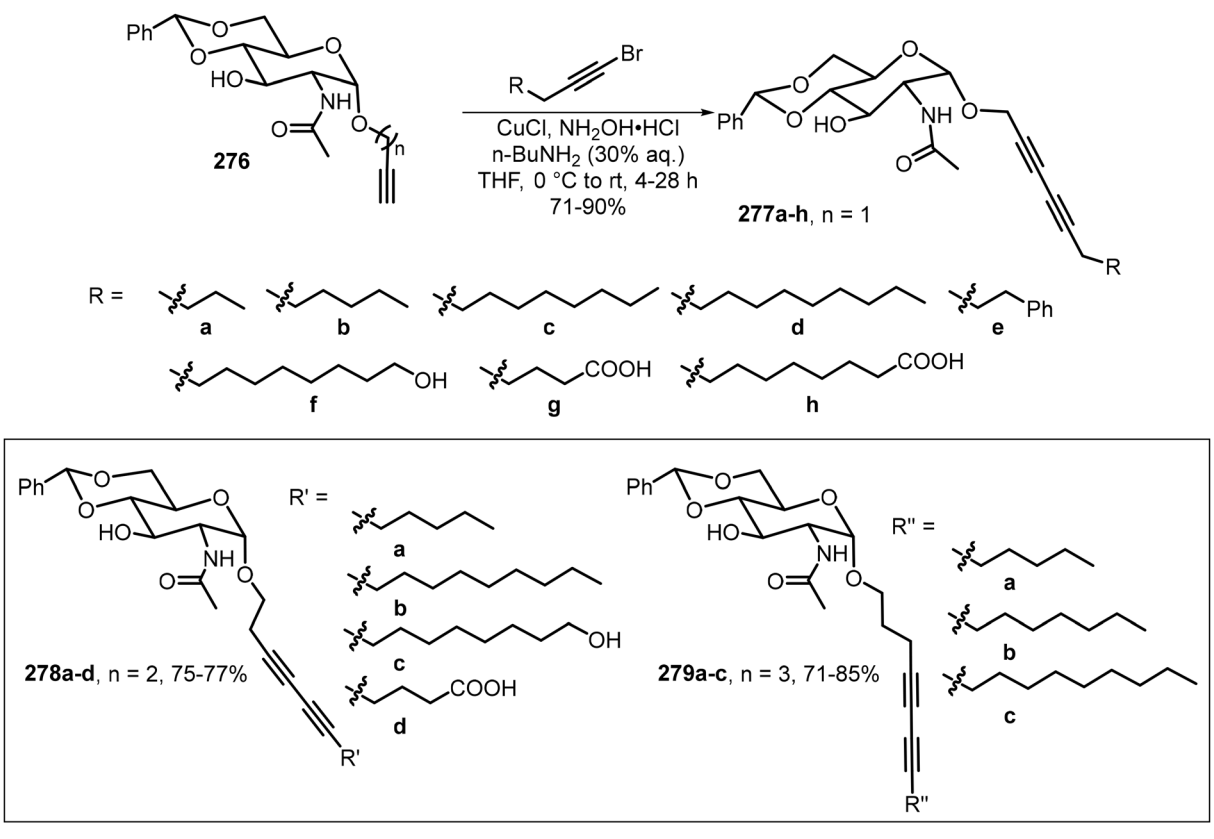

Scheme 41 Synthesis of diacetylene-containing glycosides **277–279**.

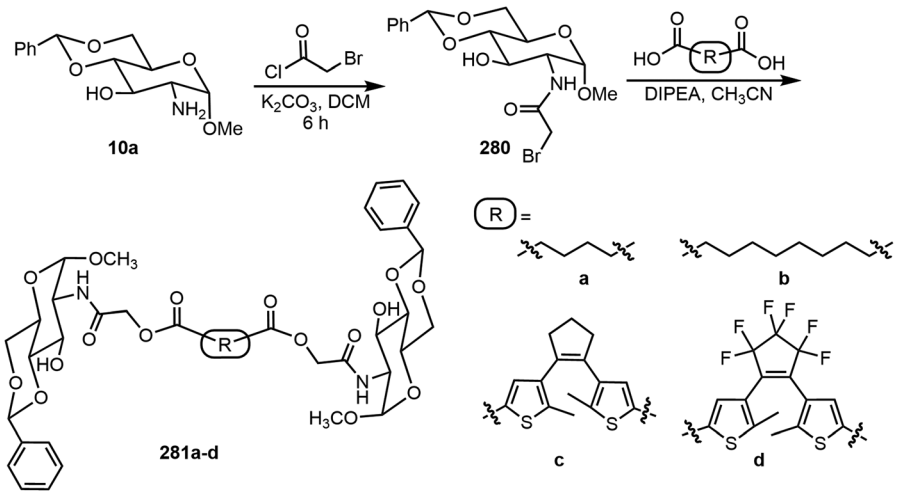

Scheme 42 Synthesis of dimeric glycolipid **281a–d**.

common intermediate (Scheme 40).[126] The hydrophilic tail was introduced by first functionalizing the phenyl OH in the azobenzene glycoside with a bifunctional spacer bearing tosyl and NHBoc or azido groups to form **272**, followed by amidation with diacetylene-containing acid or click reactions with diacetylene-containing amido alkyne. Then global deacetylation gave the targeted compounds. Glycolipid **273** formed gels in alcohol and aqueous mixture and the resulting gels underwent photoresponsive gel–sol transition upon UV irradiation. Glycoamphiphile **275b** can photopolymerize to create spherical micelles, the cavity of which can trap hydrophobic dye like Nile Red or the drug molecule docetaxel.

A library of novel α-anomeric diacetylene-containing glycosides **277–279** was designed and synthesized, in which one, two, and three methylene spacers were inserted between the anomeric oxygen and diacetylene group (Scheme 41).[127] Glycosylation of *N*-acetyl-D-glucosamine with terminal alkynyl alcohols furnished α-alkynyl glycosides **276**. Subsequent CuCl-catalyzed Cadiot–Chodkiewicz coupling completed the synthesis of the glycosides **277–279**. A majority of the prepared diacetylene glycosides are effective gelators and formed photopolymerizable red- and purple-colored gels under UV irradiation.

Recently, diarylethene (DAE) or dithienylethene (DTE) photoresponsive functional groups were incorporated into a sugar-based self-assembling system.[128] The structures and synthesis are shown in Scheme 42. Two linear dimeric glycolipid-based gelators **281a–b** were designed to be responsive to chemical stimuli. The two DTE-based photoswitchable derivatives **281c–d** were designed to be responsive to UV and visible light. Compound **281c** formed gels in DMSO aqueous solutions at low concentrations. The compound formed gels in nine different solvents and the gel formed by a DMSO and water mixture was shown to absorb rhodamine B dye or toluidine blue. The gel of **281c** in DMSO water (1 : 2 v/v) exhibited reversible opaque white to deep purple color transitions upon UV irradiation and visible light treatment. The compound **281d** formed fewer gels in the tested solvents, and the ethanol gels exhibited a transparent yellow to dark blue color change when irradiated with UV light.

7. Concluding remarks

In summary, the most recent developments of 2020 through 2023 in the field of carbohydrate-based self-assembling systems have been discussed. The review has an emphasis on the synthesis of the various carbohydrate derivatives, with a special focus on monosaccharide derivatives that can form supramolecular gels. The factors that determine the molecular assemblies are also discussed in the pertinent section. The monosaccharide derivatives that form micelles or vesicles instead of gels are also reviewed. Similar types of reaction can be used for the preparation of disaccharide derivatives, including the formation of glycosides, glycolipids, and glycopeptides. A few oligosaccharide-based systems that can be prepared by automated synthesis are also discussed. A useful reaction in the construction of sugar-based supramolecular assemblies is the click reaction, which has been employed extensively in the synthesis of various glycoclusters and glycoconjugates. These branched compounds often have additional properties depending on what functional groups are being incorporated. Finally, several stimulus-responsive carbohydrate-based self-assembling systems have been reviewed, and this section includes several dynamic covalent bonds which are reversible and can be controlled by adding different reagents; lastly, several photoresponsive molecular assemblies are also discussed. These represent interesting functional materials.

Carbohydrate-based self-assembling systems are an interesting and important class of compounds which will play a more crucial role in future multidisciplinary research fields. There are several advantages using sugars as the sources for the preparation of new functional materials. These starting materials are structurally diverse, sustainable, renewable feedstocks, and most of their derivatives are biocompatible and

biodegradable. Many methods have been developed to convert the diverse classes of sugars into useful molecular systems including those that can form supramolecular gels. Readily available monosaccharides and disaccharides can be modified to form self-assembling systems. In this review, we summarize the synthetic approaches for different classes of sugar derivatives, which are typically carried out in a few steps. It is necessary to be able to prepare these self-assemblies in short steps for the sake of efficiency and practicality. For example, the glycosylation reaction is one of the most frequently employed reactions for mono- and disaccharide modification, and many synthetic methods are available. Modifications at the hydroxyl groups, especially primary hydroxyl groups selectively, can also lead to specifically functionalized sugars with simple reactions. Natural products such as lipids, amino acids and nucleobases have been utilized for the formation of various sugar self-assembling systems. The self-assembled gels typically are not as stable as polymer gels; however the branched systems and polymerizable systems can be utilized to enhance the stability.

In comparison with other classes of natural product-based molecular self-assemblies, including peptide and nucleic acids *etc.*, carbohydrate-based self-assembling systems are inherently more complex and underexplored. Sugars are unique in their structures, and they are the only naturally available compounds containing multiple and redundant functional groups while being optically pure with great diversity. We hope to address some of these complexities and deliver the message that sugar derivatives have great potentials for the creation of soft materials and nanostructures that are applicable for catalysis and in biomedicines. Though some steps are complex in certain examples, the structures of the systems with built-in design elements are important and the knowledge gained from existing systems can be used to guide future studies. There is great promise for these classes of materials in various research fields as new biocompatible, biodegradable materials.

It is also necessary to develop new methods of designing self-assembling systems with the desired properties by introducing functional groups or scaffolds that can have a controllable response to various stimuli such as light, mechanical forces, temperature, magnetic and electrical fields, and chemical environment such as pH, ligand binding, and reactions. These unique systems with an optimal function and structure correlation are likely to have important future applications for advanced materials. The creation of these sugar derivatives has potential applications in drug delivery, therapeutic agents, tissue engineering, 3D printing, fluorescent sensors, *etc*.

Sugar-based molecular gels and new materials have endless potential and real-world utilities, they must be easy to prepare, and their properties need to be readily predicable. The future direction can focus on the element of design and achieving multifunctional stimulus-responsive molecular entities. Utilizing new catalytic reactions and incorporating automated synthesis will increase efficiency and reduce the synthetic difficulties. The advancement of machine learning and AI technology may also assist the development of novel materials and molecular assemblies. This technology may one day predict the structural requirements and functionalities needed for optimal supramolecular interactions and for binding to metal ions or ligands. Finally, collaborations of researchers from different fields including chemistry, materials sciences, engineering, and biology will ultimately lead to more impactful research discoveries that allow the carbohydrate-based self-assemblies to have practical applications.

Conflicts of interest

There are no conflicts of interest to declare.

References

1 L. Su, Y. Feng, K. Wei, X. Xu, R. Liu and G. Chen, *Chem. Rev.*, 2021, **121**, 10950–11029.
2 M. Delbianco, P. Bharate, S. Varela-Aramburu and P. H. Seeberger, *Chem. Rev.*, 2016, **116**, 1693–1752.
3 V. K. Tiwari, B. B. Mishra, K. B. Mishra, N. Mishra, A. S. Singh and X. Chen, *Chem. Rev.*, 2016, **116**, 3086–3240.
4 A. K. Agrahari, P. Bose, M. K. Jaiswal, S. Rajkhowa, A. S. Singh, S. Hotha, N. Mishra and V. K. Tiwari, *Chem. Rev.*, 2021, **121**, 7638–7956.
5 S. Cecioni, A. Imberty and S. Vidal, *Chem. Rev.*, 2015, **115**, 525–561.
6 S. Leusmann, P. Menova, E. Shanin, A. Titz and C. Rademacher, *Chem. Soc. Rev.*, 2023, **52**, 3663–3740.
7 C. Mueller, G. Despras and T. K. Lindhorst, *Chem. Soc. Rev.*, 2016, **45**, 3275–3302.
8 A. Brito, S. Kassem, R. L. Reis, R. V. Ulijn, R. A. Pires and I. Pashkuleva, *Chem*, 2021, **7**, 2943–2964.
9 A. Mittal, Krishna, Aarti, S. Prasad, P. K. Mishra, S. K. Sharma and B. Parshad, *Mater. Adv.*, 2021, **2**, 3459–3473.
10 Y. Yao, X. Meng, C. Li, K. V. Bernaerts and K. Zhang, *Small*, 2023, **19**, e2208286.
11 J. Morris, J. Bietsch, K. Bashaw and G. Wang, *Gels*, 2021, **7**, 24.
12 R. Tyagi, K. Singh, N. Srivastava and R. Sagar, *Mater. Adv.*, 2023, **4**, 3929–3950.
13 S. Datta and S. Bhattacharya, *Chem. Soc. Rev.*, 2015, **44**, 5596–5637.
14 J. Bietsch, M. Olson and G. Wang, *Gels*, 2021, **7**, 134.
15 J. Bietsch, L. Baker, A. Duffney, A. Mao, M. Foutz, C. Ackermann and G. Wang, *Gels*, 2023, **9**, 445.
16 D. Wang, A. Chen, J. Morris and G. Wang, *RSC Adv.*, 2020, **10**, 40068–40083.
17 A. J. Chen, D. Wang, L. P. Samankumara and G. J. Wang, *Synthesis*, 2019, 2897–2908.
18 P. Sharma and G. Wang, *Gels*, 2022, **8**, 191.
19 A. Chen, S. B. Adhikari, K. Mays and G. Wang, *Langmuir*, 2017, **33**, 8076–8089.

20 A. D. Ludwig, V. Gorbunova, A. Saint-Jalmes, F. Berrée and L. Lemiègre, *ChemistrySelect*, 2023, **8**, e202300213.
21 A. D. Ludwig, N. Ourvois-Maloisel, A. Saint-Jalmes, F. Artzner, J. P. Guegan, O. Tasseau, F. Berree and L. Lemiegre, *Soft Matter*, 2022, **18**, 9026–9036.
22 A. Brito, D. Dave, A. Lampel, V. I. B. Castro, D. Kroiss, R. L. Reis, T. Tuttle, R. V. Ulijn, R. A. Pires and I. Pashkuleva, *J. Am. Chem. Soc.*, 2021, **143**, 19703–19710.
23 C. He, S. Wu, D. Liu, C. Chi, W. Zhang, M. Ma, L. Lai and S. Dong, *J. Am. Chem. Soc.*, 2020, **142**, 17015–17023.
24 N. P. Pathak, A. Sengupta and S. Yadav, *Mater. Adv.*, 2022, **3**, 3906–3914.
25 N. Tsutsumi, A. Ito, A. Ishigamori, M. Ikeda, M. Izumi and R. Ochi, *Int. J. Mol. Sci.*, 2021, **22**, 1860.
26 N. Tsutsumi, A. Ito, Y. Niko, Y. Bando, K. Takahashi, M. Ikeda, K. Yoneyama, T. Nakamura, M. Izumi and R. Ochi, *ChemistrySelect*, 2022, **7**, e202202559.
27 A. George and N. Jayaraman, *ACS Omega*, 2023, **8**, 16927–16934.
28 A. George and N. Jayaraman, *Carbohydr. Res.*, 2023, **533**, 108933.
29 L. Mousavifar, J. D. Lewicky, A. Taponard, R. Bagul, M. Rivat, S. Abdullayev, A. L. Martel, N. L. Fraleigh, A. Nakamura, F. J. Veyrier, H.-T. Le and R. Roy, *Pharmaceutics*, 2022, **14**, 2300.
30 X. Xu, L. Li, L. Ye, X. Liu, Y. Feng and G. Chen, *Macromol. Rapid Commun.*, 2023, **44**, 2300359.
31 N. Baccile, A. Poirier, C. Seyrig, P. Le Griel, J. Perez, D. Hermida-Merino, P. Pernot, S. L. K. W. Roelants and W. Soetaert, *J. Colloid Interface Sci.*, 2023, **630**, 404–415.
32 G. Ben Messaoud, P. Le Griel, S. Prevost, D. Hermida-Merino, W. Soetaert, S. L. K. W. Roelants, C. V. Stevens and N. Baccile, *Soft Matter*, 2020, **16**, 2528–2539.
33 A. Poirier, P. Le Griel, T. Bizien, T. Zinn, P. Pernot and N. Baccile, *Soft Matter*, 2023, **19**, 366–377.
34 A. Poirier, P. Le Griel, I. Hoffmann, J. Perez, P. Pernot, J. Fresnais and N. Baccile, *Soft Matter*, 2023, **19**, 378–393.
35 A. Poirier, P. Le Griel, J. Perez, D. Hermida-Merino, P. Pernot and N. Baccile, *ACS Sustainable Chem. Eng.*, 2022, **10**, 16503–16515.
36 A. K. Rachamalla, V. P. Rebaka, T. Banoo, R. Pawar, M. Faizan, K. Lalitha and S. Nagarajan, *Green Chem.*, 2022, **24**, 2451–2463.
37 P. V. Bhavya, K. Soundarajan, J. G. Malecki and T. Mohan Das, *ACS Omega*, 2022, **7**, 39310–39324.
38 V. Rabecca Jenifer and T. Mohan Das, *Soft Matter*, 2022, **18**, 9017–9025.
39 R. J. Vasanthan, J. G. Malecki and T. M. Das, *Ind. Eng. Chem. Res.*, 2023, **62**, 13034–13045.
40 Y. Feng, L. Li, Q. Du, L. Gou, L. Zhang, Y. Chai, R. Zhang, T. Shi and G. Chen, *CCS Chem.*, 2022, **4**, 2228–2238.
41 O. Metelkina, B. Huck, J. S. O'Connor, M. Koch, A. Manz, C.-M. Lehr and A. Titz, *J. Mater. Chem. B*, 2022, **10**, 537–548.
42 S. Komba and R. Iwaura, *ACS Omega*, 2021, **6**, 20912–20923.
43 P. Sharma, A. Chen, D. Wang and G. Wang, *Chemistry*, 2021, **3**, 935–958.
44 G.-R. Huang, X.-W. Shi, Y.-M. Wu, B.-P. Cao, H. Okamoto and Q. Xiao, *New J. Chem.*, 2023, **47**, 84–91.
45 L. Yao, L. Wu, R. Wang, Y. Liu, F. Luo, Y. Zhang and G. Chen, *ACS Macro Lett.*, 2022, **11**, 975–981.
46 P. Aryal, S. B. Adhikari, A. Duffney and G. Wang, *New J. Chem.*, 2023, **47**, 17224–17228.
47 S. L. Higashi and M. Ikeda, *JACS Au*, 2021, **1**, 1639–1646.
48 A. Ghosh, S. K. Dubey, M. Patra, J. Mandal, N. N. Ghosh, P. Das, A. Bhowmick, K. Sarkar, S. Mukherjee, R. Saha and S. Bhattacharjee, *Chem. – Eur. J.*, 2022, **28**, e202201621.
49 V. I. B. Castro, A. R. Araujo, F. Duarte, A. Sousa-Franco, R. L. Reis, I. Pashkuleva and R. A. Pires, *ACS Appl. Mater. Interfaces*, 2023, **15**, 29998–30007.
50 D. Biswakarma, N. Dey and S. Bhattacharya, *J. Colloid Interface Sci.*, 2022, **615**, 335–345.
51 Y. Sasaoka and K. Ito, *Chem. Lett.*, 2022, **51**, 1049–1053.
52 M. Khan, S. Das, A. Roy and S. Roy, *Langmuir*, 2023, **39**, 899–908.
53 Y. Ohsedo, *Chem. – Asian J.*, 2022, **17**, e202200461.
54 K. P. C. Sekhar, D. Patel, S. A. Holey, S. Kanjilal and R. R. Nayak, *J. Mol. Liq.*, 2022, **351**, 118585.
55 S. A. Holey, K. P. C. Sekhar, D. K. Swain, S. Bojja and R. R. Nayak, *ACS Biomater. Sci. Eng.*, 2022, **8**, 1103–1114.
56 S. A. Holey, P. Basak, S. Bojja and R. R. Nayak, *Soft Matter*, 2023, **19**, 6305–6313.
57 H. S. Cooke, L. Schlichter, C. C. Piras and D. K. Smith, *Chem. Sci.*, 2021, **12**, 12156–12164.
58 M. Albino, T. J. Burden, C. C. Piras, A. C. Whitwood, I. J. S. Fairlamb and D. K. Smith, *ACS Sustainable Chem. Eng.*, 2023, **11**, 1678–1689.
59 L. Schlichter, C. C. Piras and D. K. Smith, *Chem. Sci.*, 2021, **12**, 4162–4172.
60 K. Fan, L. Wang, W. Wei, F. Wen, Y. Xu, X. Zhang and X. Guan, *Chem. Eng. J.*, 2022, **441**, 136026.
61 I. Mattsson, M. Lahtinen, R. Sitdikov, B. Wank, T. Saloranta-Simell and R. Leino, *Carbohydr. Res.*, 2022, **518**, 108596.
62 S. K. Singh, S. Dey, M. P. Schneider and S. Nandi, *New J. Chem.*, 2022, **46**, 6193–6200.
63 T. Maki, R. Yoshisaki, S. Akama and M. Yamanaka, *Polym. J.*, 2020, **52**, 931–938.
64 R. Yoshisaki, S. Kimura, M. Yokoya and M. Yamanaka, *Chem. – Asian J.*, 2021, **16**, 1937–1941.
65 D. Biswakarma, N. Dey and S. Bhattacharya, *Chem. Commun.*, 2020, **56**, 7789–7792.
66 D. Biswakarma, N. Dey and S. Bhattacharya, *J. Chem. Sci.*, 2023, **135**, 7.
67 Y.-C. Wang, L. L. Kegel, D. S. Knoff, B. S. Deodhar, A. V. Astashkin, M. Kim and J. E. Pemberton, *J. Mater. Chem. B*, 2022, **10**, 3861–3875.
68 S. Yao, R. Brahmi, F. Portier, J.-L. Putaux, J. Chen and S. Halila, *Chem. – Eur. J.*, 2021, **27**, 16716–16721.

69 S. Yao, R. Brahmi, A. Bouschon, J. Chen and S. Halila, *Green Chem.*, 2023, **25**, 330–335.
70 Y. Yu, S. Gim, D. Kim, Z. A. Arnon, E. Gazit, P. H. Seeberger and M. Delbianco, *J. Am. Chem. Soc.*, 2019, **141**, 4833–4838.
71 S. Gim, G. Fittolani, Y. Nishiyama, P. H. Seeberger, Y. Ogawa and M. Delbianco, *Angew. Chem., Int. Ed.*, 2020, **59**, 22577–22583.
72 S. Gim, G. Fittolani, Y. Yu, Y. Zhu, P. H. Seeberger, Y. Ogawa and M. Delbianco, *Chemistry*, 2021, **27**, 13139–13143.
73 P. Tsupko, S. S. Sagiri, M. Samateh, S. Satapathy and G. John, *J. Surfactants Deterg.*, 2023, **26**, 369–385.
74 X. Zhao, H. Zhang, Y. Gao, Y. Lin and J. Hu, *ACS Appl. Bio Mater.*, 2020, **3**, 648–653.
75 Q. Li, Z. L. Wan and X. Q. Yang, *Curr. Opin. Food Sci.*, 2022, **43**, 107–113.
76 A. A. Ba, J. Everaert, A. Poirier, P. Le Griel, W. Soetaert, S. L. K. W. Roelants, D. Hermida-Merino, C. V. Stevens and N. Baccile, *Green Chem.*, 2020, **22**, 8323–8336.
77 A. Poirier, P. Le Griel, T. Zinn, P. Pernot, S. L. K. W. Roelants, W. Soetaert and N. Baccile, *Chem. Mater.*, 2022, **34**, 5546–5557.
78 N. Baccile, A. Poirier, P. Le Griel, P. Pernot, M. Pala, S. Roelants, W. Soetaert and C. V. Stevens, *Colloids Surf., A*, 2023, **679**, 132518.
79 I. Russo Krauss, R. Esposito, L. Paduano and G. D'Errico, *Curr. Opin. Colloid Interface Sci.*, 2024, **70**, 101792.
80 G. Ben Messaoud, *Curr. Opin. Colloid Interface Sci.*, 2024, **71**, 101805.
81 J. Liu, Y. Zhang, K. van Dongen, C. Kennedy, M. J. G. Schotman, P. P. Marin San Roman, C. Storm, P. Y. W. Dankers and R. P. Sijbesma, *Biomacromolecules*, 2023, **24**, 2447–2458.
82 O. El Hamoui, K. Gaudin, S. Battu, P. Barthelemy, G. Lespes and B. Alies, *Langmuir*, 2021, **37**, 297–310.
83 O. El Hamoui, T. Sayde, I. Svahn, A. Gudin, E. Gontier, P. Le Coustumer, J. Verget, P. Barthelemy, K. Gaudin, S. Battu, G. Lespes and B. Alies, *ACS Biomater. Sci. Eng.*, 2022, **8**, 3387–3398.
84 N. Bansode, J. Verget and P. Barthelemy, *Soft Matter*, 2023, **19**, 6867–6870.
85 S. I. S. Hendrikse, L. Su, T. P. Hogervorst, R. P. M. Lafleur, X. Lou, G. A. van der Marel, J. D. C. Codee and E. W. Meijer, *J. Am. Chem. Soc.*, 2019, **141**, 13877–13886.
86 S. Varela-Aramburu, G. Morgese, L. Su, S. M. C. Schoenmakers, M. Perrone, L. Leanza, C. Perego, G. M. Pavan, A. R. A. Palmans and E. W. Meijer, *Biomacromolecules*, 2020, **21**, 4105–4115.
87 L. Rijns, L. Su, K. Maxeiner, G. Morgese, D. Y. W. Ng, T. Weil and P. Y. W. Dankers, *Chem. Commun.*, 2023, **59**, 2090–2093.
88 G. Wang, D. Wang, J. Bietsch, A. Chen and P. Sharma, *J. Org. Chem.*, 2020, **85**, 16136–16156.
89 A. Chen, D. Wang, J. Bietsch and G. Wang, *Org. Biomol. Chem.*, 2019, **17**, 6043–6056.
90 J. Bietsch, A. Chen, D. Wang and G. Wang, *Molecules*, 2023, **28**, 6056.
91 Q. Xiao, M. Delbianco, S. E. Sherman, A. M. R. Perez, P. Bharate, A. Pardo-Vargas, C. Rodriguez-Emmenegger, N. Y. Kostina, K. Rahimi, D. Soder, M. Moller, M. L. Klein, P. H. Seeberger and V. Percec, *Proc. Natl. Acad. Sci. U. S. A.*, 2020, **117**, 11931–11939.
92 N. Yu Kostina, D. Soder, T. Haraszti, Q. Xiao, K. Rahimi, B. E. Partridge, M. L. Klein, V. Percec and C. Rodriguez-Emmenegger, *Angew. Chem., Int. Ed.*, 2021, **60**, 8352–8360.
93 P. V. Murphy, A. Romero, Q. Xiao, A. K. Ludwig, S. Jogula, N. V. Shilova, T. Singh, A. Gabba, B. Javed, D. Zhang, F. J. Medrano, H. Kaltner, J. Kopitz, N. V. Bovin, A. M. Wu, M. L. Klein, V. Percec and H. J. Gabius, *iScience*, 2021, **24**, 101919.
94 M. Mullerova, D. Maciel, N. Nunes, D. Wrobel, M. Stofik, L. Cervenkova Stastna, A. Krupkova, P. Curinova, K. Novakova, M. Bozik, M. Maly, J. Maly, J. Rodrigues and T. Strasak, *Biomacromolecules*, 2022, **23**, 276–290.
95 T. Isono, R. Komaki, N. Kawakami, K. Chen, H.-L. Chen, C. Lee, K. Suzuki, B. J. Ree, H. Mamiya, T. Yamamoto, R. Borsali, K. Tajima and T. Satoh, *Biomacromolecules*, 2022, **23**, 3978–3989.
96 L. Dong, M. Fu, L. Liu, H.-H. Han, Y. Zang, G.-R. Chen, J. Li, X.-P. He and S. Vidal, *Chem. – Eur. J.*, 2020, **26**, 14445–14452.
97 L. Dong, M.-Y. Zhang, H.-H. Han, Y. Zang, G.-R. Chen, J. Li, X.-P. He and S. Vidal, *Chem. Sci.*, 2022, **13**, 247–256.
98 A. Barattucci, C. M. A. Gangemi, A. Santoro, S. Campagna, F. Puntoriero and P. Bonaccorsi, *Org. Biomol. Chem.*, 2022, **20**, 2742–2763.
99 L. J. Patalag, S. Ahadi, O. Lashchuk, P. G. Jones, S. Ebbinghaus and D. B. Werz, *Angew. Chem., Int. Ed.*, 2021, **60**, 8766–8771.
100 Y.-c. Liu, G.-j. Liu, W. Zhou, G.-l. Feng, Q.-y. Ma, Y. Zhang and G.-w. Xing, *Angew. Chem., Int. Ed.*, 2023, **62**, e202309786.
101 J. Treekoon, T. Pewklang, K. Chansaenpak, J. N. Gorantla, S. Pengthaisong, R.-Y. Lai, J. R. Ketudat-Cairns and A. Kamkaew, *Org. Biomol. Chem.*, 2021, **19**, 5867–5875.
102 A. K. East, M. C. Lee, C. Jiang, Q. Sikander and J. Chan, *J. Am. Chem. Soc.*, 2023, **145**, 7313–7322.
103 R. Liu, R. Zhang, L. Li, Z. Kochovski, L. Yao, M.-P. Nieh, Y. Lu, T. Shi and G. Chen, *J. Am. Chem. Soc.*, 2021, **143**, 6622–6633.
104 L. Li, L. Wu, M. Urschbach, D. Strassburger, X. Liu, P. Besenius and G. Chen, *ACS Polym. Au*, 2022, **2**, 478–485.
105 T. Tyrikos-Ergas, S. Gim, J. Y. Huang, S. Pinzon Martin, D. Varon Silva, P. H. Seeberger and M. Delbianco, *Nat. Commun.*, 2022, **13**, 3954.
106 G. Fittolani, D. Vargova, P. H. Seeberger, Y. Ogawa and M. Delbianco, *J. Am. Chem. Soc.*, 2022, **144**, 12469–12475.
107 N. Hribernik, D. Vargova, M. C. S. Dal Colle, J. H. Lim, G. Fittolani, Y. Yu, J. Fujihara, K. Ludwig, P. H. Seeberger, Y. Ogawa and M. Delbianco, *Angew. Chem., Int. Ed.*, 2023, **62**, e202310357.

108 M. G. Ricardo and P. H. Seeberger, *Chem. – Eur. J.*, 2023, **29**, e202301678.
109 Q. Chen, Y. Lv, D. Zhang, G. Zhang, C. Liu and D. Zhu, *Langmuir*, 2010, **26**, 3165–3168.
110 N. Singh, B. Lainer, G. J. M. Formon, S. De Piccoli and T. M. Hermans, *J. Am. Chem. Soc.*, 2020, **142**, 4083–4087.
111 N. Singh, A. Lopez-Acosta, G. J. M. Formon and T. M. Hermans, *J. Am. Chem. Soc.*, 2022, **144**, 410–415.
112 T. M. Hermans and N. Singh, *Angew. Chem., Int. Ed.*, 2023, **62**, e202301529.
113 R. C. Ollier, Y. Xiang, A. M. Yacovelli and M. J. Webber, *Chem. Sci.*, 2023, **14**, 4796–4805.
114 G. M. Peters and J. T. Davis, *Chem. Soc. Rev.*, 2016, **45**, 3188–3206.
115 F. Pu, J. Ren and X. Qu, *Chem. Soc. Rev.*, 2018, **47**, 1285–1306.
116 T. Giraud, P. Hoschtettler, G. Pickaert, M.-C. Averlant-Petit and L. Stefan, *Nanoscale*, 2022, **14**, 4908–4921.
117 Z. Chen, P. Zhou, Y. Guo, Anna, J. Bai, R. Qiao and C. Li, *J. Org. Chem.*, 2022, **87**, 2624–2631.
118 Umesh, S. Sarkar, S. Bera, P. Moitra and S. Bhattacharya, *Mater. Today Chem.*, 2023, **30**, 101554.
119 S. Ghosh, T. Ghosh, S. Bhowmik, M. K. Patidar and A. K. Das, *ACS Appl. Bio Mater.*, 2023, **6**, 640–651.
120 X.-Q. Xie, Y. Zhang, Y. Liang, M. Wang, Y. Cui, J. Li and C.-S. Liu, *Angew. Chem., Int. Ed.*, 2022, **61**, e202114471.
121 J. Li, Y. Cui, Y.-L. Lu, Y. Zhang, K. Zhang, C. Gu, K. Wang, Y. Liang and C.-S. Liu, *Nat. Commun.*, 2023, **14**, 5030.
122 K. A. Brown, M. K. Gugger, D. S. Roberts, D. Moreno, P. S. Chae, Y. Ge and S. Jin, *Langmuir*, 2023, **39**, 1465–1473.
123 S. Wang, M. C. Forster, K. Xue, F. Ehlers, B. Pang, L. B. Andreas, P. Vana and K. Zhang, *Angew. Chem., Int. Ed.*, 2021, **60**, 9712–9718.
124 S. Yadav, K. Naresh and N. Jayaraman, *ChemBioChem*, 2021, **22**, 3075–3081.
125 M. Negrete, E. Romero-Ben, A. Gutierrez-Valencia, C. Rosales-Barrios, E. Ales, T. Mena-Barragan, J. A. Flores, M. C. Castillejos, P. de la Cruz-Ojeda, E. Navarro-Villaran, C. Cepeda-Franco, N. Khiar and J. Muntane, *ACS Appl. Bio Mater.*, 2021, **4**, 4789–4799.
126 E. Romero-Ben, M. C. Castillejos, C. Rosales-Barrios, M. Exposito, P. Ruda, P. M. Castillo, S. Nardecchia, J. de Vicente and N. Khiar, *J. Mater. Chem. B*, 2023, **11**, 10189–10205.
127 G. Wang, D. Wang, A. Chen, I. S. Okafor and L. P. Samankumara, *ACS Omega*, 2022, **7**, 11330–11342.
128 P. Aryal, J. Morris, S. B. Adhikari, J. Bietsch and G. Wang, *Molecules*, 2023, **28**, 6228.